Acronym:	FLARE
Project full title:	Flooding Accident REsponse
Grant agreement No.	814753
Coordinator:	BALance Technology Consulting GmbH

Deliverable 4.2 – Model tests

Volume 1 - Fundamental Compartment Flooding

The project has received funding from the European's Horizon 2020 research and innovation programme (Contract No.: 814753)

Duration: 36 months - Project Start: 01/06/2019 - Project End: 31/05/2022

Deliverable data

Deliverable No	4.2 Volume 1		
Deliverable Title	Model tests: Fundamental Compartment Flooding		
Work Package no: title	WP4.2 Model tests		

Dissemination level	Public	**Deliverable type**	Report
Lead beneficiary	HSVA		
Responsible author	R. van Basten Batenburg		
Co-authors	-		
Date of delivery	15-11-2020		
Approved	**Name (partner)**		**Date [DD-MM-YYYY]**
	O. Rognebakke (DNVGL)		13-01-2021
	O. K. Olufsen (DNVGL)		13-01-2021

Document history

Version	**Date**	**Description**
1	**23-11-2020**	Draft
2	**25-11-2020**	For external review
3	**27-01-2021**	Final

The research leading to these results has received funding from the European Union Horizon 2020 Programme under grant agreement n° 814753.
This report reflects only the author's view. INEA is not responsible for any use that may be made of the information it contains.

CONTENTS

List of symbols and abbreviations

Cd	Discharge coefficient
DoF	Degree of Freedom
ITTC	International Towing Tank Conference
CFD	Computational Fluid Dynamics
RAO	Response Amplitude Operator
TD	Time domain

1 EXECUTIVE SUMMARY

The present report describes a series of model tests that focus on the fundamental flooding of compartments. The tests executed within the EU FLARE project. The goal of the tests is to provide data for benchmarking and verification of the results of numerical codes that simulate the flooding process.

The model is an assembly of three elementary compartment configurations that model specific fundamental flooding phenomena. The following compartments are made and shown in Figure 1-1 from left to right:

A - Flooding box

B - Cross flooding box

C - Up and Down flooding box

A large test matrix was set-up including inflow tests in upright and heeled conditions, oscillation tests in calm water and tests in regular waves. Most tests were executed under atmospheric pressure and some tests were executed (repeated) under depressurised condition. The test setup and adopted approaches are described in chapters 3 to 7; a summary of the results including a concise discussion of the result is given in chapter 8. The analysed data and videos are included on a USB stick that is delivered with this report.

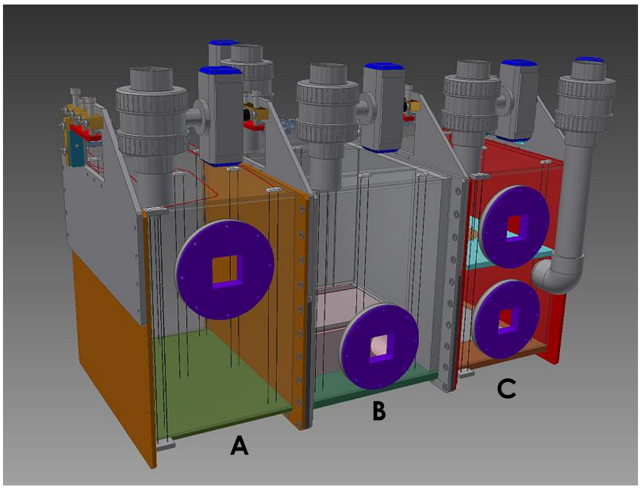

Figure 1-1 Model

1.1 Problem definition

- In the development and verification of codes that assess flooding of ships it is required to check fundamental flooding phenomena.

1.2 Technical approach and work plan

- A model with three different compartments is designed
- Model tests were executed
- The measurements were analysed and discussed

1.3 Results

- The model tests result in a data set containing a vast amount of measurements that can be used to benchmark the results of flooding simulation codes.

1.4 Conclusions

- The discharge coefficient of the vertical openings was not affected by whether the opening was partly submerged or whether the opening was dry or wet on the outflow side. The values of the discharge coefficient generally ranged between 0.6 and 0.7.
- Horizontal (down flooding) openings resulted in a varying discharge coefficient. The discharge coefficient decreased with the water depth. The discharge coefficient ranged generally between 0.7 and 1.0.
- Because of its dynamic behaviour, the cross flooding compartment was not suitable to determine the discharge coefficient when the cross-duct oscillation was near to or quicker than the model's own natural period. For relatively slow flooding, for instance the flooding under constant pressure head, the calculation resulted in a constant discharge coefficient, hence a Bernoulli method is expected to suffice for this type of flooding
- When the cross-duct undergoes dynamic motions, there is phase leg between the water level in the two compartments. Such cannot be capture by a Bernoulli model unless special additional flow momentum equations are utilized.
- A heel angle up to 10 degrees had no measurable impact on the discharge coefficients.

2 INTRODUCTION

2.1 General

The goal of this work package (WP4) is to provide measurements that can be used to benchmark simulation software that is able to predict the dynamic flooding of cruise or Ropax vessels.

Volumes 1 to 5 describe the model tests that are executed for Cruise vessels by MARIN. Volumes 6 and higher describe the model tests that are executed to investigate the flooding of Ropax vessels. The latter tests were executed by HSVA.

Volumes 1 to 5 describe

1. Fundamental compartment flooding
2. Deck flooding
3. Fundamental hydrodynamics
4. Cruise ship flooding (Part 1)
5. Cruise ship flooding (Part 2)

The model information, measured data and videos of the present model tests are provided on a USB memory stick. An HTML menu provides the metadata of each test and easy access of the results.

2.2 Volume 1

The present report describes a series of model tests that focus on the fundamental flooding of compartments. The tests are executed within the EU FLARE project. The goal of the tests is to provide data for benchmarking and verification of the results of numerical codes that simulate the flooding process.

The model is an assembly of three academic compartments that model specific flooding phenomena. The following compartments are made and shown in Figure 2-1 from left to right:

A - Flooding box

B - Cross flooding box

C - Up and Down flooding box

The test setup and adopted approaches are described in chapters 3 to 7; a summary of the results including a concise discussion of the results is given in chapter 8. The analysed data and videos are included on a USB stick that is delivered with this report.

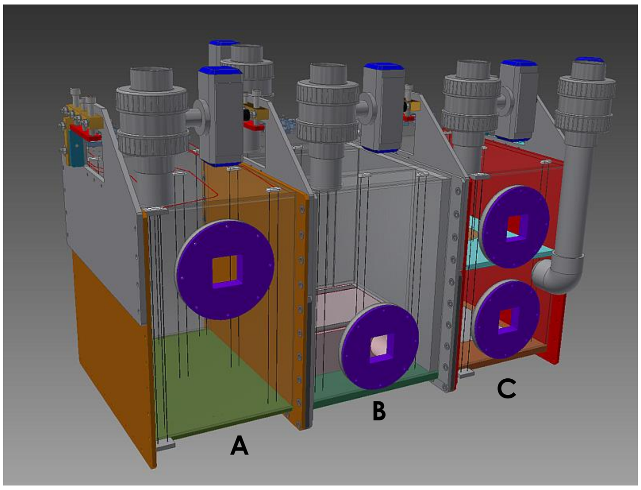

Figure 2-1 Model

2.3 FLOODING ACCIDENT RESPONSE

Despite the fact that the maritime sector is continuously investing in increasing and maintaining safety on board ships, additional effort is needed in the pathway towards zero-loss of life and zero-pollution. The highest risk for persons on board ships comes with flooding accidents, but consequences may be reduced when appropriate actions are taken following such an accident, thus greatly reducing the probability of loss of life or damage to the environment.

The FLARE project will target a risk-based methodology for "live" flooding risk assessment and control, by developing a generic (all incidents in one model) and holistic (active and passive measures) risk model with potential application to new buildings and, which is totally new, to existing ships. Innovative technical solutions in ship concepts and equipment for risk containment and control will be accompanied by proposals for the revision of relevant IMO regulations towards a risk-based approach to contain and control risk in passenger ships from flooding incidents, thereby significantly contributing to the safety of both passenger and ship.

2.4 Project partners

BALance Technology Consulting GmbH, with its headquarters in Bremen, Germany, coordinates the project in close cooperation with the University of Strathclyde, Department of Naval Architecture, Ocean and Marine Engineering. Nineteen other leading maritime stakeholders will contribute to the results of FLARE: Aalto University, Brookes Bell, Bureau Veritas Marine & Offshore, Carnival, Color Line Marine, DNV GL, Fincantieri, Hamburgische Schiffbau-Versuchsanstalt, ICAM Nantes, Lloyd's Register, MARIN, Meyer Werft, Meyer Turku, NAPA, SEA Europe, Chantiers de l'Atlantique, Rina Services, RCCL and Stena Line. This project has received funding from the European Union's Horizon 2020 research and innovation programme under Grant Agreement No 814753.

3 MODEL

3.1 General

The model is an assembly of three separate compartments that are designed to model specific flooding phenomena

A - Flooding box

B - Cross flooding box

C - Up and Down flooding box

The internal dimensions of each compartment are (L x B x H) 300 mm x 450 mm x 450 mm.

The model does not represent a vessel in reality. Therefore no scale factor is applied.

3.2 Inflow openings

Each compartment was equipped with one or two closable inflow openings. The size of the inflow opening could be changed between the tests. The sizes of the openings in each model configuration are given in Table 3-1. The location of each opening is shown in Figure 3-1

Opening names:

- A-up: Opening to single compartment to outside
- B-low: Opening wingtank to outside
- B-duct: Connection between the two wingtanks
- C-up: Upper opening to outside
- C-low: Lower opening to outside
- C-in: Opening between upper and lower compartment

All inflow openings are in a plate thickness of 2 mm with (sharp) rectangular edges (see Figure 3-2)

The deck inside the C-compartment is located at 233 mm above the base; the deck thickness is 12mm. The up/down flooding opening is made in a 2mm plate. See Figure 5-2. The inner height of the upper compartment is 205 mm.

Table 3-1 Model configuration, opening dimensions

Model configuration	Opening					
	A-up	B-low	B-duct	C-low	C-up	C-in
1	40x40	80x80	60x60	closed	80x80	40x40
2	40x40	80x80	60x60	closed	80x80	40x40
3	80X80	80x80	120x60	closed	80x80	80x40
4	80X80	80x80	120x60	closed	80x80	80x40
5	80X80	80x80	120x60	closed	80x80	80x40
6	80X80	80x80	120x60	closed	80x80	80x40
8	80x40	80x80	120x60	closed	80x80	80x40
10	80x40	80x80	120x60	80x80	closed	80x40

Note: configurations 7 and 9 were not used in the tests.

Unless stated otherwise, the openings were covered by a watertight magnetic sheet at the start of each test. The cover sheet was removed with a speed of about 2.5m/s. This implies that an 80x80 mm opening is fully opened in 0.032 s. The cover sheet moves vertically upwards.

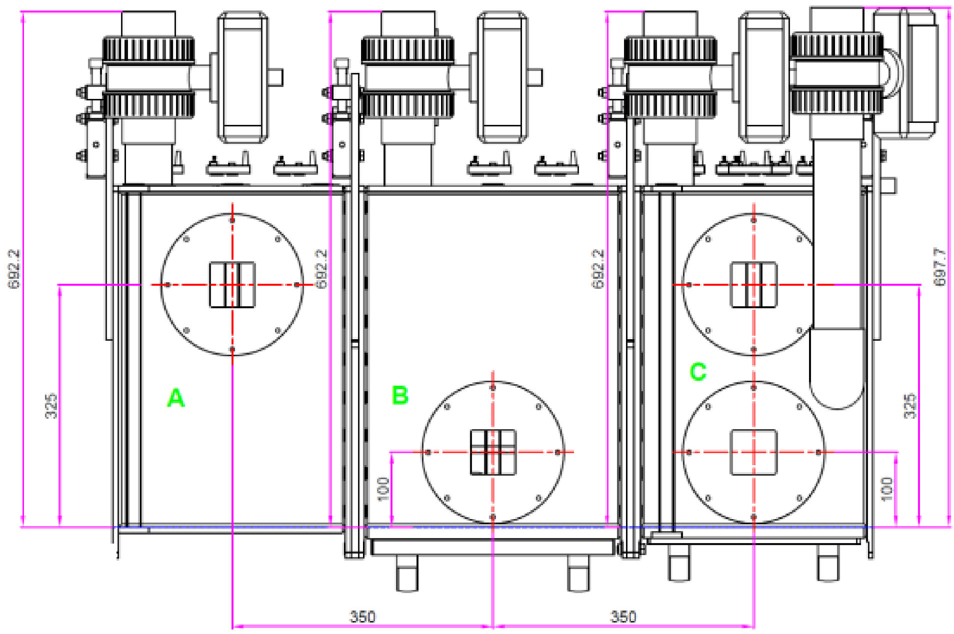

Figure 3-1: Inflow openings

Figure 3-2 shows a schematic cross section of the openings. The transparent PVS is denoted in blue, the PVC insert ring is shown in purple. The dimensions of the opening in this insert are 110x110 mm for the vertical openings and 100x100 for the horizontal opening. The thickness of the purple plate is 20mm and 12 mm for vertical and horizontal respectively.

The dimensions of the opening itself, as given in Table 3-1, are made in a 2 mm thick PVC plate with square edges; this plate is shown in black.

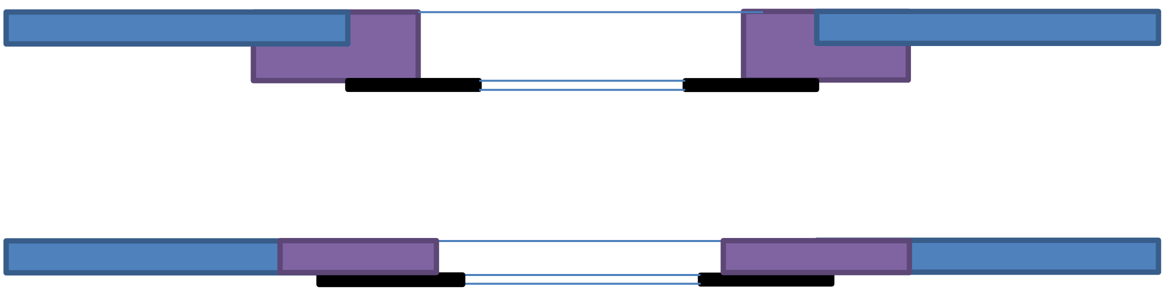

Figure 3-2: Inflow opening cross section vertical opening (upper) horizontal opening (lower)

More details of the model can be found in the drawings on the USB stick that is delivered together with this report.

3.3 Ventilation pipes

Each sub-compartment was equipped with a ventilation pipe with a closable pneumatic valve. The inner diameter of the pipes was 50mm. The status of each ventilation pipe in each model configuration is given in Table 3-2. When the valve is open, the sub-compartment is considered to be fully ventilated.

Table 3-2 Model configuration vent pipe status

Model configuration	Ventilation opening				
	Vent1 A	Vent2 B-intact	Vent3 B-breach	Vent4 C-up	Vent 5 C-low
1	open	open	open	open	open
2	closed	closed	closed	closed	closed
3	open	open	open	open	open
4	closed	open	closed	open	closed
5	open	closed	closed	closed	closed
6	closed	closed	open	closed	open
8	closed	closed	closed	closed	closed
10	open	open	open	open	open

Note: configurations 7 and 9 were not used.

Figure 3-3: Photo of the model with the inflow openings in open position.

4 TEST SETUP AND FACILITY

The tests were executed in the Depressurised Wave Basin (DWB). The DWB is a unique research facility for testing ships and offshore structures in the most realistic operational conditions. The basin is fitted with wave generators and the air pressure in the basin can be decreased to as low as 2.5 % of atmospheric pressure. In this way many important research aspects concerning cavitation, wave forces, flooding and seakeeping can be studied using properly-scaled conditions for both water and air.

The model was connected to the carriage by a controllable Hexapod and a rotating arm. The test setup is shown in Figure 4-1. The test setup was designed in such a way that the tests and drainage of the model could be executed by remote control.

The wave propagation direction was in all tests perpendicular to the inflow openings of the model. The openings were facing the incident wave.

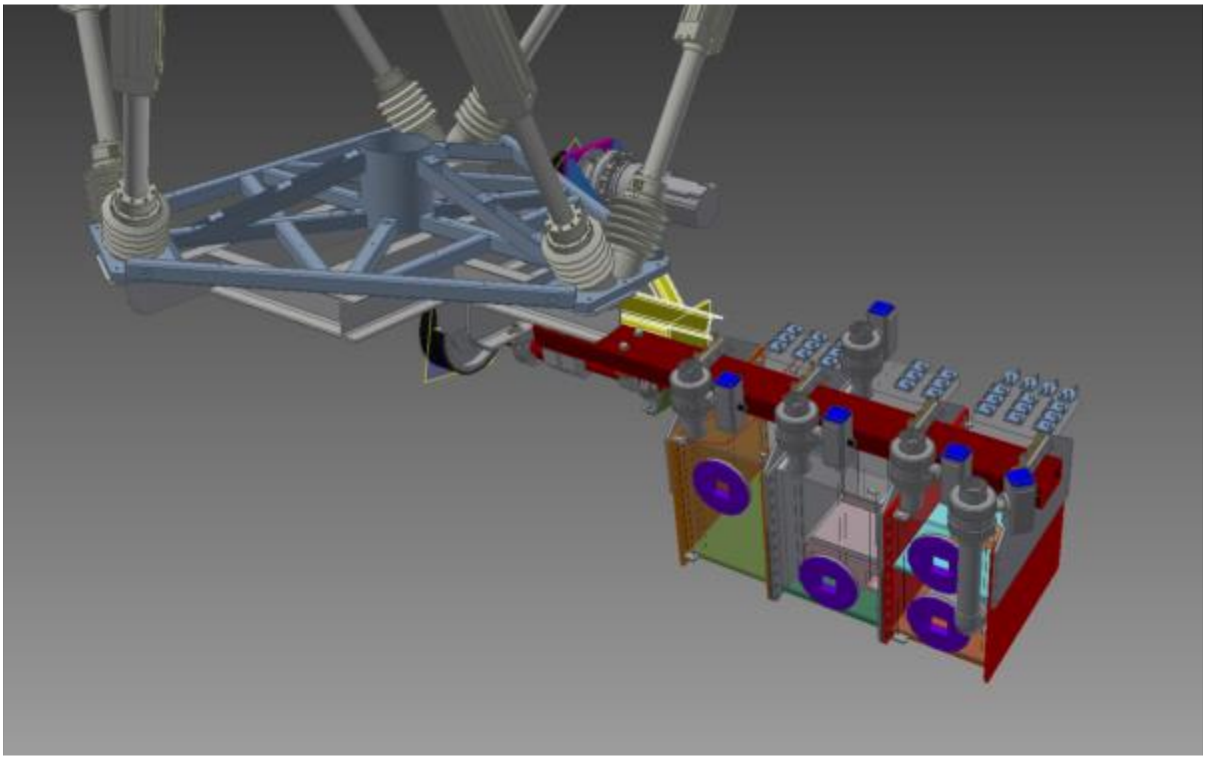

Figure 4-1: Test setup

5 MEASUREMENTS

The test setup was equipped with:

- An optical tracking system to measure the 6-DOF motions of the model in order to use the actual obtained position of the model in the test. Measured at a frequency of 100 Hz. The motions measured are translated to the origin of the model. Additionally, the motions are translated to the base of each relative wave probe to easily calculate the absolute wave elevation.
- Incident wave height in the basin to measure the incoming wave. Measured at a frequency of 200 Hz.
- The relative wave elevation was measured at 28 locations; the locations of the wave probes are given in Figure 5-1, Figure 5-2 and Table T 5 in Appendix I.

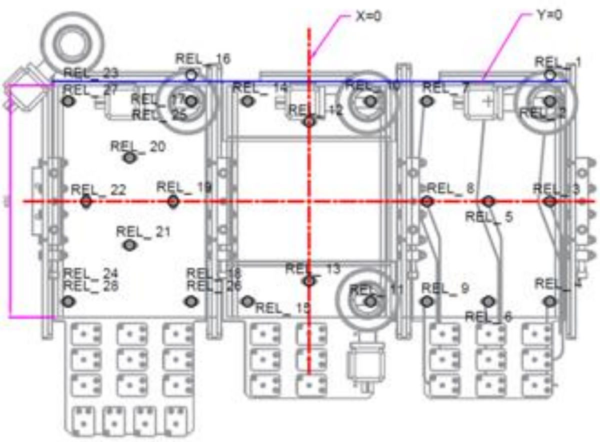

Figure 5-1: Top view of model and wave probe numbers

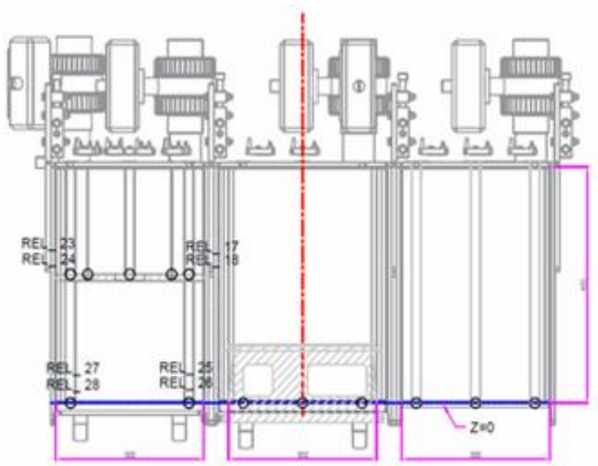

Figure 5-2: Side view of model and wave probe numbers in down-up flooding compartment (c)

The wave probe locations are relative to the axes origin of the model. (see section 6)

6 AXIS SYSTEMS AND SIGN CONVENTION

A right-handed axis system was adopted. The origin of the axis system is shown in Figure 6-1.

The origin is defined at:

- X is at the centre of compartment B
- Y is the outside of the side shell plating at the opening side
- Z is the top of the bottom plating

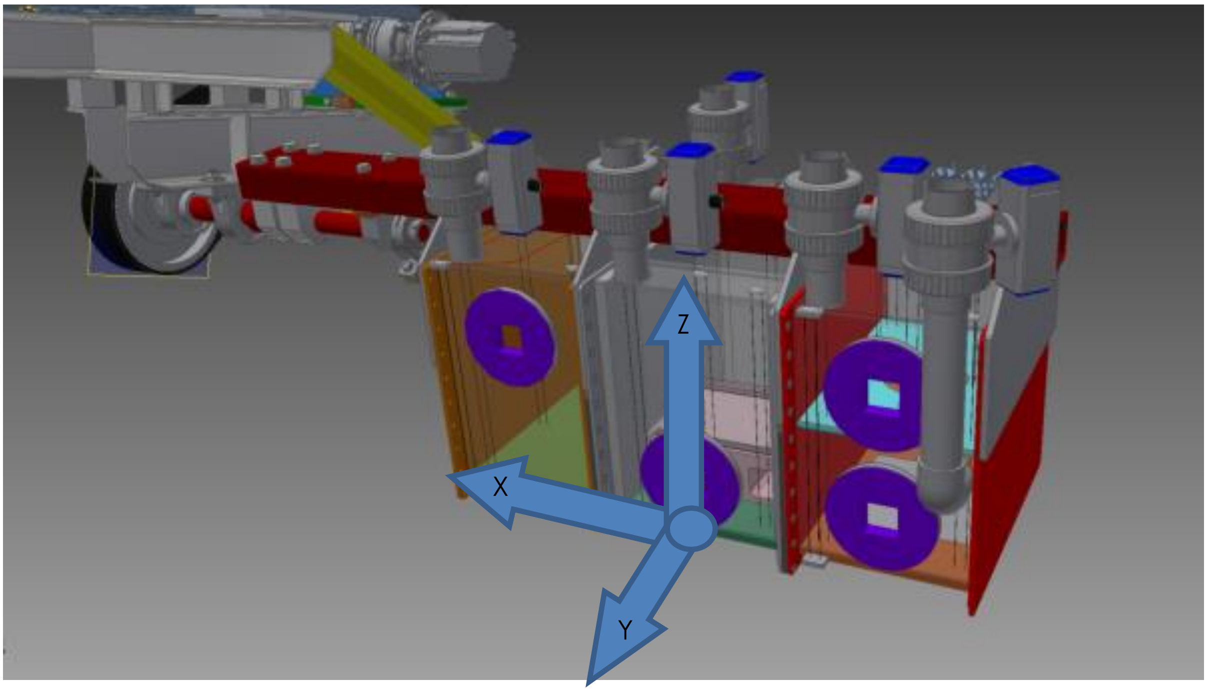

Figure 6-1: Axis system

The start position of the tests relative to the origin is given relative to the calm water level. In tests under static heel and trim or with roll and pitch oscillatory motions, the model rotates around the origin.

Draught is defined as the vertical distance between the origin and calm water level.

7 TEST PROGRAMME AND PROCEDURES

7.1 Summary of the test programme

A total of 69 flooding tests were executed. Of which:

- 4 tests at varying vertical speed
- 30 tests at constant draught in atmospheric pressure, with varying opening configurations, draught, heel and trim variations
- 13 tests in calm water with an oscillating model
- 5 tests in regular waves
- 5 tests in regular waves with an oscillating model
- 12 tests in depressurised condition with varying ventilation pipe configurations at two ambient pressures.

The full test matrix is shown in Appendix I.

7.2 Test procedures

Based on experience in previous tests, the resistive wave probes that were present in the model occasionally can show a small drift in the measured values. To avoid this phenomenon affecting the accuracy of the measurements, each wave probe starts at a known zero level and ends at a fully submerged end level. The measurements at these extreme levels are used to calibrate the wave probe in each test.

Unless stated otherwise, the following steps were conducted in each test:

A. The model was put into the start position by moving the hexapod. The start position is when the top of the bottom plating is at the calm water level
B. The measurement starts. The model stays stationary for about 30 seconds to measure the zero level of each sensor
C. Tests at constant speed only: the model descends at constant speed (continue at step L for these types of tests)
D. Tests at constant draught: the model descends to the prescribed draught
E. Tests at constant draught: the model waits a short moment to measure the start position
F. The magnetic cover sheet opens the inflow openings
G. Tests in waves: The wave generator starts
H. Oscillating tests: The oscillations start
I. The duration of the test was about 5 minutes for tests in waves or oscillations or the test ended after an equilibrium was reached. The wave generator and motions stop.
J. The model descends further to a draught of 450mm
K. Closed air valves are opened sequentially

L. After a stationary measurement of about 30 s the measurement is ended.

M. The model is prepared for the next test.

Note: for tests in waves and oscillations the steps G to I were repeated for a set of wave and oscillation conditions. The measurement stopped and started between the different conditions.

8 SUMMARY AND DISCUSSION

This section gives a summary of the test results and comparisons of the investigated phenomena.

For some tests the resulting discharge coefficients are compared. The discharge coefficient is calculated by Equation 1 if the pressure difference is constant over the opening, for horizontal openings and vertical openings which are submerged on both sides. Equation 2 is applied for openings with a (large) varying pressure difference, for instance for vertical openings. The discharge coefficient "principle" assumes a stationary flow, and in flooding calculations the Cd values are time independent, and typically only vary the geometry of the orifice.

Equation 1: Discharge coefficient for horizontal or fully submerged vertical openings

$$Cd = \frac{Q}{A\sqrt{2gh}}$$

Where:

Q is the inflow of water
A is opening area
g is the gravitational acceleration
h is the pressure difference head

Equation 2: Discharge coefficient for partial and fully submerged vertical openings

$$Cd = \frac{Q}{\frac{2}{3}b\sqrt{2g}(h_b^{\frac{3}{2}} - h_t^{\frac{3}{2}})}$$

Where:

Q is the inflow of water
b is the width of the opening
g is the gravitational acceleration
h_b is the pressure head at the bottom of the opening
h_t is the pressure head at the top of the opening, zero for partial submerged openings

8.1 Tests at constant speed

The goal of these tests is to investigate the impact of a gradually increasing water column, for instance the discharge coefficient on openings that are either wet or dry at the outflow side.

Compartment A Box

Figure 8-1 shows the calculated discharge coefficients of test 30703_03DWB_03_004_004_01 with a downward speed of 10 mm/s plotted against the time for compartment A. The opening of this compartment was 40x40 mm.

At the start of the test t=70 s the model starts to descend, as can be seen at the outside water level (blue). At just over 100 s the opening reaches the water and the internal water level rises (green). The calculated discharge coefficient varies at the start of the ingress. This is because the flow of the water is the derivative of the mean of the internal wave probes. To suppress the noise that inevitably results from deriving time traces, the wave elevation was filtered with a low pass Butterworth filter at a cut-off frequency of 0.4 Hz.

From 100 s to about 140 s the opening was submerged at the outside and the water level inside the box was below the opening. The discharge coefficient (Cd) was calculated with Equation 2. At about 140 s the water level inside the box rises above the opening and the Cd is calculated by Equation 1. (denoted with the thick black line).

Between 160 s and 230 s the model is at rest and low residual waves give a discharge coefficient. After 230 s the model submerges to the maximum position, after which the box completely fills with water.

The size of the opening was relatively small compared to the volume and close to the water plane. Hence the speed variations showed only slight difference in the measurements.

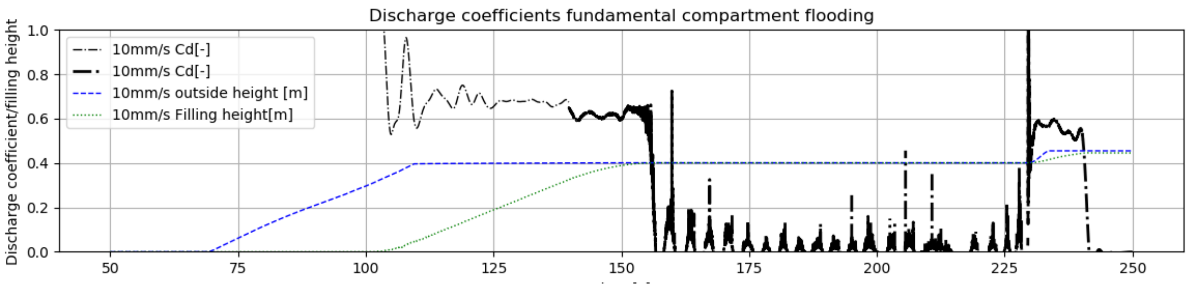

Figure 8-1: Discharge coefficient and filling height compartment A

Compartment B Cross flooding

Figure 8-2 shows the filling levels and resulting discharge coefficients for compartment B in test 30703_03DWB_03_004_006_01 with a speed of 50 mm/s. The outside water level is denoted in blue, the level at the inflow side in green, and the level at the other side of the duct in red. The discharge coefficients for the B_low opening (Cd1 and Cd2) are shown in black and the duct (Cd duct) in blue.

The graph shows the part of the measurement where the model is descending into the water to a level of 400mm.

In the calculation of the discharge coefficients the volume of water that is goes into the duct is not taken into account. This is the cause of the dip in the Cd of the inflow opening between 48 and 50 s. The discharge coefficients vary because of the dynamics in the flow. At about 55 s the Cd of the inflow opening and the duct goes to infinity as the water level at the other side of the duct exceeds the outside water level and the water level at the inflow side and hence the pressure head becomes negative.

For relatively slow sub resonance flooding as shown in these tests, the resulting discharge coefficient is quite constant, hence a simple Bernoulli method is expected to suffice.

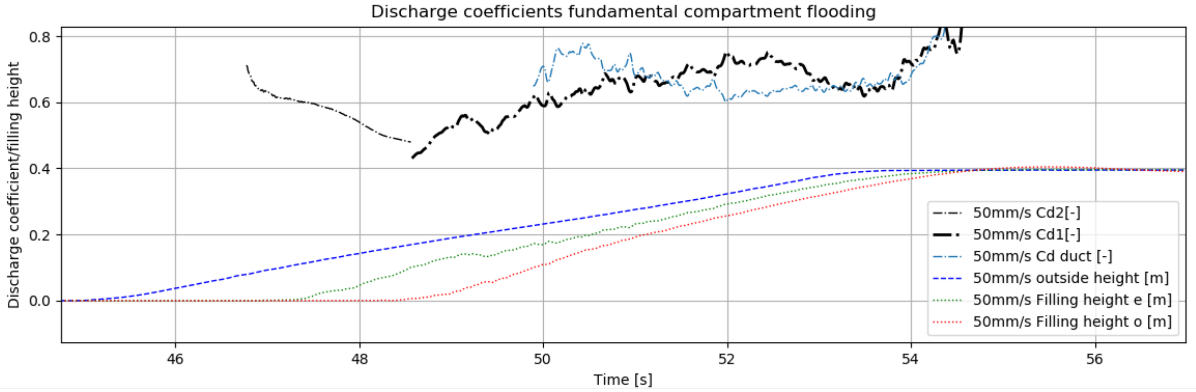

Figure 8-2: Discharge coefficient and filling height compartment B

Compartment C Down flooding

Figure 8-3 shows the water level in the upper compartment of the compartment C for test 30703_03DWB_03_004_004_01 to simulate down flooding. The green line shows the average water level near the down flooding opening. The red line shows the water level in the corners of the compartment. These values are very similar, except from the start of the ingress (between 100s and 103s), where some differences can be seen.

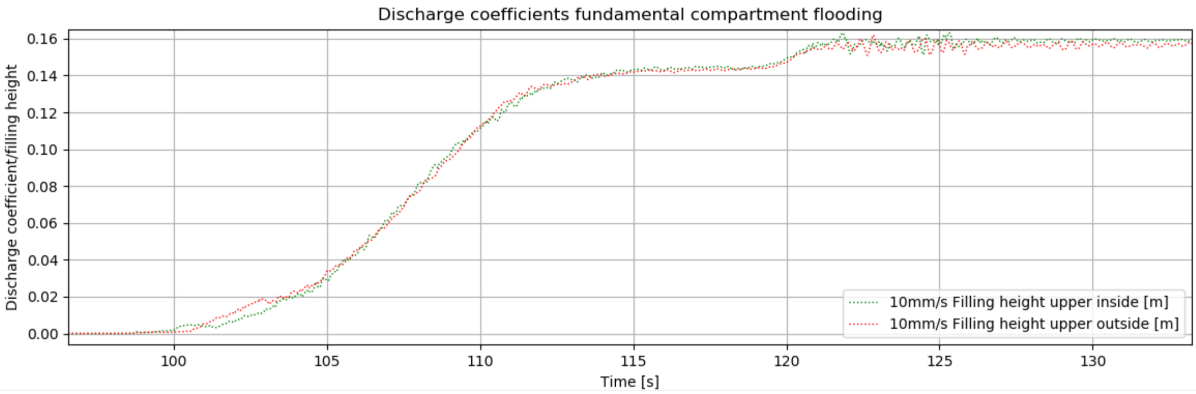

Figure 8-3: Filling height upper compartment in corners and near downloading opening

The discharge coefficient is calculated using the average water level from all wave probes in the upper compartment, and the average of all wave probes in the lower compartment. Figure 8-4 shows the discharge coefficients of the of the C_up and C_in openings; these are the inflow and down flooding openings respectively.

The discharge coefficient of the inflow opening varies at the start and stabilises at a value of about 0.6. During the ingress the coefficient seems to decrease slightly during the measurement. Note that the discharge coefficient “theory” is only valid for stationary flows, and it is not meant to capture the flow dynamics in rapid changing flow conditions.

The discharge coefficient of the down flooding opening starts at a value of about 1, without the oscillations, the value decreases to 0.75 when the lower compartment is almost filled. This is the most representative moment in the derivations. The higher discharge coefficients at start indicate large flow dynamics at the start of the measurement.

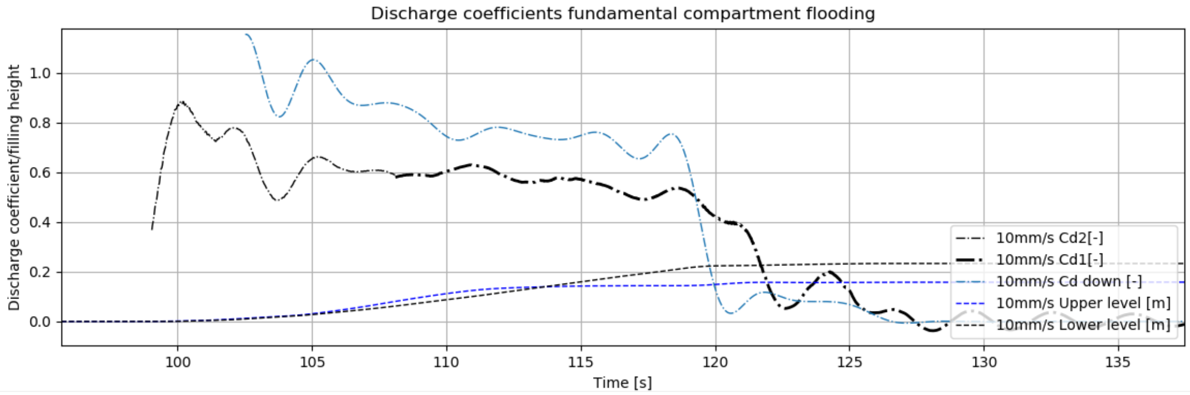

Figure 8-4: Filling heights and discharge coefficients in down flooding test

The other lowering speeds show similar decrease in the discharge coefficient values.

8.2 Tests at constant draught

The following sections show the comparisons of the observed behaviour due to changes in selection of parameter.

8.2.1 Opening sizes and partially flooded openings

Figure 8-5 shows the discharge coefficients for Compartment A for tests:

- 30703_03DWB_03_004_001_02 – opening 40x40 - T= 325 mm
- 30703_03DWB_03_004_001_03 – opening 40x40 - T= 325 mm (repeat test)
- 30703_03DWB_03_004_002_01 – opening 40x40 - T= 365 mm
- 30703_03DWB_03_004_002_02 – opening 40x40 - T= 365 mm (repeat test)
- 30703_03DWB_03_004_003_02 – opening 40x40 - T= 400 mm
- 30703_03DWB_03_004_003_03 – opening 40x40 - T= 400 mm (repeat test)
- 30703_03DWB_03_006_001_03 – opening 80x80 - T= 400 mm

The small opening of 40x40 mm was measured at three different draughts; each test was executed twice to check the repeatability of the test results. The larger opening was tested once at a draught of 400 mm. The tests result in a very similar discharge coefficient. It must be noted that the calculation of partially submerged openings is very sensitive to small deviations in the relative water level measurement at the inflow opening. To increase the accuracy of the calculation the measurements were calibrated on the calm water draught (T), which showed more consistent results compared to the calibration at the top of the compartment.

By taking the outside wave probe as source for the water head at the inflow side, the calculation automatically accounts for the flexibility of the test setup. The model got a bit deeper into the water as it filled, which has a large impact on the ingress of water in the 325 mm draught as in addition to the pressure head, this also increased the submerged area of the opening.

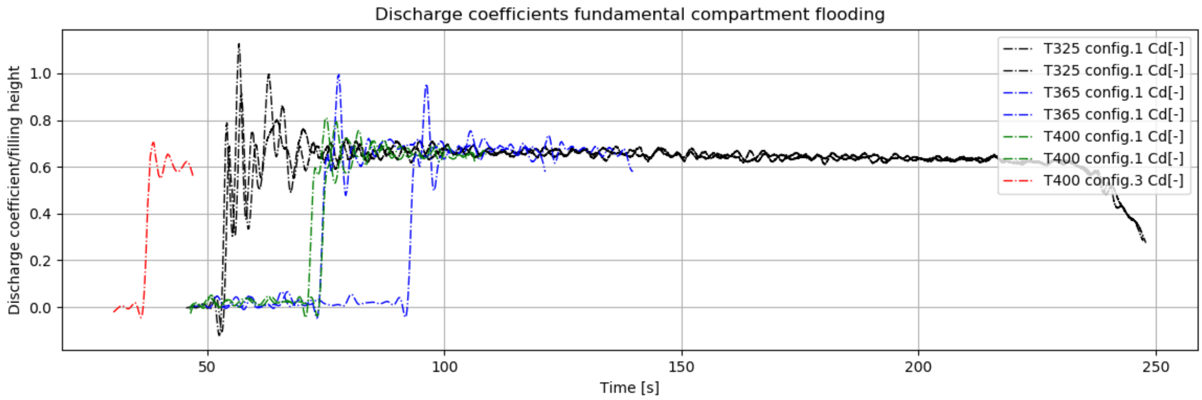

Figure 8-5: Discharge coefficients in at varying depth

Figure 8-6 shows the results for the same tests as in Figure 8-5 for Compartment C (down flooding) The discharge coefficients of the vertical opening are quite similar to each other and to the values found in Compartment A, which range between 0.6 and 0.7

The discharge coefficients of the down flooding opening show a wider spread. Generally, a larger water column results in a lower Cd. The jet of water of the inflow opening, from outside to the upper compartment, was in line with the down flooding opening. Because of this the water is assumed to have a horizontal speed above the down flooding opening.

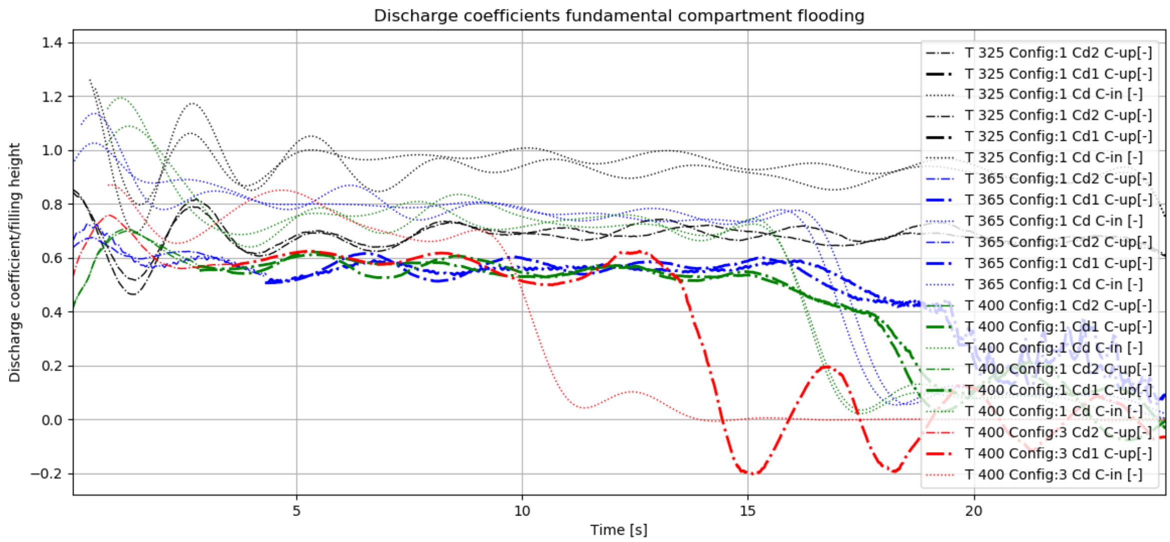

Figure 8-6: Discharge coefficients at varying depth in down flooding compartment

8.2.2 **Impact of heel**

Figure 8-7 shows the discharge coefficient of the down flooding opening at 0 3 and 10 degrees. The results are similar. The Cd is approximated using Equation 1. Hence the small pressure difference at the high and low side of the opening is neglected. The point of rotation was at the inflow opening, hence the mean water level at the down flooding opening is not exactly the same as in the zero heel condition.

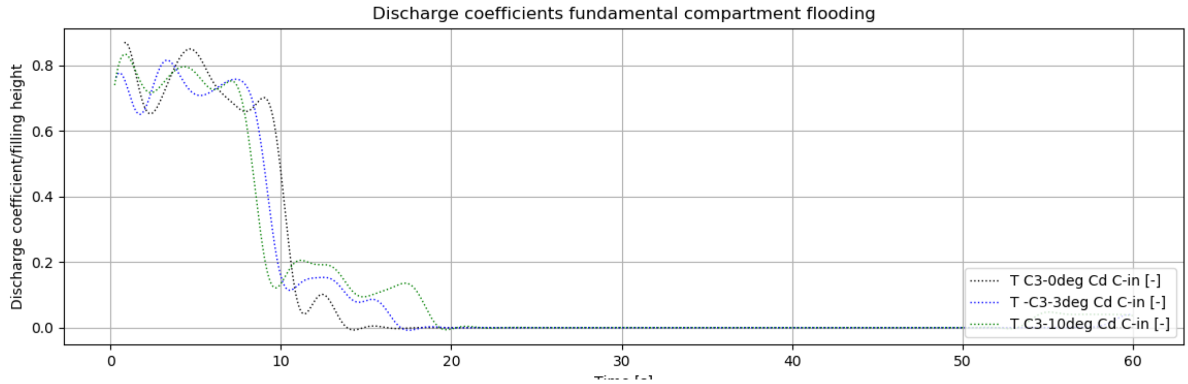

Figure 8-7: Discharge coefficients at heel

8.2.3 **Entrapped air and depressurised conditions**

Figure 8-8 shows the discharge coefficient of the down flooding opening at varying air pressure. The results are presented as a Cd to compare it to other tests, these values should not not used in Bernoulli model. In vented condition the Cd is similar to that at atmospheric pressure. In configuration 4, with closed vent pipe on the lower compartment, the entrapped air escapes through the same opening as the water. This results in a reduced inflow rate. In the graph the measurements are synchronised at the moment the ingress starts. At the start of the ingress the Cd starts at a similar level as the vented condition. After the air is compressed, presumably to a level equal to the water column, the venting starts and reduces the inflow rate. The Cd seems to reduce with the air pressure and the time. This suggests that the flexibility of the air plays a role. In the videos of the tests one can see that the bubbles are larger in depressurised condition. It is likely that this phenomenon is subject to scale effects. The time to flood the compartment was 40 sat atmospheric conditions and reduced to about 25 seconds for the depressurised conditions. Despite the fact that the pressure in the depressurised tests was a factor of two in the two depressurised test, the time to flood was quite similar.

The lower Cd values are an effect of the depressurised conditions which leads to a pressure build up in the compartments. When a Bernoulli model can capture this, the Cd values of fully vented openings should be used, not the lower values measured in this experiment.

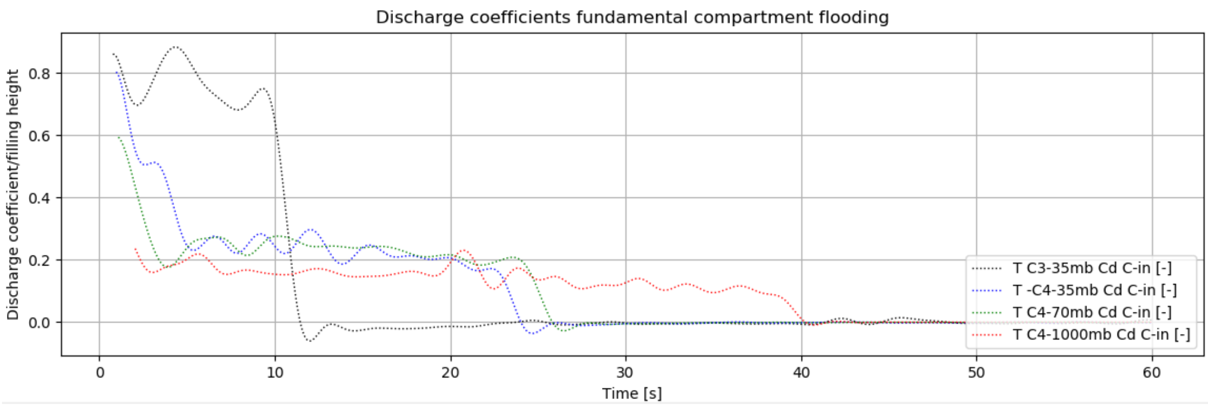

Figure 8-8: Discharge coefficients in at varying air pressure

8.2.4 **Up flooding**

Figure 8-9 shows the Cd of the up-flooding test (30703_03DWB_03_023_002_01). The short duration of the first part of the test, where the lower compartment fills, shows a turbulent flow and hence the derivative of the water level is therefore not a smooth line. At about 3.5 s the up flooding opening is reached and the flow stabilises. The Cd1 C-low is determined by the total flow and the area of the C-low opening. The Cd C-in is determined by the flow rate to the upper compartment and the smaller up-flooding area. The Cd is therefore a combined discharge coefficient for either one of the reference areas.

In the upper compartment the flow is turbulent due to the inflow. It is expected that dissipation of the energy may have an impact on the discharge coefficient.

Note, the discharge coefficients calculated in this section are only indications (verifications) for the flow rate reductions in the multiple compartment set-up. They should not be used in the flooding calculations.

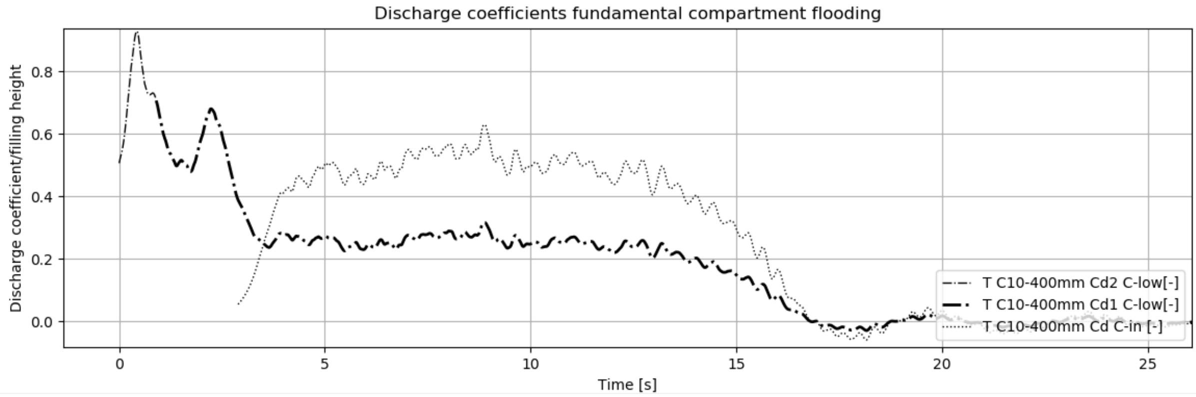

Figure 8-9: Discharge coefficients in up flooding test

8.2.5 **Compartment B**

Figure 8-10 shows the relative wave elevation inside the wing tanks of the cross flooding model. The test was executed at a draught of 400 mm. As expected the smaller duct size shows a larger difference between the two wing tanks. The intact wing tank (I) is oscillating when the outside water level is reached, whereas the breached side (B) shows no oscillations or overshoot. Because of the dynamics, the measurements did not result is a discharge coefficient within a reasonable range.

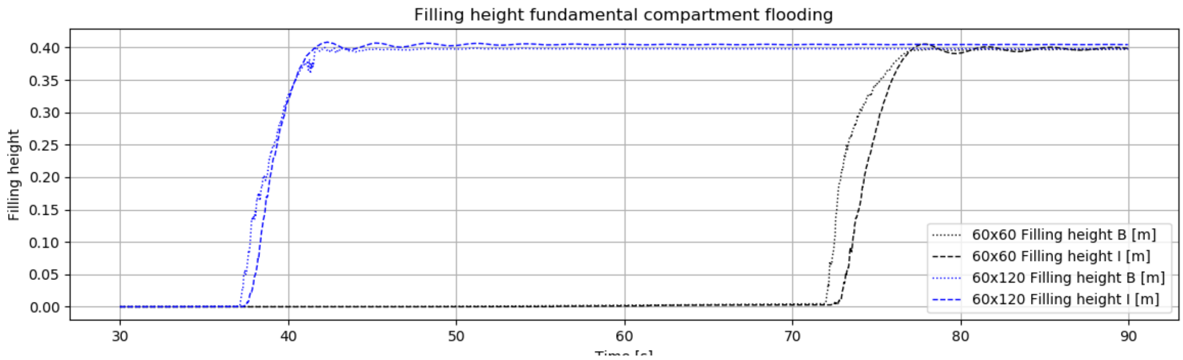

Figure 8-10: Water level in wing tanks

8.3 Regular waves and oscillations

8.3.1 Compartment A

Figure 8-11 compares the measurements in regular waves and in a regular heave motion and a wave amplitude of 40 mm and a period of 2.5 s. The wave elevation outside, the mean wave elevation inside the compartment and its low frequency component (mean water level inside). The relative wave elevation wave measurements are very similar for the waves and heave motions. In both conditions a low frequency increase of the water level can be seen at the start of the waves.

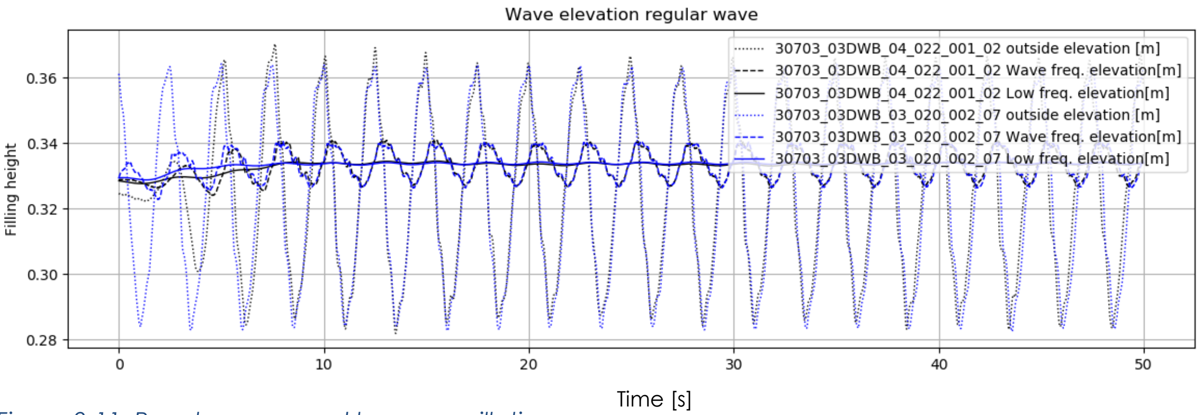

Figure 8-11: Regular wave and heave oscillation

Figure 8-12 shows the mean water level increase for the other test conditions. In shorter and/or steeper waves a larger water level rise was observed. The water level rise in the heave motions seems to be more independent from the oscillation period.

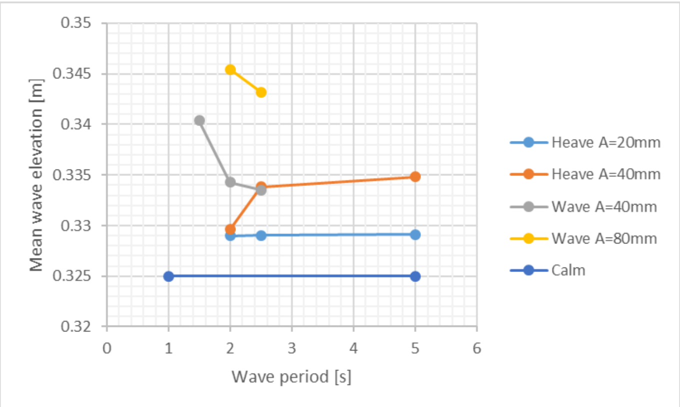

Figure 8-12: Mean water level increase in waves.

8.3.2 Compartment B

Figure 8-13 shows the wave elevation inside the wing tanks in a regular wave of 40 mm for three wave periods. The draught of the model is 400mm and the section area of the duct is 1.125 times larger than the area of the breach. The intact wing tank (I) is denoted with the solid drawn lines, the breached wing tank (B) is drawn with the dotted lines. The wave period has a significant impact on the water elevations:

- At 1.5 s wave period the oscillations at the breached side are about 2 times higher than at the intact side
- At 2 s the oscillations are similar in the two wing tanks
- At 2.5 s the oscillations are two times higher at the intact side than at the breached side. This wave period is becoming close to resonance with the oscillating water column; the natural period is about 3 s.
- There is always a phase shift between the water level in the wing tanks. This points to dynamics, or fluid momentum. The phase difference is frequency dependant. This cannot be captured by a Bernoulli model that will eliminate any phase lag or water height difference between two compartments connected by a cross-duct on the basis of pressure head equalisation.

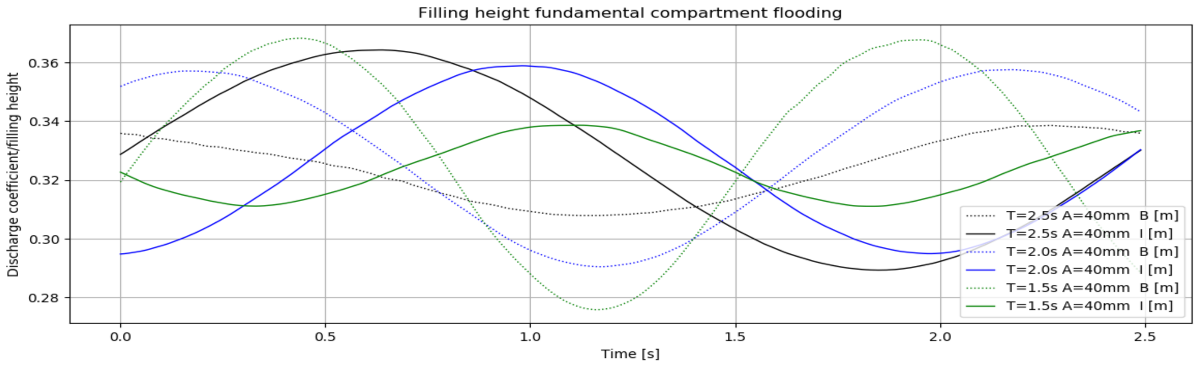

Figure 8-13: Mean water level increase in waves.

9 CONCLUSION

Model tests were conducted with a model consisting of three different elementary flooding compartments to investigate fundamental flooding physics. The goal of the tests was to generate a data set which can be used to benchmark dynamic flooding software. Based on the results of the tests the following conclusions can be drawn:

- The discharge coefficient of the vertical openings was not affected by whether the opening was partly submerged or whether the opening was dry or wet on the outflow side. The values of the discharge coefficient generally ranged between 0.6 and 0.7.
- Horizontal (down flooding) openings resulted in a varying discharge coefficient. The discharge coefficient decreased with the water depth. The discharge coefficient ranged generally between 0.7 and 1.0.
- Because of its dynamic behaviour, the cross flooding compartment was not suitable to determine the discharge coefficient when the cross-duct oscillation was near to or quicker than the model's own natural period. For relatively slow flooding, for instance the flooding under constant pressure head, the calculation resulted in a constant discharge coefficient, hence a Bernoulli method is expected to suffice for this type of flooding

- When the cross-duct undergoes dynamic motions, there is phase leg between the water level in the two compartments. Such cannot be capture by a Bernoulli model unless special additional flow momentum equations are utilized.
- A heel angle up to 10 degrees had no measurable impact on the discharge coefficients.

Appendix I – Tables

Table T 1: Tests at constant speed

Test no	Test type	Configuration	Speed
-	-	-	m/s
30703_03DWB_03_004_004_01	Constant speed	1	10
30703_03DWB_03_004_005_01	Constant speed	1	25
30703_03DWB_03_004_006_01	Constant speed	1	50
30703_03DWB_03_004_008_01	Constant speed	1	100
30703_03DWB_03_023_003_01	Constant speed (outflow)	10	-20

Table T 2: Tests in calm water

Test no	**Test type**	**Config.**	Draught	Heel (Rx)	Trim (Ry)
-	-	-	mm	deg	deg
30703_03DWB_03_004_001_02	Constant draught	1	325	0	0
30703_03DWB_03_004_001_03	Constant draught	1	325	0	0
30703_03DWB_03_004_002_01	Constant draught	1	365	0	0
30703_03DWB_03_004_002_02	Constant draught	1	365	0	0
30703_03DWB_03_004_003_02	Constant draught	1	400	0	0
30703_03DWB_03_004_003_03	Constant draught	1	400	0	0
30703_03DWB_03_005_001_01	Constant draught	2	400	0	0
30703_03DWB_03_005_002_01	Constant draught	2	400	0	0
30703_03DWB_03_006_001_03	Constant draught	3	400	0	0
30703_03DWB_03_007_001_01	Constant draught	4	400	0	0
30703_03DWB_03_008_001_01	Constant draught	5	400	0	0
30703_03DWB_03_009_001_01	Constant draught	6	400	0	0
30703_03DWB_03_010_001_02	Constant draught and heel	3	400	1	0
30703_03DWB_03_010_001_03	Constant draught and heel	3	400	1	0
30703_03DWB_03_011_001_01	Constant draught and heel	3	400	2	0
30703_03DWB_03_011_001_02	Constant draught and heel	3	400	2	0
30703_03DWB_03_012_001_01	Constant draught and heel	3	400	3	0
30703_03DWB_03_012_001_02	Constant draught and heel	3	400	3	0
30703_03DWB_03_013_001_01	Constant draught and heel	3	400	10	0
30703_03DWB_03_013_001_02	Constant draught and heel	3	400	10	0
30703_03DWB_03_014_001_01	Constant draught and trim	3	400	0	2
30703_03DWB_03_014_001_02	Constant draught and trim	3	400	0	2
30703_03DWB_03_015_001_01	Constant draught and heel	3	400	0	-2
30703_03DWB_03_016_001_01	Constant draught and heel	3	300	-10	0
30703_03DWB_03_017_001_03	Constant draught and heel	3	300	10	0
30703_03DWB_03_019_001_01	Constant draught and heel	3	325	10	0
30703_03DWB_03_018_001_01	Constant draught and heel	8	400	10	0
30703_03DWB_03_018_001_02	Constant draught and heel	8	400	10	0
30703_03DWB_03_023_002_01	Constant draught	10	400	0	0

Table T 3: Tests in waves and oscillations

Test no	Test type	Config.	Draught	Oscillation	Wave
-	-	-	mm	-	
30703_03DWB_03_020_002_02	Oscillation	3	325	Heave A=20mm T=1.525s	CALM
30703_03DWB_03_020_002_03	Oscillation	3	325	Heave A=20mm T=2.03s	CALM
30703_03DWB_03_020_002_04	Oscillation	3	325	Heave A=20mm T=2.54s	CALM
30703_03DWB_03_020_002_05	Oscillation	3	325	Heave A=20mm T=5.08s	CALM
30703_03DWB_03_020_002_06	Oscillation	3	325	Heave A=40mm T=2.03s	CALM
30703_03DWB_03_020_002_07	Oscillation	3	325	Heave A=40mm T=2.54s	CALM
30703_03DWB_03_020_002_08	Oscillation	3	325	Heave A=40mm T=5.08s	CALM
30703_03DWB_03_023_001_01	Oscillation	10	325	Heave A=40mm T=2.03s	CALM
30703_03DWB_03_020_002_09	Oscillation	3	325	roll A=2deg T=1.0s	CALM
30703_03DWB_03_020_002_10	Oscillation	3	325	roll A=2deg T=1.5s	CALM
30703_03DWB_03_020_002_11	Oscillation	3	325	roll A=2deg T=2s	CALM
30703_03DWB_03_020_002_12	Oscillation	3	325	roll A=2deg T=2.5s	CALM
30703_03DWB_04_022_001_02	Regular waves	3	325	-	H=0.08m T=2.5s
30703_03DWB_04_022_002_01	Regular waves	3	325	-	H=0.08m T=2s
30703_03DWB_04_022_003_01	Regular waves	3	325	-	H=0.08m T=1.5s
30703_03DWB_04_022_004_03	Regular waves	3	325	-	H=0.16m T=2.5s
30703_03DWB_04_022_005_01	Regular waves	3	325	-	H=0.16m T=2s
30703_03DWB_04_022_006_01	Wave and Osc.	3	325	Heave A=20mm T=1.525s	H=0.08m T=1.5s
30703_04DWB_01_030_001_05	Wave and Osc.	3	325	Heave A=20mm T=2.03s	H=0.08m T=2s
30703_03DWB_04_022_008_02	Wave and Osc.	3	325	Heave A=20mm T=2.54s	H=0.08m T=2.5s
30703_04DWB_01_030_002_01	Wave and Osc.	3	325	Heave A=40mm T=2.03s	H=0.16m T=2s
30703_04DWB_01_030_003_01	Wave and Osc.	3	325	Heave A=40mm T=2.54s	H=0.16m T=2.5s

Table T 4: Tests in depressurised ambient pressure

Test no	Test type	Config.	Draught	Heel (Rx)	Air pressure
-	-	-	mm	deg	mbar
30703_03DWB_05_024_001_01	Depressurised	3	400	0	35
30703_03DWB_05_025_001_01	Depressurised	4	400	0	35
30703_03DWB_05_026_001_01	Depressurised	5	400	0	35
30703_03DWB_05_027_001_02	Depressurised	6	400	0	35
30703_03DWB_05_024_002_01	Depressurised	3	400	10	35
30703_03DWB_05_028_001_01	Depressurised	8	400	10	35
30703_03DWB_05_024_003_01	Depressurised	3	400	0	70
30703_03DWB_05_025_002_01	Depressurised	4	400	0	70
30703_03DWB_05_026_002_01	Depressurised	5	400	0	70
30703_03DWB_05_027_002_01	Depressurised	6	400	0	70
30703_03DWB_05_024_004_01	Depressurised	3	400	10	70
30703_03DWB_05_028_002_01	Depressurised	8	400	10	70

Table T 5: Wave probe location

Description	Name	X-coordinate	Y-coordinate	Z-coordinate	Probe length
	[-]	[mm]	[mm]	[mm]	[mm]
Relative wave probe	REL_ 1	470	13	0	450
Relative wave probe	REL_ 2	470	-38	0	450
Relative wave probe	REL_ 3	470	-233	0	450
Relative wave probe	REL_ 4	470	-428	0	450
Relative wave probe	REL_ 5	350	-233	0	450
Relative wave probe	REL_ 6	350	-428	0	450
Relative wave probe	REL_ 7	230	-38	0	450
Relative wave probe	REL_ 8	230	-233	0	450
Relative wave probe	REL_ 9	230	-428	0	450
Relative wave probe	REL_ 10	120	-38	0	450
Relative wave probe	REL_ 11	120	-428	0	450
Relative wave probe	REL_ 12	0	-78	0	450
Relative wave probe	REL_ 13	0	-388	0	450
Relative wave probe	REL_ 14	-120	-38	0	450
Relative wave probe	REL_ 15	-120	-428	0	450
Relative wave probe	REL_ 16	-230	13	0	450
Relative wave probe	REL_ 17	-230	-38	245	205
Relative wave probe	REL_ 18	-230	-428	245	205
Relative wave probe	REL_ 19	-265	-233	245	205
Relative wave probe	REL_ 20	-350	-148	245	205
Relative wave probe	REL_ 21	-350	-318	245	205
Relative wave probe	REL_ 22	-435	-233	245	205
Relative wave probe	REL_ 23	-470	-38	245	205
Relative wave probe	REL_ 24	-470	-428	245	205
Relative wave probe	REL_ 25	-230	-38	0	233
Relative wave probe	REL_ 26	-230	-428	0	233
Relative wave probe	REL_ 27	-470	-38	0	233
Relative wave probe	REL_ 28	-470	-428	0	233

Acronym:	FLARE
Project full title:	Flooding Accident REsponse
Grant agreement No.	814753
Coordinator:	BALance Technology Consulting GmbH

Deliverable 4.2 – Model tests

Volume 2 – Fundamental Deck Flooding

The project has received funding from the European's Horizon 2020 research and innovation programme (Contract No.: 814753)

Duration: 36 months - Project Start: 01/06/2019 - Project End: 31/05/2022

Deliverable data

Deliverable No	4.2 Volume 2		
Deliverable Title	Model tests: Fundamental Deck Flooding		
Work Package no: title	WP4.2 Model tests		

Dissemination level	Public	**Deliverable type**	Report
Lead beneficiary	HSVA		
Responsible author	R. van Basten Batenburg		
Co-authors	-		
Date of delivery	24-11-2020		
Approved	**Name (partner)**		**Date [DD-MM-YYYY]**
Peer reviewer 1	O. Rognebakke (DNVGL)		13-01-2021
Peer reviewer 2	O. K. Olufsen (DNVGL)		13-01-2021

Document history

Version	**Date**	**Description**
1	**24-11-2020**	Draft
2	**25-11-2020**	For peer review
3	**28-11-2021**	**Final**

The research leading to these results has received funding from the European Union Horizon 2020 Programme under grant agreement n° 814753.
This report reflects only the author's view. INEA is not responsible for any use that may be made of the information it contains.

CONTENTS

List of symbols and abbreviations

DoF	Degree of Freedom
ITTC	International Towing Tank Conference
CFD	Computational Fluid Dynamics
Cd	Discharge coefficient
RAO	Response Amplitude Operator

1 EXECUTIVE SUMMARY

The present report describes a series of model tests that focus on the fundamental flooding of a cruise vessel deck. The tests were executed within the EU FLARE project. The goal of the tests is to provide data for benchmarking and verification of the results of numerical codes that simulate the flooding process.

The model represents a large portion of deck 4 in various degree of complexity of internal compartment division (see Figure 3-3). The following division is made:

- Simplified: Considered to be oversimplified. Even static flooding calculations will use a more detailed compartmentation.
- Intermediate: This is assumed a feasible simplification for dynamic flooding models, a kind of industry standard Static flooding calculation tools will most likely use a somewhat simpler model.
- Detailed: This model was designed to have more detail than what is expected to be required for reliable test results.

The test setup and adopted approaches are described in chapters 3 to 7; a summary of the results including a concise discussion of the results is given in chapter 8. The analysed data and videos are included on a USB stick that is delivered with this report.

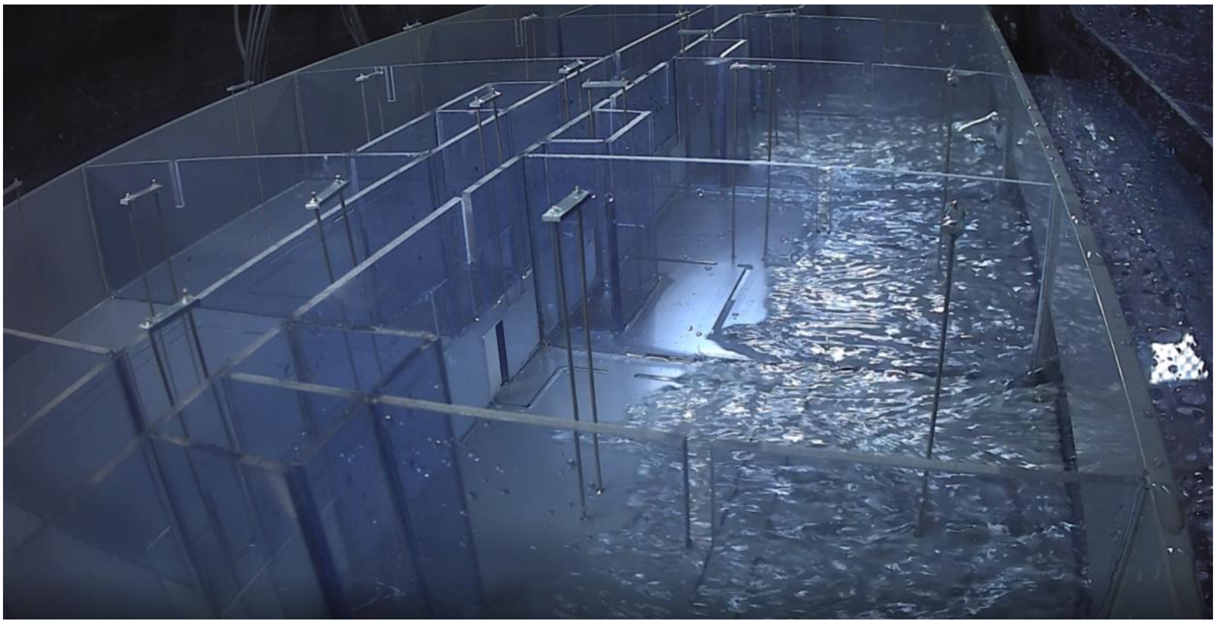

Figure 1-1 Intermediate deck model during a test.

1.1 Problem definition

- In the development and verification of codes that assess flooding of ships it is required to check the sequential flooding of connected compartments.

1.2 Technical approach and work plan

- Three models were created with different levels of modelling detail

- Model tests were executed
- The measurements were analysed and discussed

1.3 Results

- The measurements result is a data set containing a vast amount of measurements that can be used to benchmark the results of flooding simulation codes.

1.4 Conclusions and recommendation

- The discharge coefficient of the internal doors was not affected by whether the opening was partly submerged or whether the opening was dry or wet on the outflow side or whether the outflow opening had a deck at the bottom or not. The values of the discharge coefficient generally ranged between 0.6 and 0.75.
- The detailed model shows a significant delay in the progressive flooding rate compared to the intermediate and simplified model.
- The model test show that the detailed modelling resulted in a longer flooding times and a lower down flooding rates than the intermediate and simplified model.
- The Simplified model showed considerably more sloshing in tests with roll motions than the Intermediate and Detailed models. The simplified model will not represent the floodwater behaviour very well under dynamic conditions.
- Design choices for amount of detail in the flooding model may have significant impact on the outcome of the tests. The model therefore should be tailored to the expected flooding phenomena.

It is recommended to validate the numerical flooding models against the experimental results with the intermediate and detailed modelling. This should be feasible for Bernoulli based models. It is recommended to assess the impact of the modelling on the outcome of the dynamic flooding in calm water and waves, so that within FLARE it is possible to conclude on the modelling impact in time to capsize predictions.

2 INTRODUCTION

2.1 General

The goal of this work package is to provide measurements that can be used to benchmark simulation software that is able to predict the flooding of cruise or Ropax vessels.

Volumes 1 to 5 describe the model tests that are executed for Cruise vessels by MARIN. Volumes 6 to 8 describe the model tests that are executed to investigate the flooding of Ropax vessels. The latter tests were executed by HSVA.

Volumes 1 to 5 describe

1. Fundamental compartment flooding
2. **Deck flooding (present report)**
3. Fundamental hydrodynamics
4. Cruise ship flooding (Part 1)
5. Cruise ship flooding (Part 2)

The model information, measured data and videos of the present model tests are provided on a USB memory stick. An HTML menu provides the metadata of each test and easy access of the results.

2.2 Volume 2

The present report describes a series of model tests that focus on the deck flooding of a section of a cruise vessel. The tests are executed within the EU FLARE project. The goal of the tests is to provide data for benchmarking and verification of the results of numerical codes that simulate the flooding process.

These model tests are executed with a typical deck geometry and various openings/flooding scenarios, which are representative for the sample ship. The impact of three different modelling detail levels is investigated and the results will aid in the design of models in which flooding is considered. The water levels are measured in an area with long corridors with cabins.

The test setup and adopted approaches are described in chapters 3 to 7; a summary of the results including a concise discussion of the results is given in chapter 8. The analysed data and videos are included on a USB stick that is delivered with this report.

The appendices are presented in Annex 1.

Figure 2-1 Model

2.3 FLOODING ACCIDENT RESPONSE

Despite the fact that the maritime sector is continuously investing in increasing and maintaining safety on board ships, additional effort is needed in the pathway towards zero-loss of life and zero-pollution. The highest risk for persons on board ships comes with flooding accidents, but

consequences may be reduced when appropriate actions are taken following such an accident, thus greatly reducing the probability of loss of life or damage to the environment.

The FLARE project will target a risk-based methodology for "live" flooding risk assessment and control, by developing a generic (all incidents in one model) and holistic (active and passive measures) risk model with potential application to new buildings and, which is totally new, to existing ships. Innovative technical solutions in ship concepts and equipment for risk containment and control will be accompanied by proposals for the revision of relevant IMO regulations towards a risk-based approach to contain and control risk in passenger ships from flooding incidents, thereby significantly contributing to the safety of both passenger and ship.

2.4 Project partners

BALance Technology Consulting GmbH, with its headquarters in Bremen, Germany, coordinates the project in close cooperation with the University of Strathclyde, Department of Naval Architecture, Ocean and Marine Engineering. Nineteen other leading maritime stakeholders will contribute to the results of FLARE: Aalto University, Brookes Bell, Bureau Veritas Marine & Offshore, Carnival, Color Line Marine, DNV GL, Fincantieri, Hamburgische Schiffbau-Versuchsanstalt, ICAM Nantes, Lloyd's Register, MARIN, Meyer Werft, Meyer Turku, NAPA, SEA Europe, Chantiers de l'Atlantique, Rina Services, RCCL and Stena Line. This project has received funding from the European Union's Horizon 2020 research and innovation programme under Grant Agreement No 814753.

3 MODEL

3.1 General

The model design is based on deck 4 of the sample cruise ship vessel (Vessel #3). FLARE partner Chantiers de Atlantique provided the vessel design. Figure 3-1 shows the considered model section in the green rectangle on Deck 4. This is chosen because of its typical deck layout for a cruise vessel with relatively small compartments connected at a long hallway at the centre of the ship. Additionally this deck is located at a relatively low position in the vessel, which makes it more likely to be part of a flooding scenario than higher decks.

Figure 3-1 Deck 4 of sample ship 3

Figure 3-2 shows the deck model, which is mounted inside a box to enable the measurement of the weight of the total amount of water on deck. The model was built to a geometric scale ratio of 1 to 60.

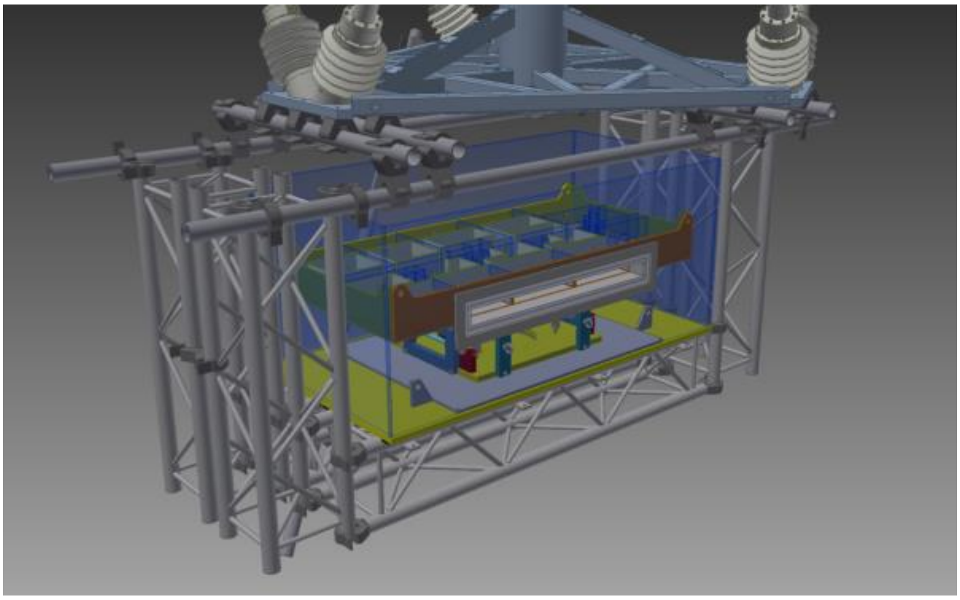

Figure 3-2 Model design

3.2 Modelling detail levels

The deck section was modelled to three levels of detail as shown in Figure 3-3.

From top to bottom the model detailing levels are:

- Simplified: Considered to be oversimplified. Even static flooding calculations will use a more detailed compartmentation.
- Intermediate: This is assumed a feasible simplification for dynamic flooding models, a kind of industry standard Static flooding calculation tools will most likely use a somewhat simpler model.
- Detailed: This model was designed to have more detail than what is expected to be required for reliable test results.

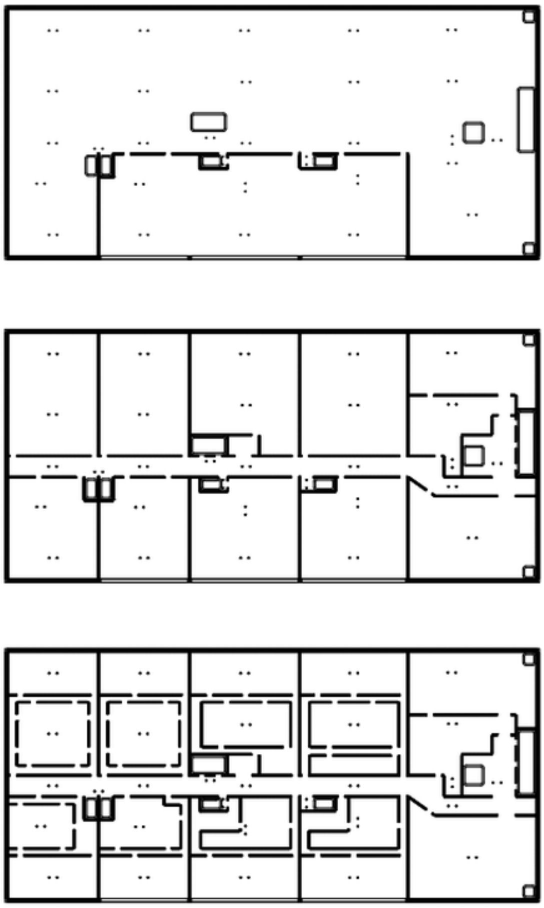

Figure 3-3: Model-detailing levels

To avoid uncertainty about the ventilation of the model, it was not closed at the top. The bulkheads were extended to a height of 6 m to prevent overtopping from one compartment to the other.

The internal bulkheads in the simplified and intermediate model were glued at the deck and therefore are water-tight connections. The detailed model was created by placing extra bulkheads in the intermediate model. These were screw-in connections and were not sealed to establish a complete watertight connection. This is accepted for the present purpose as it is expected that possible leakage though this connections is negligible compared to the water that flows through the many door openings that are modelled in these compartments.

3.3 Openings

The model was able to flood though the openings that are marked red in Figure 3-4. This figure shows the inflow and down flooding openings.

3.3.1 Inflow openings (breach)

Unless stated otherwise all inflow openings were in open condition after the water-tight cover sheet opened at the start of the tests. A selection of tests was executed with only one of the three inflow openings open. Because of the water-tight connection between the outer box and the deck section an extension was made to the starboard side of the deck. The shape of the inflow opening is therefore different from reality. It is recommended to model this extension.

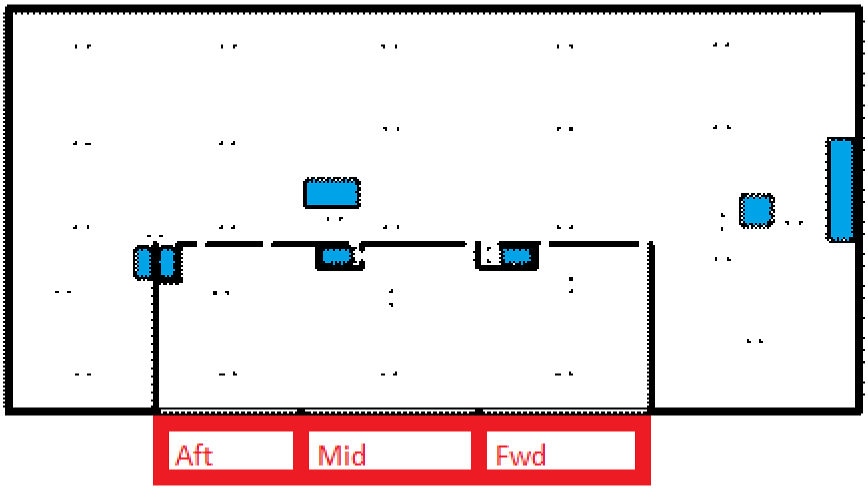

Figure 3-4: Model openings

3.3.2 Inflow openings

Unless stated otherwise the down flooding openings were in closed position. A selection of tests was executed with the down flooding openings open. The down flooding openings are marked blue in Figure 3-4.

4 TEST SETUP AND FACILITY

The tests were executed in the Depressurised Wave Basin (DWB). The DWB is a unique research facility for testing ships and offshore structures in the most realistic operational conditions. The basin is fitted with wave generators and the air pressure in the basin can be decreased to as low as 2.5% of atmospheric pressure. This way many important research aspects concerning cavitation, wave forces, flooding and seakeeping can be studied using a properly-scaled condition for both water and air.

The model was connected to the carriage by a controllable Hexapod. The test setup is shown in Figure 4-1. The test setup was designed in such a way that the tests and drainage of the model could be executed by remote control.

The inflow opening was covered with a water-tight sheet that was removed almost instantly at the start of the test. The cover sheet is shown in closed position, which is the black rectangle at the centre of the box around the deck.

The wave propagation direction was in all tests perpendicular to the inflow openings of the model. The damage was facing the waves.

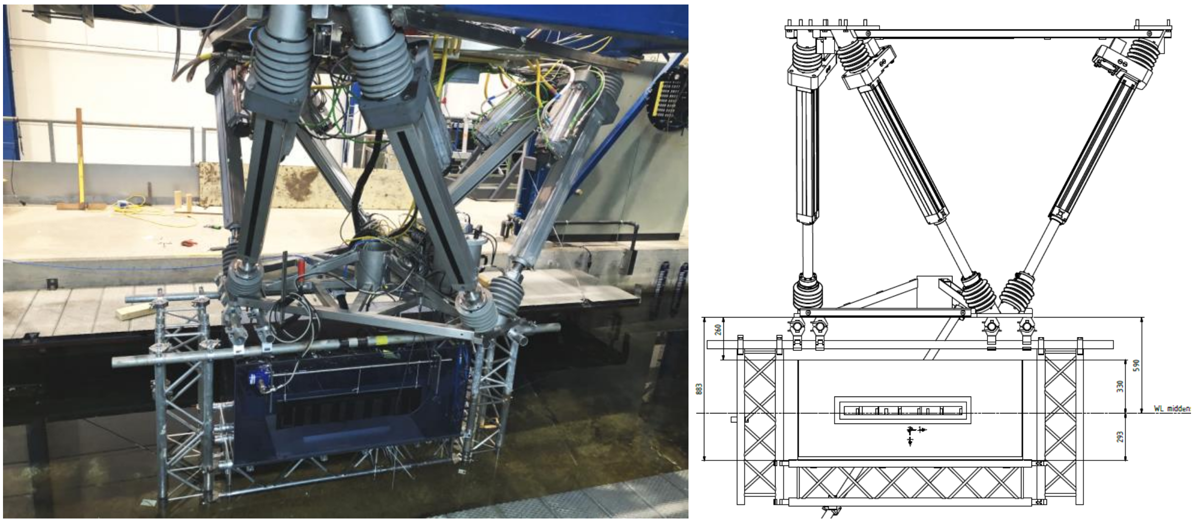

Figure 4-1: Photo and front view of the test setup

5 MEASUREMENTS

The test setup was equipped with:

- An optical tracking system to measure the 6-DOF motions of the model in order to use the actual obtained position of the model in the test. Measured at a frequency of 100 Hz. The motions measured are translated to the origin of the model. Additionally, the motions are translated to the base of each relative wave probe to easily calculate the absolute wave elevation.
- Incident wave height in the basin to measure the incoming wave. Measured at a frequency of 200 Hz (all sample rates in this section are given in model scale).
- The relative wave elevation was measured at 28 locations at a rate of 200 Hz. The locations of the wave probes are given in Figure 5-1and Table T 4 in Appendix I.
- The weight of the incoming water was measured with a force frame between the deck section and the box at a rate of 200 Hz.
- The weight of the total test setup was measured by the force measurement of the Hexapod at a rate of 100 Hz.

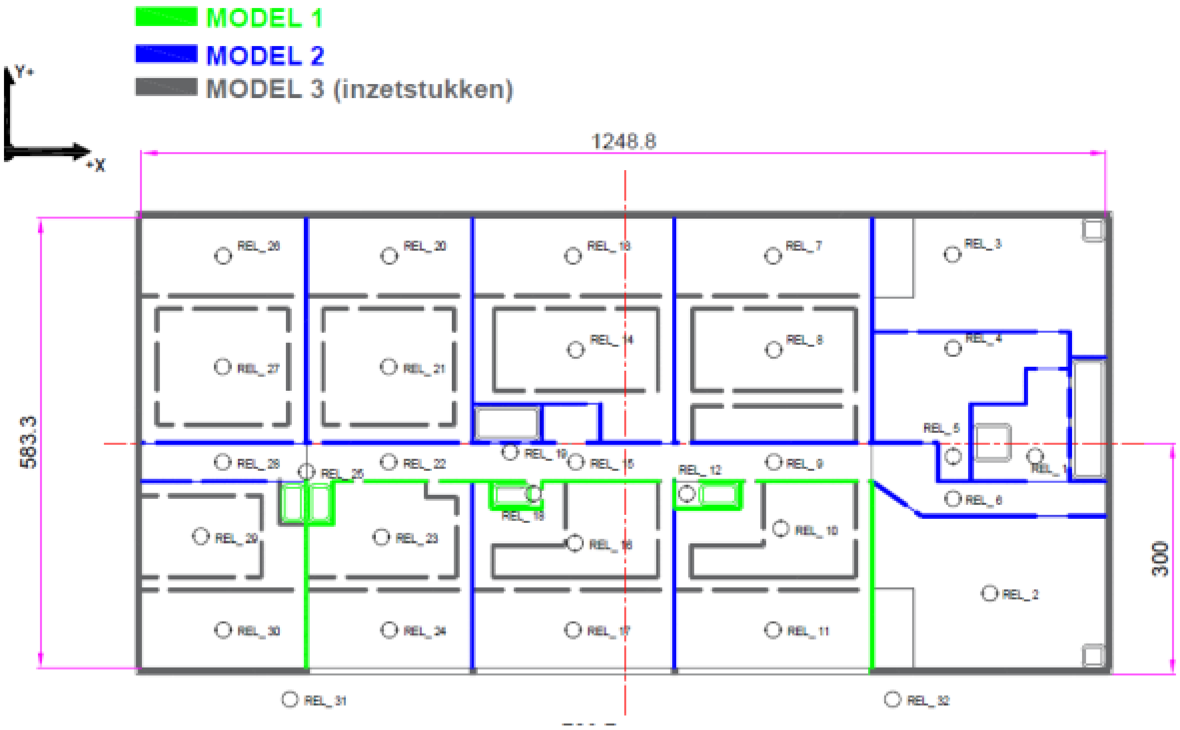

Figure 5-1: Top view of model and wave probe numbers

The wave probe locations are relative to the origin point of the model (see section 6).

6 AXIS SYSTEMS AND SIGN CONVENTION

A right-handed axis system was adopted. The origin of the axis system is shown in Figure 6-1.

The zero position of the axis system is:

- X is at the centre of the deck section (red line in Figure 5-1)
- Y is the centreline of the model
- Z is the top of the deck plating

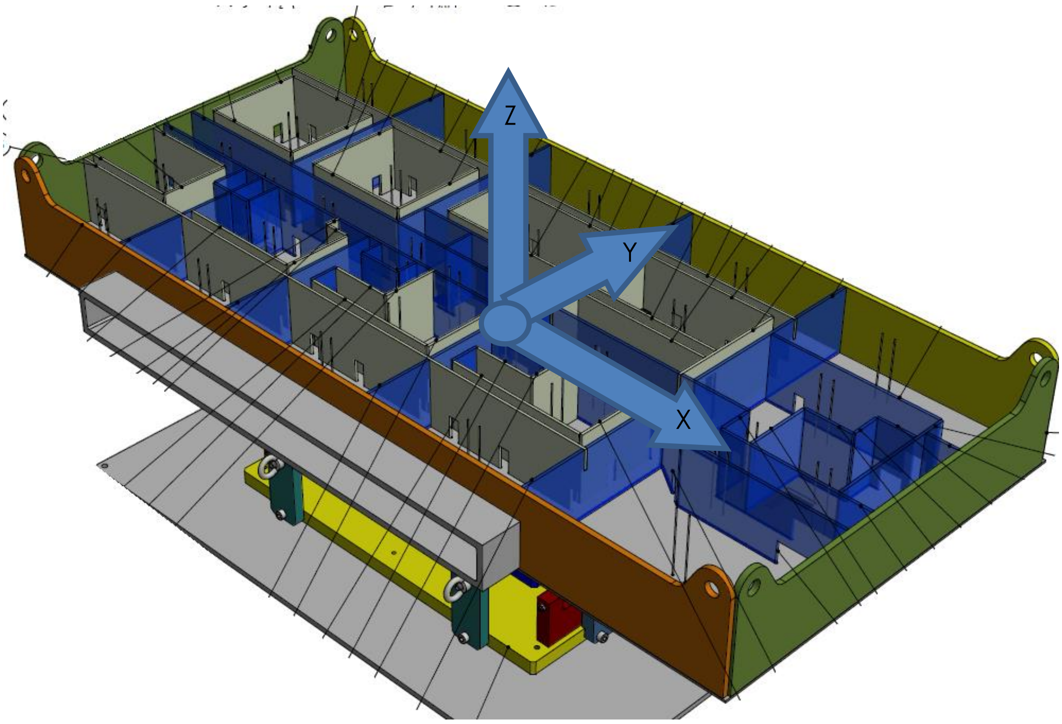

Figure 6-1: Axis system

The start position of the tests relative to the origin is given relative to the calm water level. In tests with roll and pitch motions and oscillations the model rotates around the origin.

Draught is defined as the vertical distance between the origin and calm water level.

7 TEST PROGRAMME AND PROCEDURES

7.1 Summary of the test programme

For each deck model the same set of 21 tests were executed. This set comprised:

- 7 tests at constant draught
- 6 tests at heel or trim
- 2 tests in regular waves
- 4 tests with reduced opening size
- 2 tests with down flooding.

The full test matrix is shown in Table T 1 to Table T 3 in Appendix I.

7.2 Test procedures

Based on experience in previous tests, the resistive wave probes that were present in the model occasionally can show a small drift in the measured values. To avoid this phenomenon affecting the accuracy of the measurements, each wave probe starts at a known zero level and ends at a stationary known end level. The measurements at these levels are used to calibrate the wave probe in each test.

Unless stated otherwise, the following steps were conducted in each test:

A. The model was put into the start position by moving the hexapod. The start position is when the top of the bottom plating is at the calm water level.

B. The measurement starts. The model stays stationary for about 30 seconds to measure the zero level of each sensor.

C. The model descends to the prescribed draught.

D. The model stays stationary for a short moment to measure the start position.

E. Test in waves: The wave generator starts and sufficient time is taken in to account for the wave to reach the model.

F. Oscillating tests: The oscillations start.

G. The magnetic cover sheet opens the inflow openings.

H. The duration of the test was about 5 minutes for tests in waves or oscillations or the test ended after an equilibrium was reached. The wave generator and motions stop.

I. The model stays for a moment (about 30s) at the prescribed draught.

J. The model is prepared for the next test.

8 SUMMARY AND DISCUSSION

This section gives a summary of the test results and comparisons of the three deck sections investigated. The purpose of this section is to give an idea of the implications for choices that are to be made in the design of a deck level.

For benchmarking purposes the flooding sequence can be compared to the results of simulations. This is not part of this report.

8.1 Discharge coefficients

The discharge coefficients of the internal door openings are determined in a separate test using the lower part of Compartment C and described in Volume 1 of this report.

For some tests the resulting discharge coefficients are compared. The discharge coefficient is calculated by Equation 1.

Equation 1: Discharge coefficient for vertical openings

$$Cd = \frac{Q}{\frac{2}{3} b\sqrt{2g}(h_b^{\frac{3}{2}} - h_t^{\frac{3}{2}})}$$

Where:

Q is the inflow of water
b is the width of the opening
g is the gravitational acceleration
h_b is the pressure head of the bottom of the opening
h_t is the pressure head of the top of the opening

Two door sizes were taken to determine discharge coefficient:

- Wide 47x34mm – test number: 30703_15SMB_01_001_004_01
- Narrow 17x34mm – test number: 30703_15SMB_01_001_003_01(

To check if the presence of a deck has an impact we mounted a balcony (100mm x 50mm) at the outflow side; this test is denoted as Narrow_b. This setup is shown in Figure 8-1, the balcony is marked with a green outline and the narrow outflow opening is marked yellow. This setup is used in test number: 30703_15SMB_01_001_005_01.

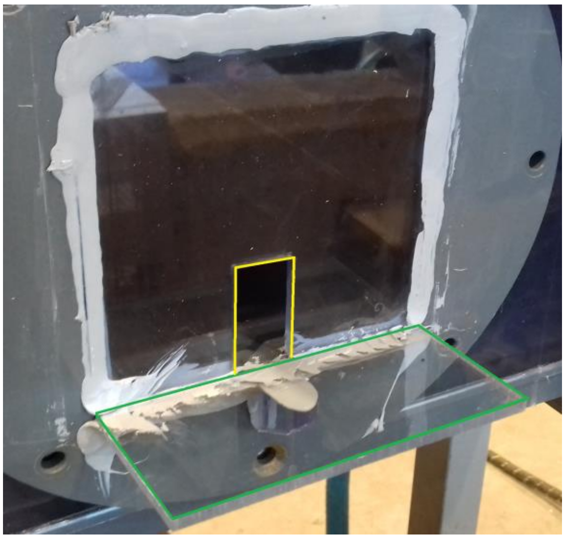

Figure 8-1: Outflow opening with balcony 'narrow_b'

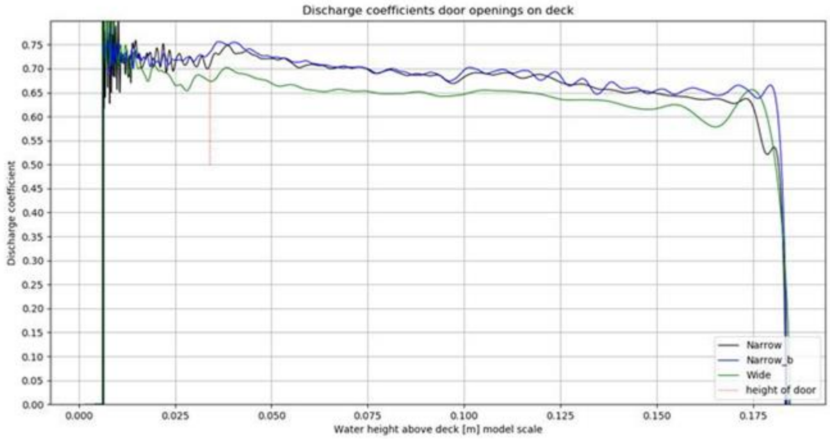

Figure 8-2: Discharge coefficient for internal doors.

Figure 8-2 shows the discharge coefficient against the water level on deck during a discharge measurement. The Cd increases somewhat towards lower water levels. As the deck height in the model is only 50mm the figures imply a Cd between 0.72 and 0.75 for the narrow openings and 0.66 and 0.70 for the wide opening. The balcony at the outflow side did not have an impact on the Cd.

8.2 Tests at constant draught

Figure 8-3 shows the water level in metres above deck for “Rel 3” and “Rel 15”, against the time in seconds. The water depth is 1.8m. The measurements are shown in black, blue and green for the Detailed (D) Intermediate (I) and Simplified (S) model respectively.

The location of Rel 15 was chosen to demonstrate the water level at the centre of the hallway though which the water is distributed through the model. Rel 3 is at one of the locations that are at the end of the flooding sequence. Plots of measurements at other locations are attached as Appendix II.

At Rel 15, the water level in the Simplified and Intermediate models are relatively similar; at first, the water level in the intermediate model is higher, water needs time to leave the water through the door openings. At a level about 1.5m, the Simplified model shows higher water levels.

At Rel 3, it can be seen that the delay where the compartment starts to fill increases with the amount of detail. The slope of the curve is similar for all tests.

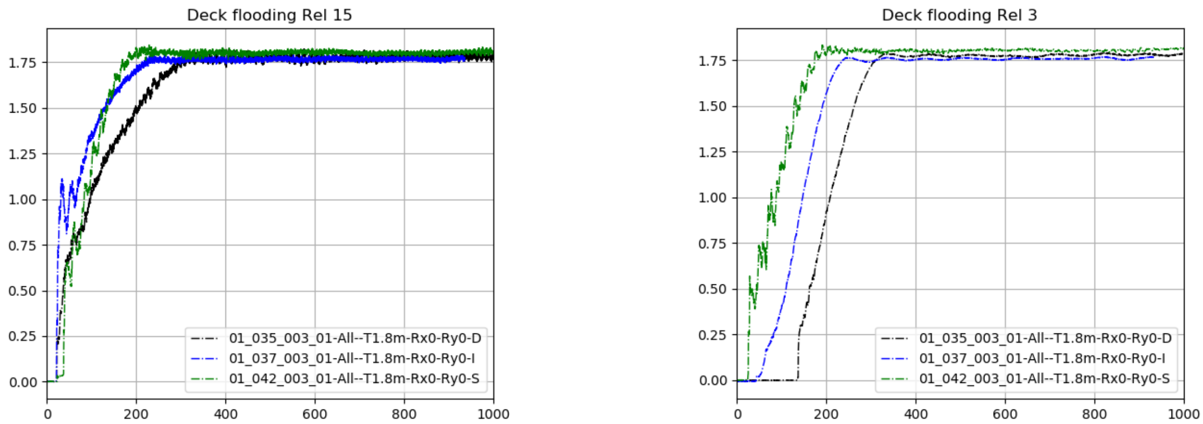

Figure 8-3: Water level above deck T=1.8m for "Rel 15" and "Rel 3"

Figure 8-4 shows the total weight of water on the deck section in kN, at a draught of 1.8m. The total weight of the water is similar for the Intermediate and Simplified model. The Detailed model requires about 50% more time to fill. Concerning the amount of water on the deck, the Intermediate model seems not to have an added value compared to the Simplified model, but the water distribution over the deck will be different (see Rel 3 differences) The detailed deck clearly floods at a lower rate.

The results presented on the left and right are repeat tests that were executed in this condition; the results were almost identical.

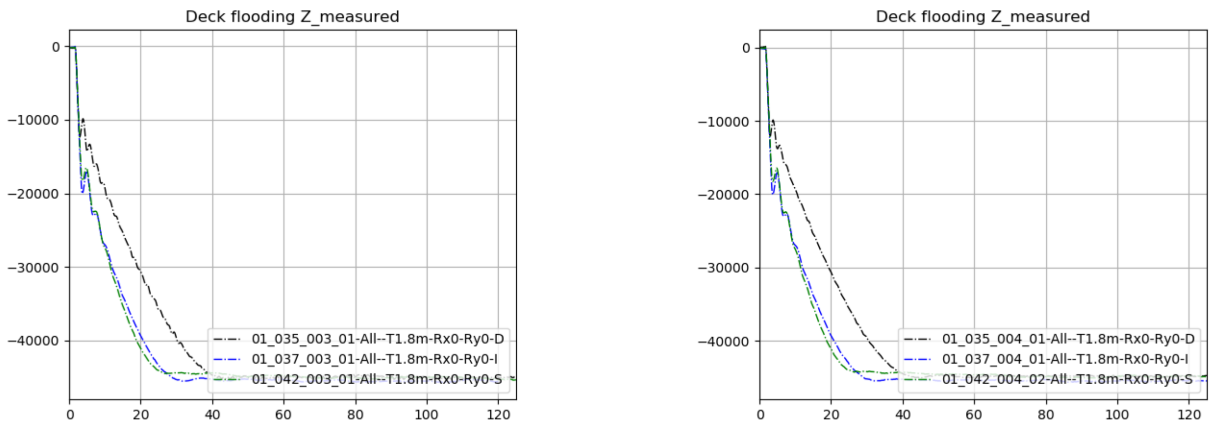

Figure 8-4: Total weight of water T=1.8m

At the lowest water level of 0.6m, the surface tension in the water starts to play a significant role in the test result.

8.3 Test at heel or trim

Figure 8-5 shows, similar to Figure 8-3, the water level at the locations of Rel 3 and Rel 15. This test was at a higher draught and at a 5 degree heel to port. Because of the higher draught and the heel, more water enters the deck, whereas the submerged part of the opening is similar at the edge of the extension of the deck. Again, the water levels at Rel 15 are similar for the Simplified and Intermediate models. The water level in the detailed model rises more slowly. At Rel 3, the ingress decreased with the amount of detail. However, the results of the Intermediate model are closer to those of the Simplified model than to those of the Detailed model.

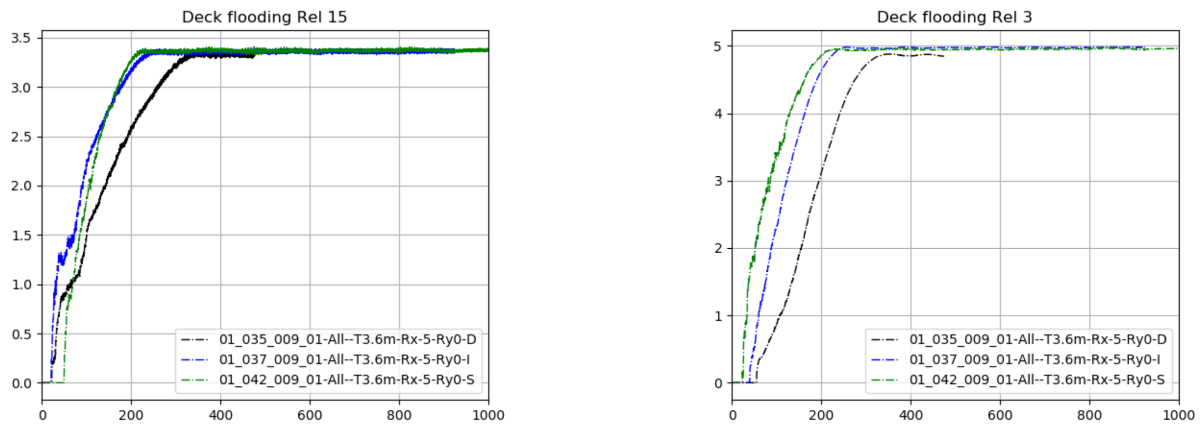

Figure 8-5: Water level above deck for "Rel 15" and "Rel 3" T=3.6m at 5 degree heel to port.

8.4 Tests in roll oscillations

Figure 8-6 shows the relative wave elevation with a roll oscillation of 2.5 deg and a period of 20s the roll motion is similar to the ship's natural period of roll. Figure 8-7 shows a part of the time trace for one stationary oscillation between 600 and 620 s. In the simplified model, the measurements show significant sloshing above the deck level. The water elevations in the Detailed and Intermediate model are similar. In theory, depending on the phasing of the bore of the wave, which is running on the deck, the mean water level can be affected. The mean water level at Rel 3 shows a slight increase of the mean water level compared to the calm water level. This phenomenon is expected to be frequency dependent; this was not investigated in the present tests.

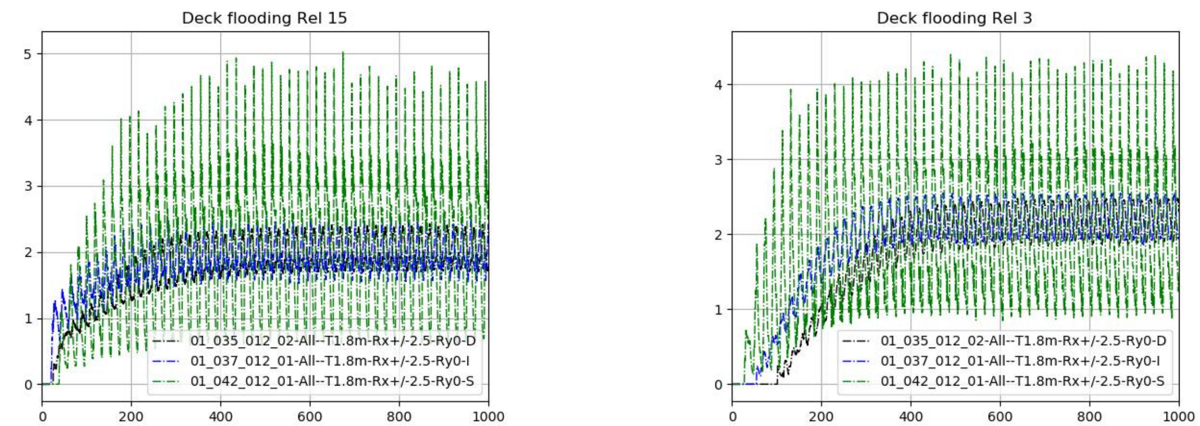

Figure 8-6 Water level above deck for "Rel 15" and "Rel 3" T=1.8 m at 2.5 degree roll oscillation.

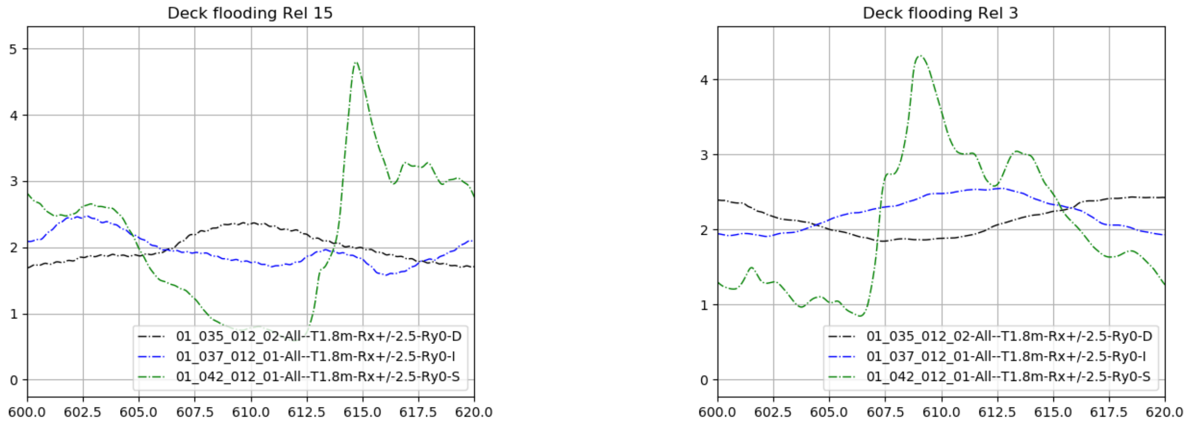

Figure 8-7 Water level above deck for "Rel 15" and "Rel 3" T=1.8 m at 2.5 degree roll oscillation for one oscillation

8.5 Tests in regular waves

Figure 8-8 shows the wave elevations at the two selected locations with the model in a regular wave with a height of 4 m and a period of 11.6 seconds. The measurements at Rel 3 show a clear increase of the mean water level, which is highest for the Detailed model. The relative wave elevations on the decks were highest at Rel 15 in the Detailed model.

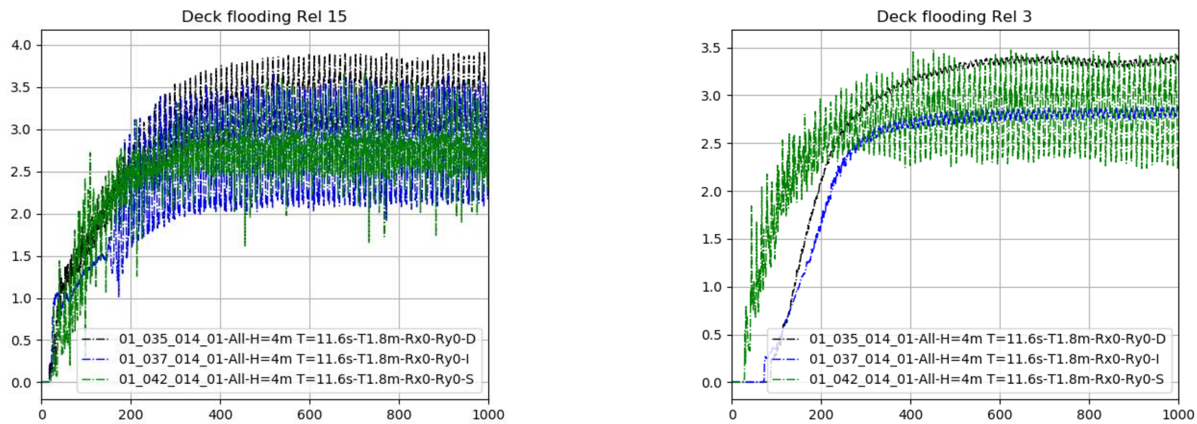

Figure 8-8 Water level above deck for "Rel 15" and "Rel 3" T=1.8 m in regular waves

8.6 Reduced opening size

Figure 8-9 shows the relative wave elevation for the two locations with a reduced breach size. With only the middle part opened the size is about one third of the total opening. In contrast with the results of the tests of the large opening, the results of the Intermediate model are closer to those of the Detailed model than those of the Simplified model.

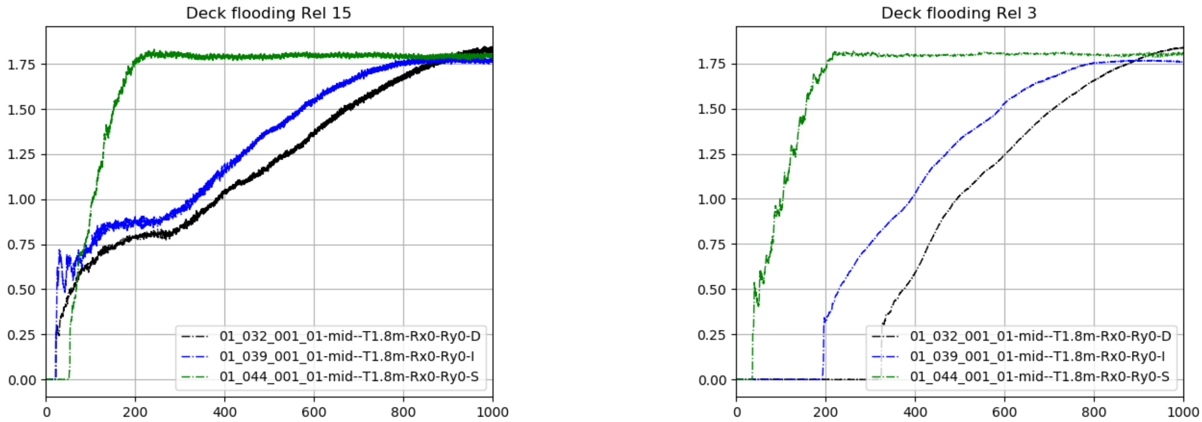

Figure 8-9 Water level above deck for "Rel 15" and "Rel 3" T=1.8 m - reduced opening size.

The total weight on the deck shows the same result; see Figure 8-9. The Simplified model is completely filled at 200 seconds whereas the Intermediate and Detailed model need 4 to 6 times more time respectively.

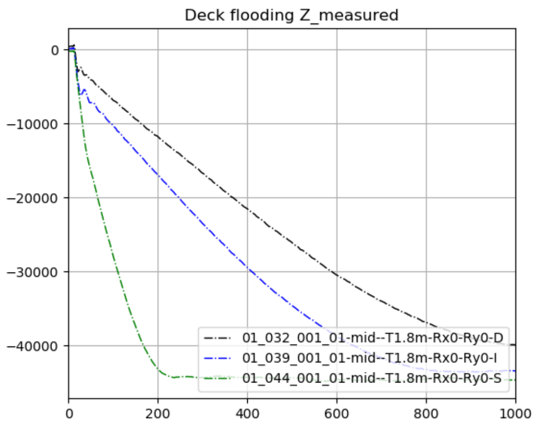

Figure 8-10: Total weight of water T=1.8m - reduced opening size.

If transverse bulkheads are added at the fore and aft side of the breach in the Simplified model, the results are expected to be similar to those of the Intermediate model.

8.7 Tests with down flooding

Figure 8-11 shows the total vertical load on the Hexapod. This measures the complete weight of the test setup. Therefore, this measurement can be used to measure the amount of water that flows inside the box around the deck section. The results are shown for two test conditions: at 1.8 m draught without heel and at the same draught with 5 degree heel to starboard (breach deeper into the water).

In the two conditions tested, the down flooding rate decreases with the level of modelling detail. The difference between the Intermediate and the Simplified model is less than half the difference between the Intermediate and Detailed model.

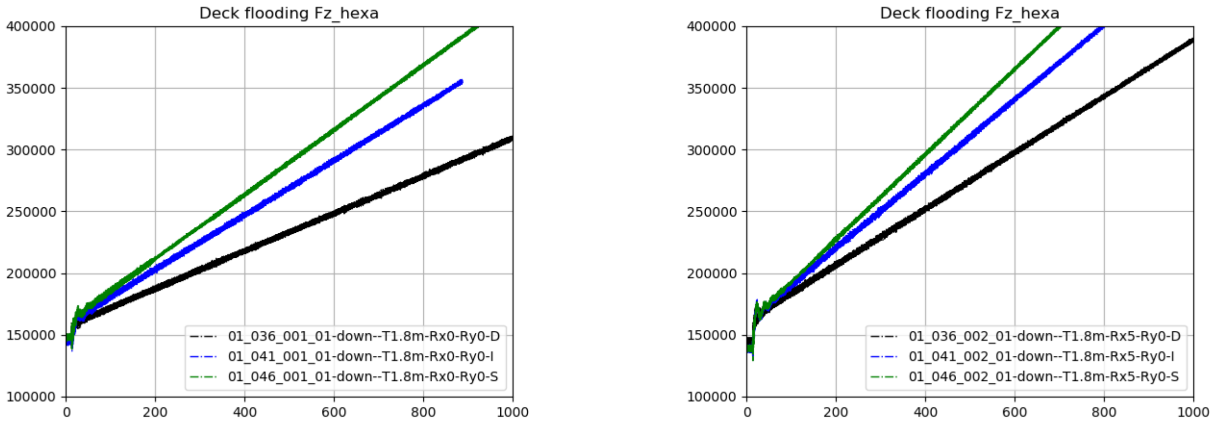

Figure 8-11: Vertical load on Hexapod in down flooding test.

9 CONCLUSION

Model tests were conducted with a model with three realisations of a deck section of a cruise vessel, a Detailed, Intermediate and a Simplified model.

Based on the results of the tests the following conclusions can be drawn:

- The discharge coefficient of the internal doors was not affected whether the opening was partly submerged or whether the opening was dry or wet on the outflow side or whether the outflow opening had a deck at the bottom or not. The values of the discharge coefficient generally ranged between 0.6 and 0.75.
- In various static test conditions, the water height at specific points is comparable between the intermediate and simplified model for the larger damage opening.
- The detailed model shows a significant delay in the progressive flooding rate compared to the intermediate model for the larger damage opening.
- The Simplified model showed considerably more sloshing in tests with roll motions than the Intermediate and Detailed models. The simplified model will not represent the floodwater behaviour very well under dynamic conditions.
- Design choices for amount of detail in the flooding model may have significant impact on the outcome of the tests.

It is recommended to validate the numerical flooding models against the experimental results with the intermediate and detailed modelling. This should be feasible for Bernoulli based models. It is recommended to assess the impact of the modelling on the outcome of the dynamic flooding in calm water and waves, so that within FLARE it is possible to conclude on the modelling impact in time to capsize predictions.

Appendix I – Tables

Table T 1: Tests with simplified model

Simplified

Test no	Openings	Waves	Draught	Heel	Trim
-		-	[m]	[deg]	[deg]
30703_05DWB_01_042_001_01	All	CALM	0.6	0	0
30703_05DWB_01_042_002_01	All	CALM	1.2	0	0
30703_05DWB_01_042_003_01	All	CALM	1.8	0	0
30703_05DWB_01_042_004_02	All	CALM	1.8	0	0
30703_05DWB_01_042_005_01	All	CALM	2.4	0	0
30703_05DWB_01_042_006_01	All	CALM	3.0	0	0
30703_05DWB_01_042_007_01	All	CALM	3.6	0	0
30703_05DWB_01_042_008_01	All	CALM	1.8	5	0
30703_05DWB_01_042_009_01	All	CALM	3.6	-5	0
30703_05DWB_01_042_010_01	All	CALM	1.8	0	2.5
30703_05DWB_01_042_011_01	All	CALM	1.8	5	-2.5
30703_05DWB_01_042_012_01	All	CALM	1.8	+/-2.5	0
30703_05DWB_01_042_013_01	All	CALM	1.8	+/-5.0	0
30703_05DWB_01_042_014_01	All	H=7m T=15.5s	1.8	0	0
30703_05DWB_01_042_015_01	All	H=4m T=11.6s	1.8	0	0
30703_05DWB_01_043_001_01	aft	CALM	1.8	0	0
30703_05DWB_01_044_001_01	mid	CALM	1.8	0	0
30703_05DWB_01_044_002_01	mid	CALM	1.8	0	0
30703_05DWB_01_045_001_01	fwd	CALM	1.8	0	0
30703_05DWB_01_046_001_01	down	CALM	1.8	0	0
30703_05DWB_01_046_002_01	down	CALM	1.8	5	0

Table T 2: Tests with intermediate model

Intermediate

Test no	Openings	Waves	Draught	Heel	Trim
-		-	[m]	[deg]	[deg]
30703_05DWB_01_037_001_01	All	CALM	0.6	0	0
30703_05DWB_01_037_002_01	All	CALM	1.2	0	0
30703_05DWB_01_037_003_01	All	CALM	1.8	0	0
30703_05DWB_01_037_004_01	All	CALM	1.8	0	0
30703_05DWB_01_037_005_01	All	CALM	2.4	0	0
30703_05DWB_01_037_006_01	All	CALM	3.0	0	0
30703_05DWB_01_037_007_01	All	CALM	3.6	0	0
30703_05DWB_01_037_008_02	All	CALM	1.8	5	0
30703_05DWB_01_037_009_01	All	CALM	3.6	-5	0
30703_05DWB_01_037_010_01	All	CALM	1.8	0	2.5
30703_05DWB_01_037_011_01	All	CALM	1.8	5	-2.5
30703_05DWB_01_037_012_01	All	CALM	1.8	+/-2.5	0
30703_05DWB_01_037_013_03	All	CALM	1.8	+/-5.0	0
30703_05DWB_01_037_014_01	All	H=7m T=15.5s	1.8	0	0
30703_05DWB_01_037_015_01	All	H=4m T=11.6s	1.8	0	0
30703_05DWB_01_038_001_01	aft	CALM	1.8	0	0
30703_05DWB_01_039_001_01	mid	CALM	1.8	0	0
30703_05DWB_01_039_002_01	mid	CALM	1.8	0	0
30703_05DWB_01_040_001_01	fwd	CALM	1.8	0	0
30703_05DWB_01_041_001_01	down	CALM	1.8	0	0
30703_05DWB_01_041_002_01	down	CALM	1.8	5	0

Table T 3: Tests with detailed model

Detailed

Test no	Openings	Waves	Draught	Heel	Trim
-		-	[m]	[deg]	[deg]
30703_05DWB_01_035_001_03	All	CALM	0.6	0	0
30703_05DWB_01_035_002_01	All	CALM	1.2	0	0
30703_05DWB_01_035_003_01	All	CALM	1.8	0	0
30703_05DWB_01_035_004_01	All	CALM	1.8	0	0
30703_05DWB_01_035_005_01	All	CALM	2.4	0	0
30703_05DWB_01_035_006_01	All	CALM	3.0	0	0
30703_05DWB_01_035_007_01	All	CALM	3.6	0	0
30703_05DWB_01_035_008_01	All	CALM	1.8	5	0
30703_05DWB_01_035_009_01	All	CALM	3.6	-5	0
30703_05DWB_01_035_010_01	All	CALM	1.8	0	2.5
30703_05DWB_01_035_011_02	All	CALM	1.8	5	-2.5
30703_05DWB_01_035_012_02	All	CALM	1.8	+/-2.5	0
30703_05DWB_01_035_013_14	All	CALM	1.8	+/-5.0	0
30703_05DWB_01_035_014_01	All	H=7m T=15.5s	1.8	0	0
30703_05DWB_01_035_015_01	All	H=4m T=11.6s	1.8	0	0
30703_05DWB_01_033_001_01	aft	CALM	1.8	0	0
30703_05DWB_01_032_001_01	mid	CALM	1.8	0	0
30703_05DWB_01_032_002_01	mid	CALM	1.8	0	0
30703_05DWB_01_034_001_01	fwd	CALM	1.8	0	0
30703_05DWB_01_036_001_01	down	CALM	1.8	0	0
30703_05DWB_01_036_002_01	down	CALM	1.8	5	0

Table T 4: Wave probe locations

Sensor	Signal name	X	Y	Zbottom	Ztop
-	-	[m]	[m]	[m]	[m]
Relative wave probe	REL_ 1	31.92	-1.08	0	7.2
Relative wave probe	REL_ 2	28.44	-11.64	0	7.2
Relative wave probe	REL_ 3	25.5	14.64	0	7.2
Relative wave probe	REL_ 4	25.56	7.32	0	7.2
Relative wave probe	REL_ 5	25.56	-1.08	0	7.2
Relative wave probe	REL_ 6	25.56	-4.38	0	7.2
Relative wave probe	REL_ 7	11.58	14.52	0	7.2
Relative wave probe	REL_ 8	11.64	7.2	0	7.2
Relative wave probe	REL_ 9	11.64	-1.5	0	7.2
Relative wave probe	REL_ 10	12.18	-6.66	0	7.2
Relative wave probe	REL_ 11	11.58	-14.52	0	7.2
Relative wave probe	REL_ 12	4.86	-3.96	0	7.2
Relative wave probe	REL_ 13	-3.96	14.52	0	7.2
Relative wave probe	REL_ 14	-3.72	7.2	0	7.2
Relative wave probe	REL_ 15	-3.72	-1.5	0	7.2
Relative wave probe	REL_ 16	-3.78	-7.8	0	7.2
Relative wave probe	REL_ 17	-3.96	-14.52	0	7.2
Relative wave probe	REL_ 18	-7.02	-3.96	0	7.2
Relative wave probe	REL_ 19	-8.82	-0.72	0	7.2
Relative wave probe	REL_ 20	-18.24	14.52	0	7.2
Relative wave probe	REL_ 21	-18.3	5.88	0	7.2
Relative wave probe	REL_ 22	-18.3	-1.5	0	7.2
Relative wave probe	REL_ 23	-18.84	-7.32	0	7.2
Relative wave probe	REL_ 24	-18.24	-14.52	0	7.2
Relative wave probe	REL_ 25	-24.66	-2.28	0	7.2
Relative wave probe	REL_ 26	-31.14	14.52	0	7.2
Relative wave probe	REL_ 27	-31.2	5.88	0	7.2
Relative wave probe	REL_ 28	-31.2	-1.5	0	7.2
Relative wave probe	REL_ 29	-32.88	-7.26	0	7.2
Relative wave probe	REL_ 30	-31.14	-14.52	0	7.2
Relative wave probe	REL_ 31	-25.98	-19.92	0	7.2
Relative wave probe	REL_ 32	20.88	-19.92	0	7.2
Force frame 6DOF	6CFF	0	0	-9.78	[-]

Acronym: FLARE
Project full title: Flooding Accident REsponse
Grant agreement No. 814753
Coordinator: BALance Technology Consulting GmbH

Deliverable 4.2 – Model tests

Volume 3 – Cruise ship hydrodynamics

The project has received funding from the European's Horizon 2020 research and innovation programme (Contract No.: 814753)

Deliverable data

Deliverable No	4.2 Volume 3		
Deliverable Title	Model tests: Cruise ship hydrodynamics		
Work Package no: title	WP4.2 Model tests		

Dissemination level	Public	**Deliverable type**	Report
Lead beneficiary	HSVA		
Responsible author	R. van Basten Batenburg		
Co-authors	-		
Date of delivery	30-11-2020		
Approved	**Name (partner)**		**Date [DD-MM-YYYY]**
Peer reviewer 1	O. Rognebakke (DNVGL)		13-01-2021
Peer reviewer 2	O. K. Olufsen (DNVGL)		13-01-2021

Document history

Version	**Date**	**Description**
1	**26 Nov. 20**	Draft
2	**30 Nov**	For peer review
3	**28-11-2021**	Final

The research leading to these results has received funding from the European Union Horizon 2020 Programme under grant agreement n° 814753.
This report reflects only the author's view. INEA is not responsible for any use that may be made of the information it contains.

CONTENTS

List of symbols and abbreviations

Cd	Discharge coefficient
CoG	Centre of Gravity
DoF	Degree of Freedom
ITTC	International Towing Tank Conference
CFD	Computational Fluid Dynamics
GM	Metacentric height
RAO	Response Amplitude Operator
TD	Time domain

1 EXECUTIVE SUMMARY

The present report describes a series of model tests that focus on the hydrodynamics of a cruise vessel in damaged condition that were executed within the EU FLARE project. The goal is to provide data for benchmarking and verification of the results of numerical codes that simulate the flooding process.

The test setup and adopted approaches are described in chapters 3 to 7; a summary of the results including a concise discussion of the results is given in chapter 8. The analysed data and videos are included on a USB stick that is delivered with this report.

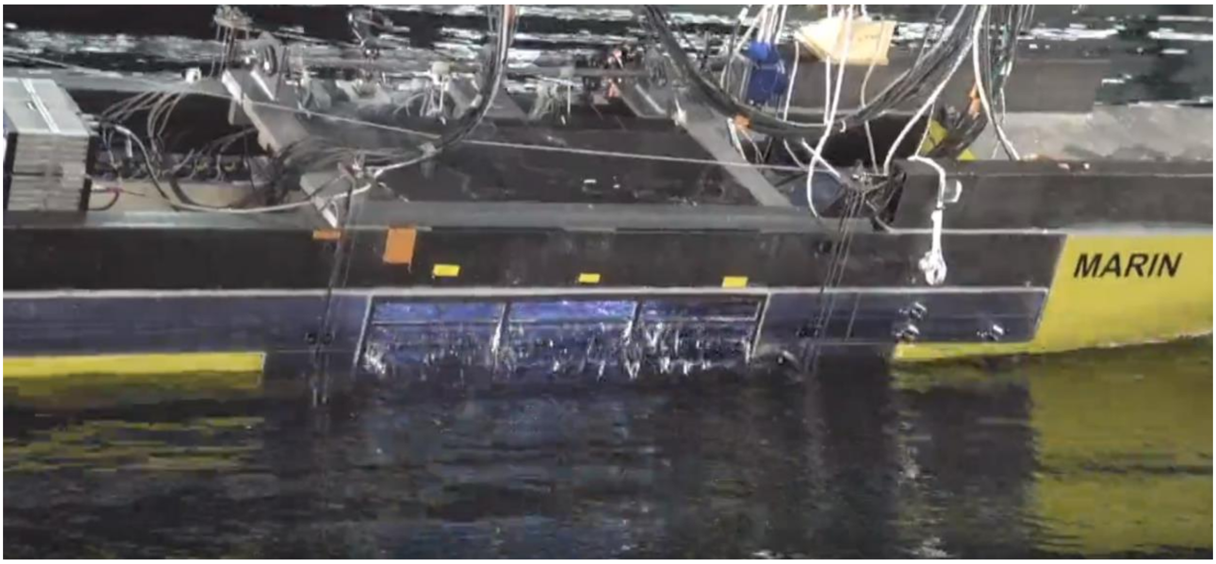

Figure 1-1 Model in irregular waves

1.1 Problem definition

- In the development and verification of codes that assess flooding of ships it is required to benchmark the result of numerical simulations and to gain insight into the hydrodynamics of a vessel which is in damaged condition.

1.2 Technical approach and work plan

- A ship model with a floodable internal geometry was built to simulate a given flooding scenario
- Basin tests were executed in calm water and a selection of irregular waves for a range of metacentric heights
- The measurements were analysed and discussed

1.3 Results

- The measurements contribute to the understanding of the most important differences in the hydrodynamics of a cruise vessel in intact and damaged condition. These results can be used to benchmark the results of flooding simulations

1.4 Conclusions

- The analysis of the roll decay tests for the damaged ship did not result in consistent damping values suitable for numerical simulations
- It is recommended to use intact roll damping coefficients in numerical simulations and to assume that the flood water dynamics change the roll behaviour "as in the model basin". This needs validation.
- The analysis of the roll decay tests did not result in consistent damping values.
- The additional roll damping due to the breach openings was very similar for all configurations with two of the four breaches open. The exact location of the compartments did not seem to have an impact.
- The roll damping in transverse drift increased with the square of the drift speed. At a drift speed of 4 knots, the roll damping was twice the roll damping at zero speed.
- At zero drift, the RAO for roll in beam seas reduced by about 40% with all breaches open.
- In irregular seas, the damage openings in the model can reduce the roll motions by about 40% in beam seas. On the other hand, the roll in damaged condition in head seas was significantly increased to an even higher rms value than in beam seas.

2 INTRODUCTION

2.1 General

The goal of this work package is to provide measurements that can be used to benchmark simulation software that is able to predict the flooding of cruise or Ropax vessels.

Volumes 1 to 5 describe the model tests that were executed for Cruise vessels by MARIN. Volumes 6 to 8 describe the model tests that were executed to investigate the flooding of Ropax vessels. The latter tests were executed by HSVA.

Volumes 1 to 5 describe

1. Fundamental compartment flooding
2. Deck flooding
3. **Fundamental hydrodynamics**
4. Cruise ship flooding (Part 1)
5. Cruise ship flooding (Part 2)

The model information, measured data and videos of the present model tests are provided on a USB memory stick. An HTML menu provides the metadata of each test and easy access of the results.

2.2 Volume 3

The present report describes a series of model tests that focus on the fundamental hydrodynamics of a cruise vessel model that are executed within the EU FLARE project. The goal of the tests is to provide data for benchmarking and verification of the results of numerical codes that simulate the flooding process.

The model is based on the geometry of Sample ship 3, which is a cruise vessel design of Flare partner Chantiers de l'Atlantique. The present volume describes the fundamental hydrodynamics that may play a role in the flooding of vessels, such as, roll damping at excessive heel and roll damping due to breach openings.

The test setup and adopted approaches are described in chapters 3 to 7; a summary of the results including a concise discussion of the results is given in chapter 8. The analysed data and videos are included on a USB stick that is delivered with this report.

2.3 FLOODING ACCIDENT RESPONSE

Despite the fact that the maritime sector is continuously investing in increasing and maintaining safety on board ships, additional effort is needed in the pathway towards zero-loss of life and zero-pollution. The highest risk for persons on board ships comes with flooding accidents, but consequences may be reduced when appropriate actions are taken following such an accident, thus greatly reducing the probability of loss of life or damage to the environment.

The FLARE project will target a risk-based methodology for "live" flooding risk assessment and control, by developing a generic (all incidents in one model) and holistic (active and passive measures) risk model with potential application to new buildings and, which is totally new, to existing ships. Innovative technical solutions in ship concepts and equipment for risk containment and control will be accompanied by proposals for the revision of relevant IMO regulations towards a risk-based approach to contain and control risk in passenger ships from flooding incidents, thereby significantly contributing to the safety of both passenger and ship.

2.4 Project partners

BALance Technology Consulting GmbH, with its headquarters in Bremen, Germany, will coordinate the project in close cooperation with the University of Strathclyde, Department of Naval Architecture, Ocean and Marine Engineering. Nineteen other leading maritime stakeholders will contribute to the results of FLARE: Aalto University, Brookes Bell, Bureau Veritas Marine & Offshore, Carnival, Color Line Marine, DNV GL, Fincantieri, Hamburgische Schiffbau-Versuchsanstalt, ICAM Nantes, Lloyd's Register, MARIN, Meyer Werft, Meyer Turku, NAPA, SEA Europe, Chantiers de l'Atlantique, Rina Services, RCCL and Stena Line. This project has received funding from the European Union's Horizon 2020 research and innovation programme under Grant Agreement No 814753.

3 MODEL

3.1 General

A ship model was made to a geometric scale of 1:60 (Model number 10155). This is the same model as described in Volumes 4 and 5. However the breach opening was reduced and a longitudinal bulkhead 6m inward from the side shell prevented ingress in the floodable geometry of the model.

The model was assembled out of the following segments:

- The bow and stern are Styrofoam filled and shown in yellow in Figure 3–1.
- The floodable compartments are made from transparent PVC. In the present tests a small portion of these compartments can be flooded.
- The sections are stiffened by two carbon fibre box beams.

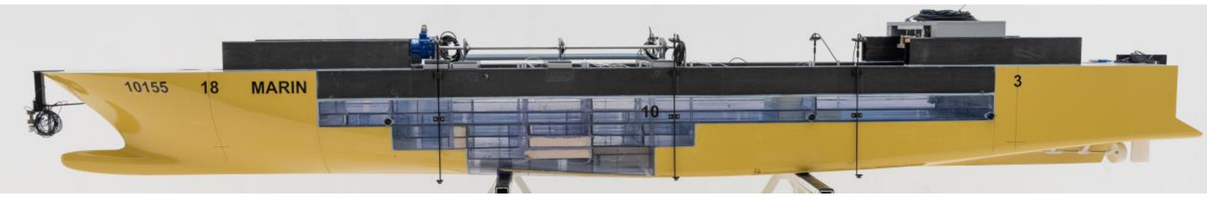

Figure 3-1: Side view of the model (intact side)

3.2 Compartments

Figure 3-2 and Figure 3-3 show the location and the dimensions of the breached compartments. The two blue compartments are on deck 2 and are below the waterline; the green compartments are on deck 3, which is above the waterline.

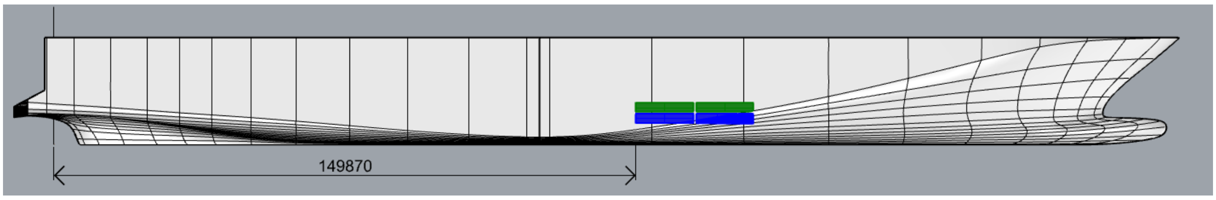

Figure 3-2: Location of breaches

The aft side of compartments start at 149.9m forward of the aft perpendicular.

Each compartment could be filled with a tight fitting Styrofoam block to model the intact condition.

Five configurations are tested:

- Setup 1: Intact, all compartments closed
- Setup 2: The two forward compartments open
- Setup 3: All compartments open
- Setup 4: The two compartments below the waterline open
- Setup 5: The two compartments above the waterline open

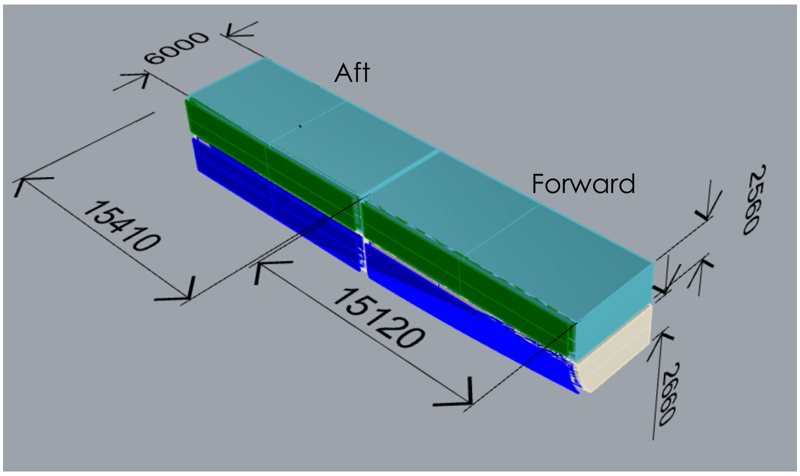

Figure 3-3: Dimensions of the breach

Because of the relatively small compartment size and the fact that the compartments are completely open at the side shell, no additional vent pipes were mounted.

3.3 Appendages

The model is equipped with the following appendages:

- Passive rudders (rapid prototyping).
- Passive propeller arrangement (rapid prototyping).
- Wooden bilge keels with a total length of 90 m and a height of 430mm. The bilge keel is divided into a forward and aft part. The bilge keel is removed at the location of the damage opening. The length on the damaged side was 45 m

Figure 3-4: Photo of appendages

3.4 Loading condition

The properties of the loading conditions as used in the tests are given in Table T 1. The loading condition was based on the loading conditions as reported in Volume 4. No effort was made to obtain a specified GM value. The measured GM was 2.88 m

Note that in model tests the GM is measured via the inclination test. The intact KM is known from the hydrostatics, hence the intact KG is known when the GM is determined. The KG is not measured in dry condition.

4 TEST SETUP AND FACILITY

4.1 Facility

This part of the test programme was executed in the Seakeeping and Manoeuvring Basin. This basin is equipped with a wave generator and a moving carriage. Current is mimicked by moving the model slowly through the basin.

Figure 4-1: Seakeeping and Manoeuvring basin

4.2 Test setup

The vessel was kept at location by a soft spring mooring system. The mooring lines were connected at the bow and stern of the vessel. The angle of the mooring lines was 45 degrees with the centreline. Figure 4-2 and Figure 4-3 show a sketch of the mooring system and a photo of the model connected in the mooring.

The stiffness of the lines was designed in such a way that resonance with the ship motions was avoided. The yaw motion is the shortest period in this type of mooring system; in the present setup the yaw period was about twice the natural period of roll with a yaw period of 37 s. The results of the mooring decay tests are included in Appendix II.

The stiffness and pre-tension of each mooring line was:

Line stiffness: 241 kN/m

Pretension: 6516 kN

The mooring line attachment height on the vessel was located between the CoG and the waterline. The mooring lines run parallel to the calm water level.

A lightweight slack bundle of flexible measurement cables provided the transfer of data between the model and the carriage; care was taken that these wires did not restrict the motions of the model.

Four flexible synthetic safety wires were installed to retrieve the model at the end of the test and to make sure that the model did not sink or capsize in flooded condition.

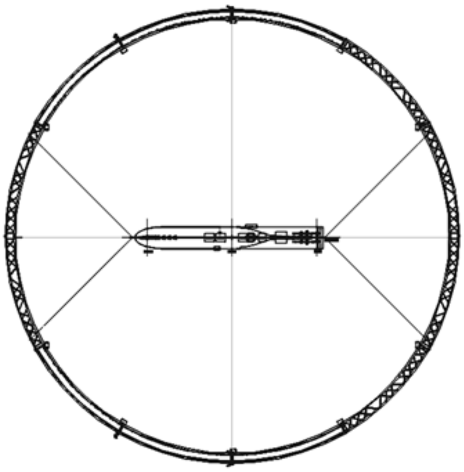

Figure 4-2: Soft spring mooring arrangement

In forced roll tests the model was connected to a cardan shaft and a force frame to a roll motor that was mounted on the carriage. The setup is shown in Figure 4-4. The motor provided a constantly oscillating roll moment. The resulting roll amplitude was measured.

Figure 4-3: Photo of the model in "Setup 2" in a forced roll test(two forward compartments open).

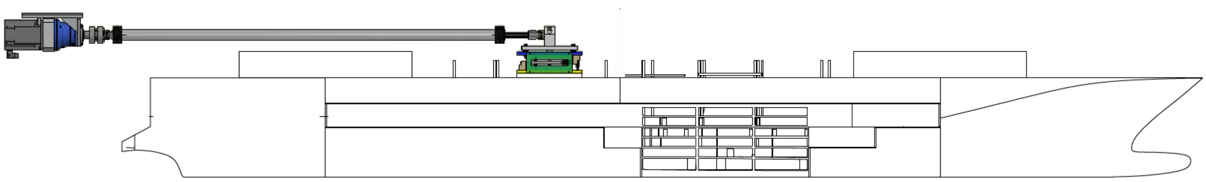

Figure 4-4: Sketch of the forced roll setup

5 MEASUREMENTS

The test setup was equipped with:

- An optical tracking system to measure the 6-DoF motions of the model in order to use the actual obtained position of the model in the test. Measured at a frequency of 100 Hz. The motions measured are translated to the CoG of the model.
- Incident wave height in the basin at 3 locations by an acoustical wave probe, to measure the incoming wave. Measured at a frequency of 50 Hz.

The relative wave elevation was measured at 4 locations inside the breach openings; the locations of the wave probes are given in

- Table T 5 in Appendix I.
- Relative wave elevation at 6 positions at the side shell of the vessel. Measured at a frequency of 200 Hz.
- 3 DoF accelerations at four locations at 200Hz. The results were translated to determine the 6 DoF accelerations at the CoG.
- 3 DoF mooring forces (Surge, Sway and Yaw) at 200Hz
- 6 component force frame in forced roll tests at 200Hz

Drawings of the wave probe instrumentation can be found on the memory stick that is delivered with this report.

6 AXIS SYSTEMS AND SIGN CONVENTION

The ITTC axis and heading system was used in this report, as Figure 6-1.

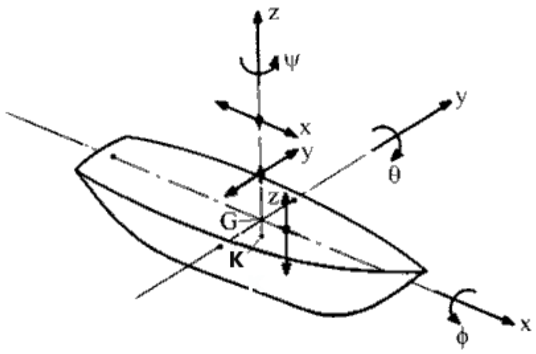

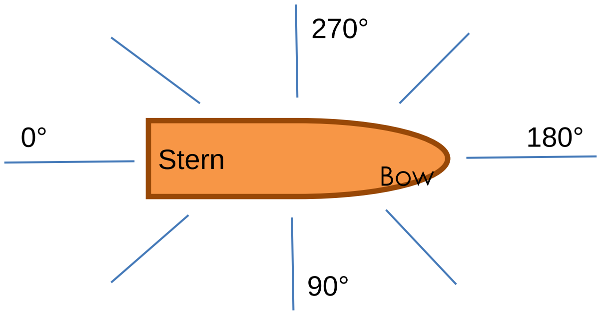

Figure 6-1: Axis system and heading convention.

The origin of the vessel is at the aft perpendicular, centreline and keel for longitudinal, transverse and vertical directions respectively.

Draught is defined as the vertical distance between the keel and calm water level.

7 TEST PROGRAMME AND PROCEDURES

7.1 Summary of the test programme

A total of 191 tests were executed. Of which:

- 59 decay tests
- 84 Forced roll tests
- 32 tests in regular waves
- 16 tests in irrregular waves

7.2 Test procedures

The following test procedures were followed:

Roll decay tests

- The measurement starts
- The model is held at a heel angle of about 10 deg. manually
- The model is released
- The measurements stopped after the roll motion was negligible
- Each decay test was executed over port side and starboard.

Forced roll

- The measurement starts
- The roll motor starts
- After about 60 seconds the roll moment increases
- A total of 4 amplitudes is measured
- The roll motor stops
- The measurement stops

Tests in regular waves

- The measurement starts
- The wave generator starts
- After a measurement time of 300s (model scale) measurement stops

8 SUMMARY AND DISCUSSION

This section gives a summary of the main observations, including a brief discussion.

8.1 Roll decay tests

The roll decay tests in damaged condition did not result in consistent damping results. Therefore the roll decay tests are not included in this report. A decay analysis is sensitive to small vitiations, the dynamic behaviour of the flood water seemed to have a larger impact between oscillations than the differences between the model configurations. The duration of the measurement is too short to average the differences.

It is recommended to use intact roll damping coefficients in numerical simulations and to assume that the flood water dynamics change the roll behaviour "as in the model basin". This needs validation. The intact roll decay analysis is found in Appendix XX and Figure 8.1

8.2 Forced roll

Figure 8-1 shows the roll damping resulting from the forced roll tests at zero speed. The frequency of 0.38 rad/s is close to the natural period of roll. The damping in intact condition is shown in green. Setups 2, 4 and 5 are all different configurations with two of the four compartments breached.

The resulting damping in damaged condition is quite similar for all cases, and higher than for the intact case (as expected). This indicates that the exact location of the damaged compartment(s) does not have a notable impact.

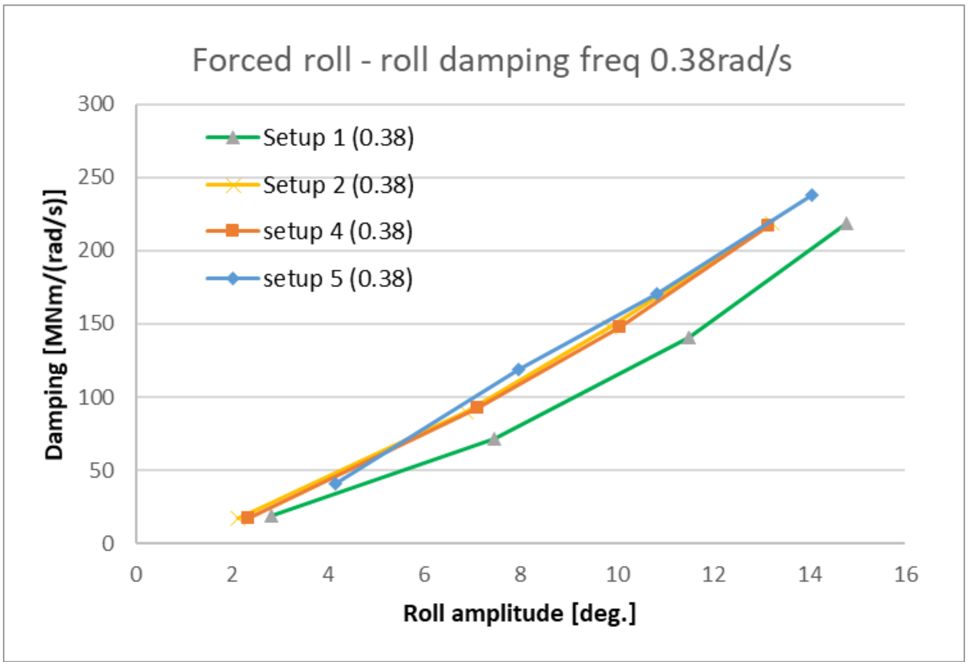

Figure 8-1: Roll damping with various opening configurations at 0.38 rad/s

Figure 8- 2 shows the roll damping at drift speed. The roll damping speed increases with the speed. At a drift speed of 4 kn the damping is about twice the damping at zero drift. The damping seems to increase with the square of the drift speed. This can be understood since the damping is associated with the square of the local relative velocity at the bilge keels, and with drift, this velocity increases considerable.

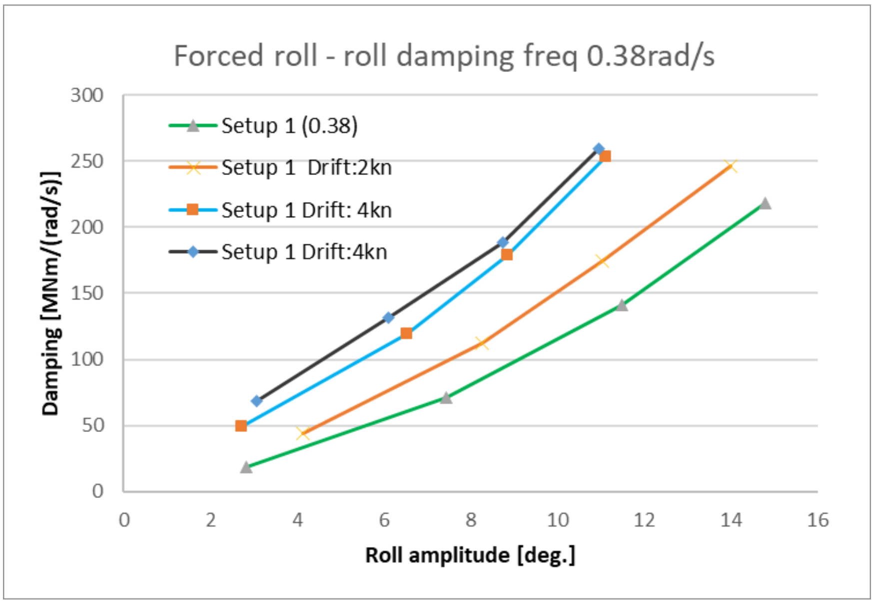

Figure 8- 2: Roll damping at drift speed

8.3 Regular waves

Figure 8-3 shows the RAO in beam regular waves. The wave condition is given below the bars. The numbers in the legend are the defined setup numbers. The results show that the intact conditions have the highest RAOs and Setup 3 results in the lowest value for the RAO. The values for Setup 3 are reduced by about 40% to 50% compared to the Intact conditions. The comparison at drift speed is affected by the change in encounter frequency. The drift with the waves shifts the encounter frequency closer to roll resonance, hence increasing the roll motion. Keeping the encounter frequency constant would change the steepness of the waves and therefore have an impact also on the roll RAO.

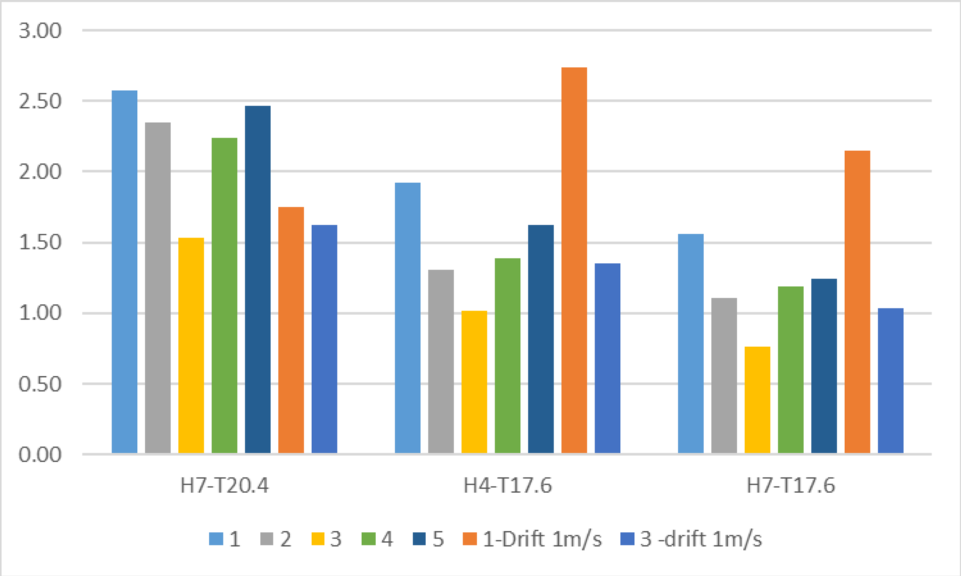

Figure 8-3: rms of RAO [deg/m]of roll in regular waves

8.4 Irregular waves

Figure 8- shows the rms of roll in head and beam seas as measured in the irregular wave tests. The tests were executed for the intact condition and the setup with the four compartments opened. The roll motion was the most remarkable difference. Other differences found were a resulting from the difference in roll, such as the relative wave elevation at the side shell, which is partly driven by the roll motion.

In beam seas (Hs=7m) the breach gives a clear reduction in roll: at a wave period of 14 s the roll motion reduces from 2 deg to about 1.2 deg rms.

On the other hand, in head seas, the roll motion significantly increases. Due to the asymmetry in the hull shape because of the breach, the roll increases from about 0.4 deg to 1.3 deg rms. Hence, in the damaged condition the roll excitation in head seas was larger than in beam seas.

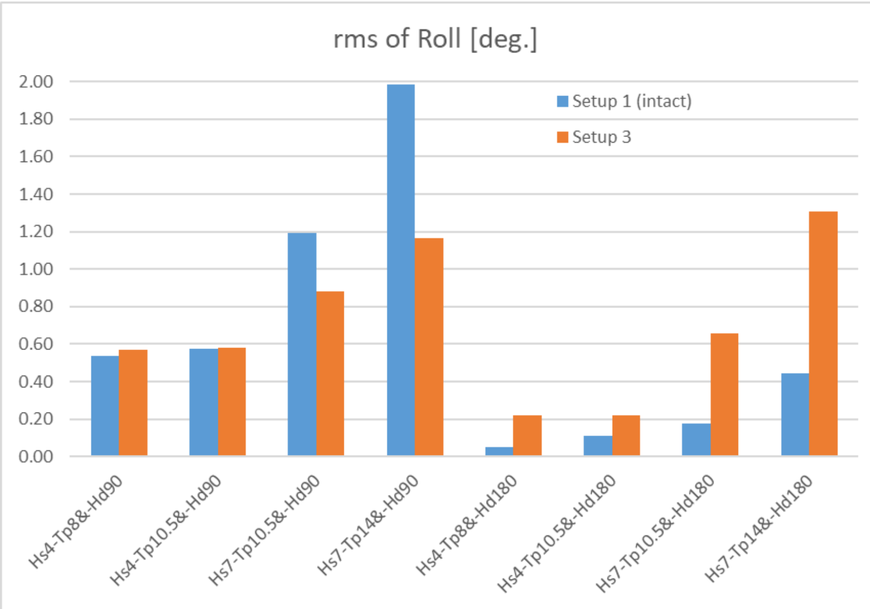

Figure 8-4: rms of roll in beam and head seas

The above-described behaviour can clearly be seen in the RAO of roll in beam and head seas (Figure 8-5). In beam seas the damaged condition, Setup 3, the RAO is lower in the low frequency range. In head seas, the RAO of the damaged condition is significantly higher than the intact condition. Note that the RAOs in head and beam seas are not plotted to the same vertical scale.

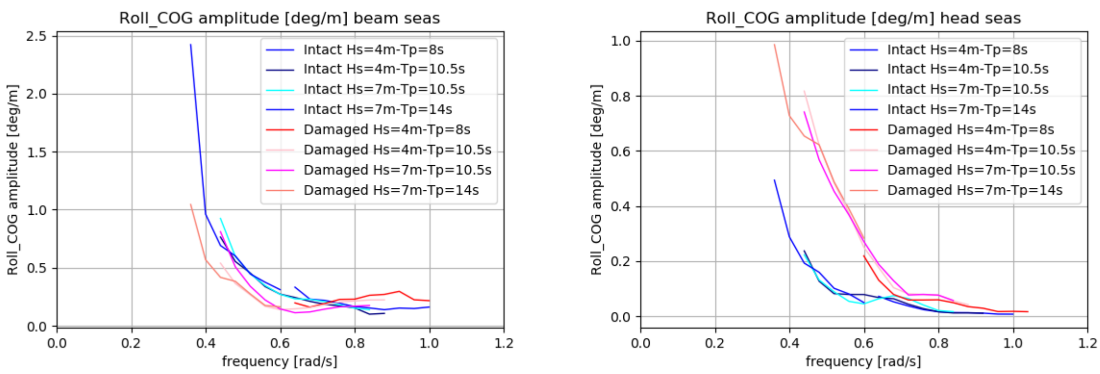

Figure 8-5 RAO of roll in beam and head seas

9 CONCLUSION

Model tests were conducted with a model of a cruise vessel with four damage openings to investigate the fundamental hydrostatics of a vessel in damaged condition. The goal of the tests was to generate a data set which can be used to benchmark flooding software. Based on the results of the tests the following conclusions can be drawn:

- The analysis of the roll decay tests for the damaged ship did not result in consistent damping values suitable for numerical simulations
- It is recommended to use intact roll damping coefficients in numerical simulations and to assume that the flood water dynamics change the roll behaviour "as in the model basin". This needs validation.
- The dynamic behaviour of the flood water seemed to have a larger impact between oscillations than the differences between the model configurations. The duration of the measurement is too short to average the differences. Hence the roll decay tests did not materialise in trustworthy damping numbers.
- The additional roll damping, in forced roll tests, due to the breach openings was very similar for all configurations with two of the four breaches open. The exact location of the compartments did not seem to have an impact.
- The roll damping in transverse drift increased with the square of the drift speed. At a drift speed of 4 knots, the roll damping was roughly twice the roll damping at zero speed.
- At zero drift, the RAO for roll in beam seas reduced by about 40% with all breaches open.
- In irregular seas, the damage openings in the model can reduce the roll motions by about 40% in beam seas. On the other hand, the roll in damaged condition in head seas was significantly increased to an even higher rms value than in beam seas.

Appendix I – Tables

Table T 1: Loading condition

Main particulars			
Designation	**Symbol**	**Magnitude**	**Unit**
Length	Lpp	270	m
Breadth	B	35	m
Height	H	12.6	m
Draught fore	T fore	8.2	m
Draught aft	T aft	8.2	m
Displacement mass	displ	52850	ton
VCG position from Keel (approx.)	KG	17	m
Metacentric height	GM	2.88	m
Natural period of roll (intact)	Tphi	18.3	s
LCG position from AP	LCG	127.92	m
Radius of inertia for roll	Kxx	13.904	m
Radius of inertia for pitch	Kyy	70.708	m
Radius of inertia for yaw	Kzz	71.223	m

Table T 2: Location of measurement devices

Wave probes	X [m]	Y [m]	Z [m] (zero level)	Compartment number	Deck
Number					
REL.9	157.2	-15	5.3	8	2
REL.10	172.74	-15	5.3	9	2
REL.11	157.2	-15	8.22	15	3
REL.18	172.74	-15	8.22	16	3
REL.PSA	82.2	18	8.2	outside	-
REL.SBA	82.2	-18	8.2	outside	-
REL.PSM	129	18	8.2	outside	-
REL.SBM	129	-18	8.2	outside	-
REL.PSF	190	18	8.2	outside	-
REL.SBF	190	-18	8.2	outside	-

Table T 3: Decay tests

Decay tests	Type
Test No	
30703_09SMB_02_002_001_01_4	Roll
30703_07SMB_03_002_001_01_1	Surge
30703_07SMB_03_003_001_01_1	Sway
30703_07SMB_03_004_001_01_1	Yaw

Table T 4: Forced roll tests

Forced roll tests	Freq	Amplitude	Drift
Test No	[rad/s]	[deg.]	[kn]
Intact, config 1			
30703_09SMB_03_001_001_01	0.38	2.825484	0
30703_09SMB_03_001_002_02	0.38	7.448727	0
30703_09SMB_03_001_003_01	0.38	11.49032	0
30703_09SMB_03_001_004_01	0.38	14.78233	0
Intact, config 1			
30703_09SMB_03_001_005_01	0.41	4.05376	0
30703_09SMB_03_001_006_01	0.41	8.295085	0
30703_09SMB_03_001_007_01	0.41	10.89316	0
30703_09SMB_03_001_008_01	0.41	13.94246	0
Intact, config 1			
30703_09SMB_03_001_009_01	0.44	5.364384	0
30703_09SMB_03_001_010_02	0.44	8.869268	0
30703_09SMB_03_001_011_02	0.44	10.60229	0
30703_09SMB_03_001_012_01	0.44	13.11213	0
Setup 1 Drift:2kn			
30703_09SMB_06_001_001_01	0.38	4.133311	2
30703_09SMB_06_001_001_02	0.38	8.274502	2
30703_09SMB_06_001_001_03	0.38	11.03829	2
30703_09SMB_06_001_001_04	0.38	13.99523	2
Setup 1 Drift:4kn			
30703_09SMB_06_002_001_01	0.38	3.057758	4
30703_09SMB_06_002_001_02	0.38	6.103908	4
30703_09SMB_06_002_001_03	0.38	8.739011	4
30703_09SMB_06_002_001_04	0.38	10.96251	4
Setup 1 Drift: 4kn			
30703_09SMB_06_003_001_01	0.38	2.714478	-4
30703_09SMB_06_003_001_02	0.38	6.541207	-4
30703_09SMB_06_003_001_03	0.38	8.841198	-4
30703_09SMB_06_003_001_04	0.38	11.10217	-4

Forced roll tests	Freq	Amplitude	Drift
Test No	[rad/s]	[deg.]	[kn]
Setup 2			
30703_09SMB_13_001_001_01	0.38	2.123425	0
30703_09SMB_13_001_002_01	0.38	6.854858	0
30703_09SMB_13_001_003_02	0.38	9.858688	0
30703_09SMB_13_001_004_01	0.38	13.21785	0
Setup 2			
30703_09SMB_13_001_005_01	0.41	3.52359	0
30703_09SMB_13_001_006_01	0.41	6.73189	0
30703_09SMB_13_001_007_01	0.41	9.119065	0
30703_09SMB_13_001_008_01	0.41	12.3214	0
Setup 2			
30703_09SMB_13_001_009_01	0.44	4.747269	0
30703_09SMB_13_001_010_01	0.44	7.155674	0
30703_09SMB_13_001_011_01	0.44	8.91173	0
30703_09SMB_13_001_012_01	0.44	11.56649	0
setup 3			
30703_09SMB_23_001_001_01	0.38	2.18253	2
30703_09SMB_23_001_002_01	0.38	5.945816	2
30703_09SMB_23_001_003_01	0.38	8.301889	2
30703_09SMB_23_001_004_01	0.38	11.39801	2
setup 3			
30703_09SMB_23_001_005_01	0.38	2.566275	4
30703_09SMB_23_001_006_01	0.38	5.45354	4
30703_09SMB_23_001_007_01	0.38	7.371975	4
30703_09SMB_23_001_008_01	0.38	10.78745	4
setup 3			
30703_09SMB_23_001_009_01	0.38	3.848951	-4
30703_09SMB_23_001_010_01	0.38	5.947417	-4
30703_09SMB_23_001_011_01	0.38	7.565571	-4
30703_09SMB_23_001_012_01	0.38	10.3761	-4
setup 3			
30703_09SMB_26_001_001_01	0.41	3.372186	2
30703_09SMB_26_001_001_02	0.41	6.038723	2
30703_09SMB_26_001_001_03	0.41	7.941951	2
30703_09SMB_26_001_001_04	0.41	10.33446	2
setup 3			
30703_09SMB_26_002_001_01	0.41	1.750956	4
30703_09SMB_26_002_001_02	0.41	4.117044	4
30703_09SMB_26_002_001_03	0.41	5.964189	4
30703_09SMB_26_002_001_04	0.41	7.808472	4

Forced roll tests	Freq	Amplitude	Drift
Test No	[rad/s]	[deg.]	[kn]
setup 3			
30703_09SMB_26_005_001_02	0.41	1.940428	-4
30703_09SMB_26_005_001_03	0.41	3.829625	-4
30703_09SMB_26_005_001_04	0.41	6.247895	-4
30703_09SMB_26_005_001_05	0.41	8.918602	-4
setup 3			
30703_09SMB_33_001_001_01	0.38	2.337226	0
30703_09SMB_33_001_002_01	0.38	7.115891	0
30703_09SMB_33_001_003_01	0.38	10.07348	0
30703_09SMB_33_001_004_01	0.38	13.15806	0
setup 3			
30703_09SMB_33_001_005_01	0.41	3.975623	0
30703_09SMB_33_001_006_01	0.41	6.819279	0
30703_09SMB_33_001_007_01	0.41	9.19314	0
30703_09SMB_33_001_008_01	0.41	12.41675	0
setup 3			
30703_09SMB_33_001_009_01	0.44	4.707295	0
30703_09SMB_33_001_010_01	0.44	7.358481	0
30703_09SMB_33_001_011_01	0.44	9.097637	0
30703_09SMB_33_001_012_01	0.44	11.82061	0
setup 3			
30703_09SMB_43_001_001_03	0.38	4.149333	0
30703_09SMB_43_001_002_03	0.38	7.960884	0
30703_09SMB_43_001_003_02	0.38	10.84589	0
30703_09SMB_43_001_004_02	0.38	14.04336	0
setup 3			
30703_09SMB_43_001_005_02	0.41	4.978229	0
30703_09SMB_43_001_006_02	0.41	7.608516	0
30703_09SMB_43_001_007_02	0.41	9.575026	0
30703_09SMB_43_001_008_02	0.41	12.72877	0
setup 3			
30703_09SMB_43_001_009_02	0.44	5.417488	0
30703_09SMB_43_001_010_02	0.44	7.753998	0
30703_09SMB_43_001_011_02	0.44	9.116946	0
30703_09SMB_43_001_012_02	0.44	11.84349	0

Table T 5: Regular waves

Test no	Model	Wave no.	Heading	H	T	Drift speed
			deg.	m	s	kn
30703_09SMB_05_001_001_01	1	100	90	4.0	20.4	0
30703_09SMB_05_002_001_01	1	101	90	7.0	20.4	0
30703_09SMB_05_003_001_01	1	102	90	4.0	17.6	0
30703_09SMB_05_004_001_02	1	103	90	7.0	17.6	0
30703_09SMB_05_005_001_01	1	104	90	4.0	7.0	0
30703_09SMB_05_006_001_01	1	105	90	7.0	10.0	0
30703_09SMB_05_007_001_01	1-Drift 1m/s	100	90	4.0	20.4	1.9
30703_09SMB_05_008_001_01	1	101	90	7.0	20.4	1.9
30703_09SMB_05_009_001_01	1	102	90	4.0	17.6	1.9
30703_09SMB_05_010_001_01	1	103	90	7.0	17.6	1.9
30703_09SMB_15_001_001_01	2	100	90	4.0	20.4	0.0
30703_09SMB_15_002_001_01	2	101	90	7.0	20.4	0.0
30703_09SMB_15_003_001_01	2	102	90	4.0	17.6	0.0
30703_09SMB_15_004_001_01	2	103	90	7.0	17.6	0.0
30703_09SMB_25_001_001_01	3	100	90	4.0	20.4	0.0
30703_09SMB_25_002_001_01	3	101	90	7.0	20.4	0.0
30703_09SMB_25_003_001_01	3	102	90	4.0	17.6	0.0
30703_09SMB_25_004_001_01	3	103	90	7.0	17.6	0.0
30703_09SMB_25_007_001_01	3 -drift 1m/s	100	90	4.0	20.4	1.9
30703_09SMB_25_008_001_01	3	101	90	7.0	20.4	1.9
30703_09SMB_25_009_001_01	3	102	90	4.0	17.6	1.9
30703_09SMB_25_010_001_01	3	103	90	7.0	17.6	1.9
30703_09SMB_25_005_001_01	3	104	90	4.0	7.0	0
30703_09SMB_25_006_001_01	3	105	90	7.0	10.0	0
30703_09SMB_35_001_001_01	4	100	90	4.0	20.4	0
30703_09SMB_35_002_001_01	4	101	90	7.0	20.4	0
30703_09SMB_35_003_001_01	4	102	90	4.0	17.6	0
30703_09SMB_35_004_001_01	4	103	90	7.0	17.6	0
30703_09SMB_45_001_001_01	5	100	90	4.0	20.4	0
30703_09SMB_45_002_001_01	5	101	90	7.0	20.4	0
30703_09SMB_45_003_001_01	5	102	90	4.0	17.6	0
30703_09SMB_45_004_001_01	5	103	90	7.0	17.6	0

Table T 6: Tests in irregular waves

Test number	Setup	Wave number	heading	Hs	Tp
			deg.	m	s
30703_09SMB_04_001_001_01	Setup 1 (intact)	1	90	4.0	8.0
30703_09SMB_04_002_001_01	1	2	90	4.0	10.5
30703_09SMB_04_002_001_02	1	3	90	7.0	10.5
30703_09SMB_04_004_001_01	1	4	90	7.0	14.0
30703_09SMB_04_005_001_01	1	1	180	4.0	8.0
30703_09SMB_04_006_001_01	1	2	180	4.0	10.5
30703_09SMB_04_007_001_01	1	3	180	7.0	10.5
30703_09SMB_04_008_001_01	1	4	180	7.0	14.0
30703_09SMB_24_001_001_01	Setup 3	1	90	4.0	8.0
30703_09SMB_24_002_001_01	4	2	90	4.0	10.5
30703_09SMB_24_003_001_01	4	3	90	7.0	10.5
30703_09SMB_24_004_001_01	4	4	90	7.0	14.0
30703_09SMB_24_005_001_01	4	1	180	4.0	8.0
30703_09SMB_24_006_001_01	4	2	180	4.0	10.5
30703_09SMB_24_007_001_01	4	3	180	7.0	10.5
30703_09SMB_24_008_001_01	4	4	180	7.0	14.0

Appendix II – Decay tests

Flare 30703
Roll decay - Vs = 0 kn
Test ID: 30703_09SMB_02_001_001_04_1 - Intact, config 1 - Soft mooring

Parameter	Magnitude	Unit
P	0.152	-
Q	0.021	1/deg
BCrit	8.67E+06	kNm/(rad/s)
BLin	2.4	%*
BQua	1.1	%/(deg·rad/s)*
Natural Period	18.3	s
Damped Period	18.3	s

* percentage critical damping

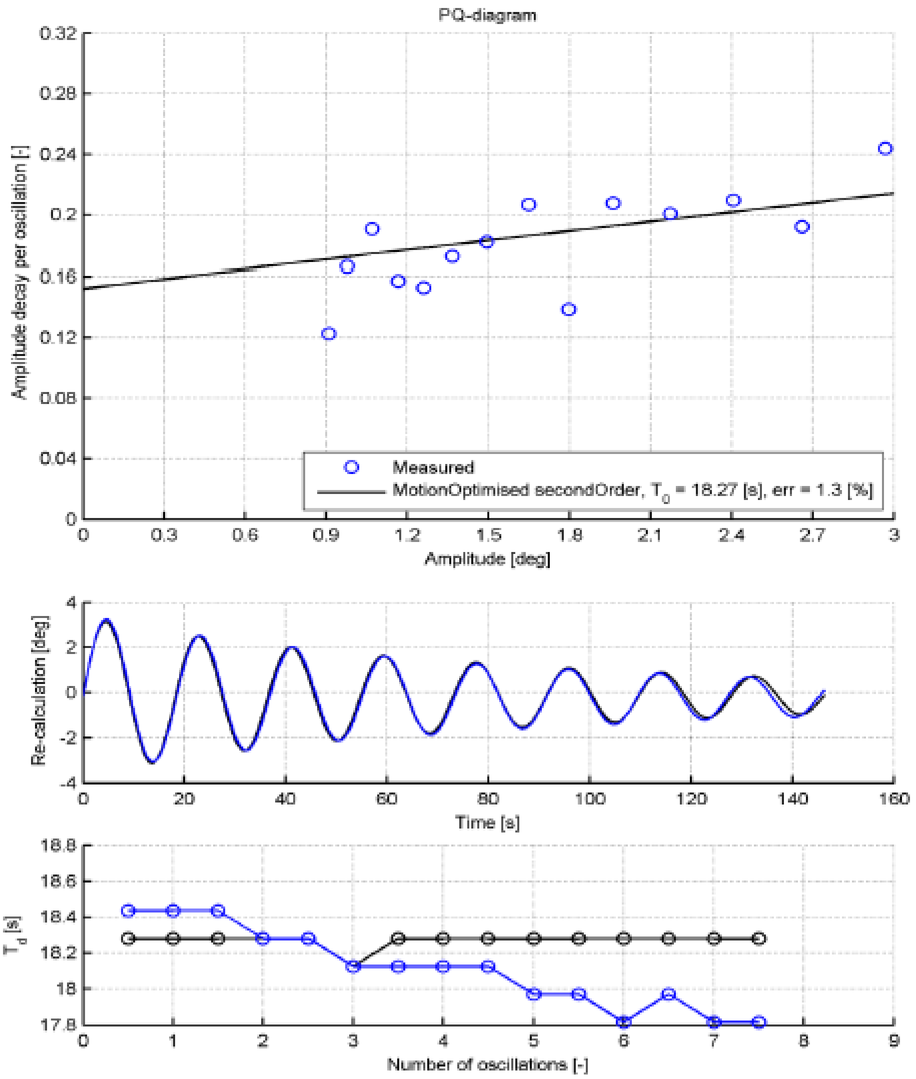

Flare 30703
Surge decay - Vs = 0 kn
Test ID: 30703_07SMB_03_002_001_01_1 - Intact, config 1 - Soft mooring

Parameter	Magnitude	Unit
P	0.117	-
Q	0.000	1/m
BCrit	2.75E+07	kN/(m/s)
BLin	1.9	%*
BQua	0.0	%/(m·rad/s)*
Natural Period	65.5	s
Damped Period	65.5	s

* percentage critical damping

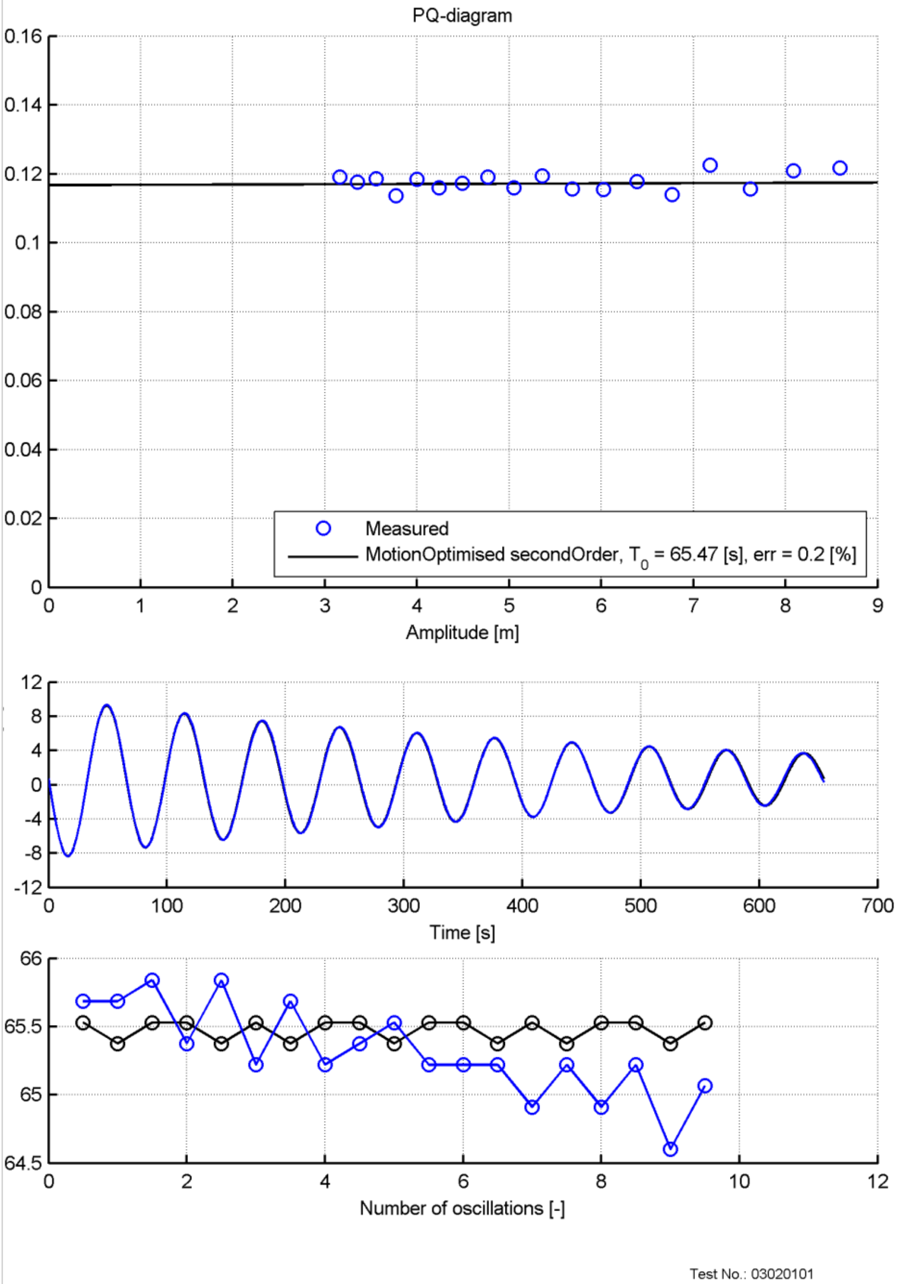

Flare 30703
Sway decay - Vs = 0 kn
Test ID: 30703_07SMB_03_003_001_01_1 - Intact, config 1 - Soft mooring

Parameter	Magnitude	Unit
P	0.099	-
Q	0.048	1/m
BCrit	3.52E+07	kN/(m/s)
BLin	1.6	%*
BQua	11.9	%/(m·rad/s)*
Natural Period	83.9	s
Damped Period	83.9	s

* percentage critical damping

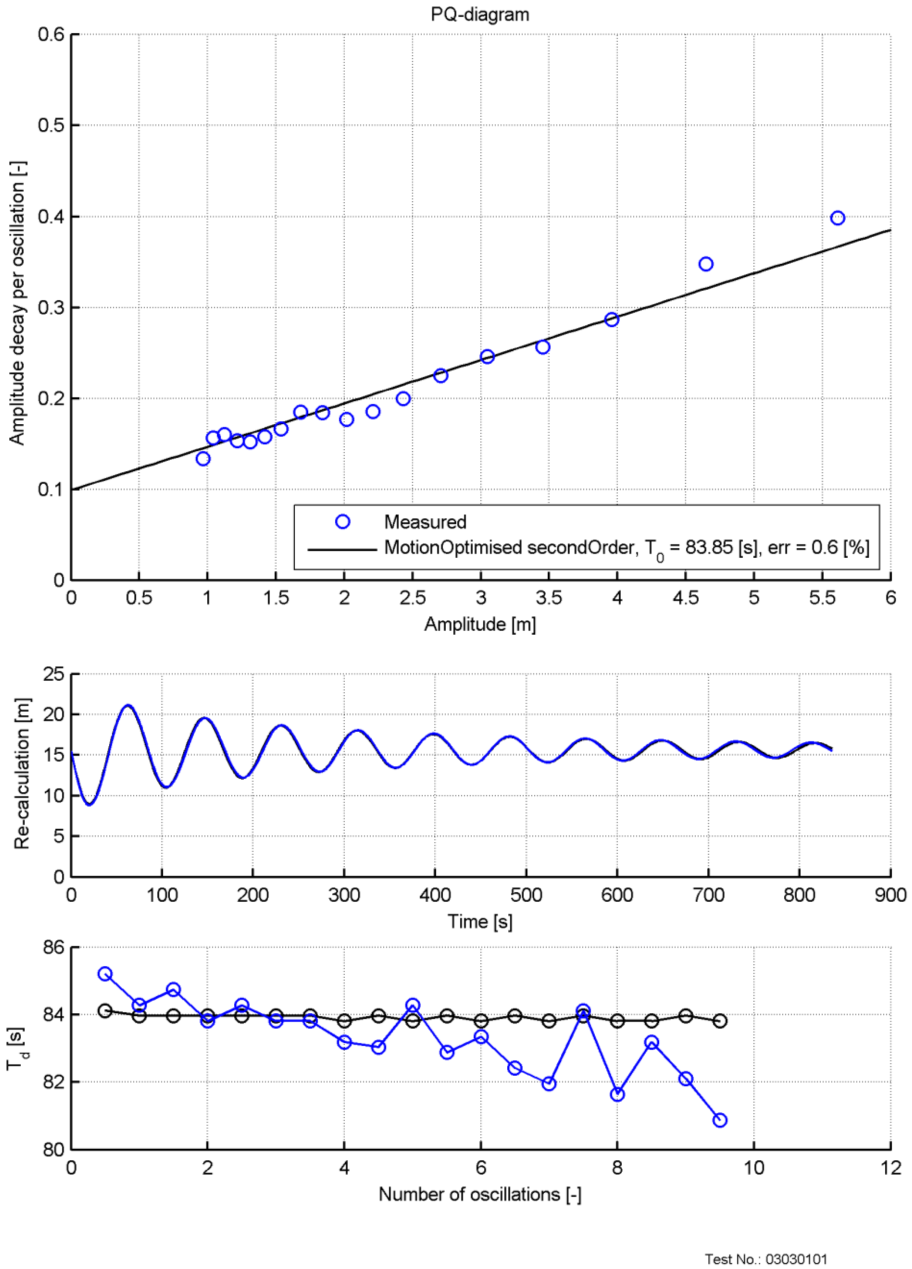

Flare 30703		
Yaw decay - Vs = 0 kn		
Test ID: 30703_07SMB_03_004_001_01_1 - Intact, config 1 - Soft mooring		

Parameter	Magnitude	Unit
P	0.018	-
Q	0.265	1/deg
BCrit	1.52E+07	kNm/(rad/s)
BLin	0.3	%*
BQua	28.7	%/(deg·rad/s)*
Natural Period	36.3	s
Damped Period	36.3	s

* percentage critical damping

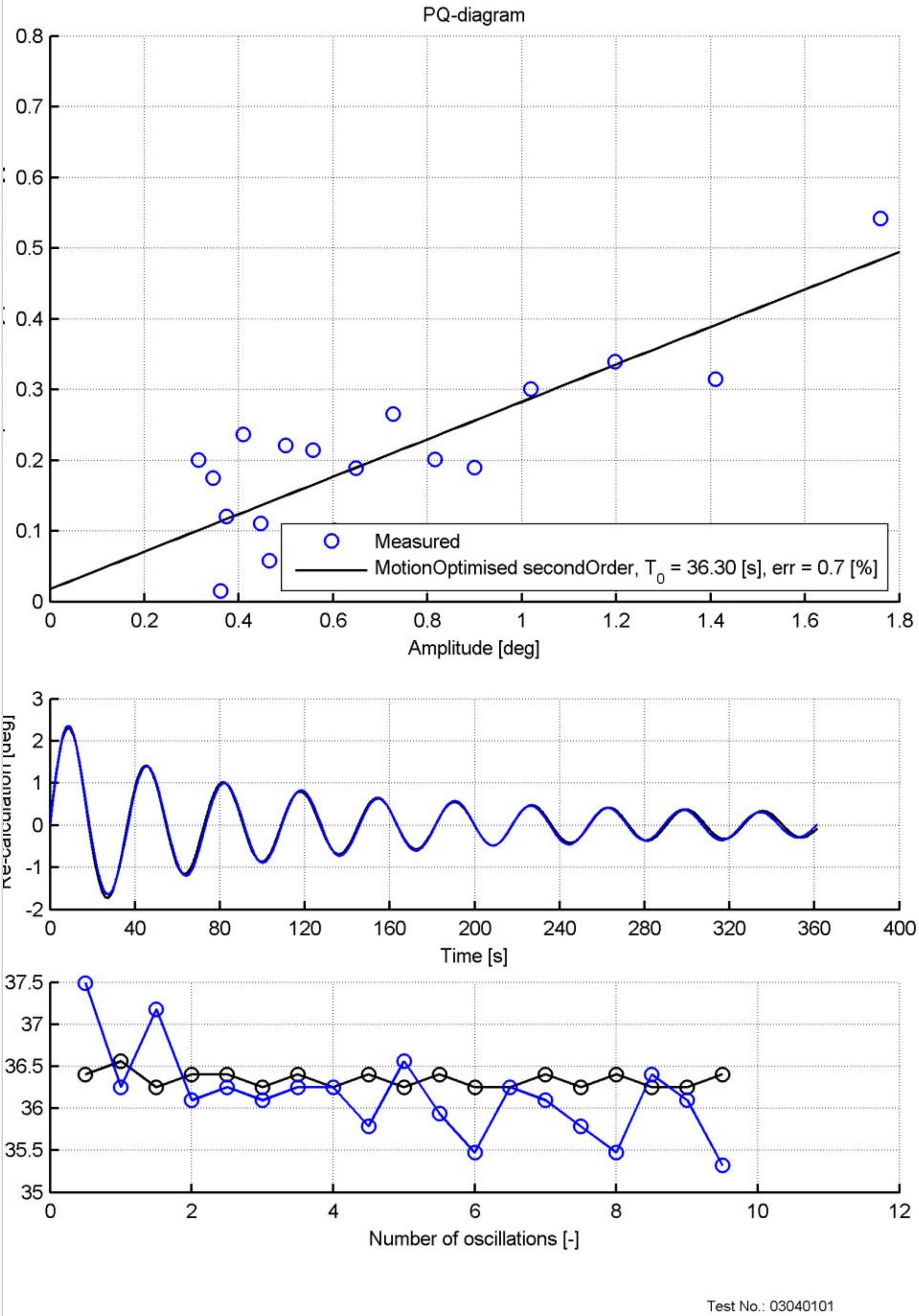

Acronym:	FLARE
Project full title:	Flooding Accident REsponse
Grant agreement No.	814753
Coordinator:	BALance Technology Consulting GmbH

Deliverable 4.2 – Model tests

Volume 4 – Cruise ship flooding I

The project has received funding from the European's Horizon 2020 research and innovation programme (Contract No.: 814753)

Duration: 36 months - Project Start: 01/06/2019 - Project End: 31/05/2022

Deliverable data

Deliverable No	4.2 Volume 4		
Deliverable Title	Model tests: Cruise ship flooding I		
Work Package no: title	WP4.2 Model tests		

Dissemination level	Public	**Deliverable type**	Report
Lead beneficiary	HSVA		
Responsible author	R. van Basten Batenburg		
Co-authors	-		
Date of delivery	28-01-2021		
Approved	**Name (partner)**		**Date [DD-MM-YYYY]**
Peer reviewer 1	O. Rognebakke (DNVGL)		13-01-2021
Peer reviewer 2	O. K. Olufsen (DNVGL)		13-01-2021

Document history

Version	**Date**	**Description**
1	**24 Nov. 20**	Draft
2	**25 Nov. 20**	For peer review
3	**27 Jan. 21**	Final

The research leading to these results has received funding from the European Union Horizon 2020 Programme under grant agreement n° 814753.
This report reflects only the author's view. INEA is not responsible for any use that may be made of the information it contains.

CONTENTS

List of symbols and abbreviations

Cd	Discharge coefficient
CoG	Centre of Gravity
DoF	Degree of Freedom
ITTC	International Towing Tank Conference
CFD	Computational Fluid Dynamics
GM	Metacentric height
RAO	Response Amplitude Operator
TD	Time domain

1 EXECUTIVE SUMMARY

The present report describes a series of model tests that focus on the flooding of cruise vessel that are executed within the EU FLARE project. The goal of the tests is to provide data for benchmarking and verification of the results of numerical codes that simulate the flooding process.

The test setup and adopted approaches are described in chapters 3 to 0; a summary of the results including a concise discussion of the results is given in chapter 8. The analysed data and videos are included on a USB stick that is delivered with this report.

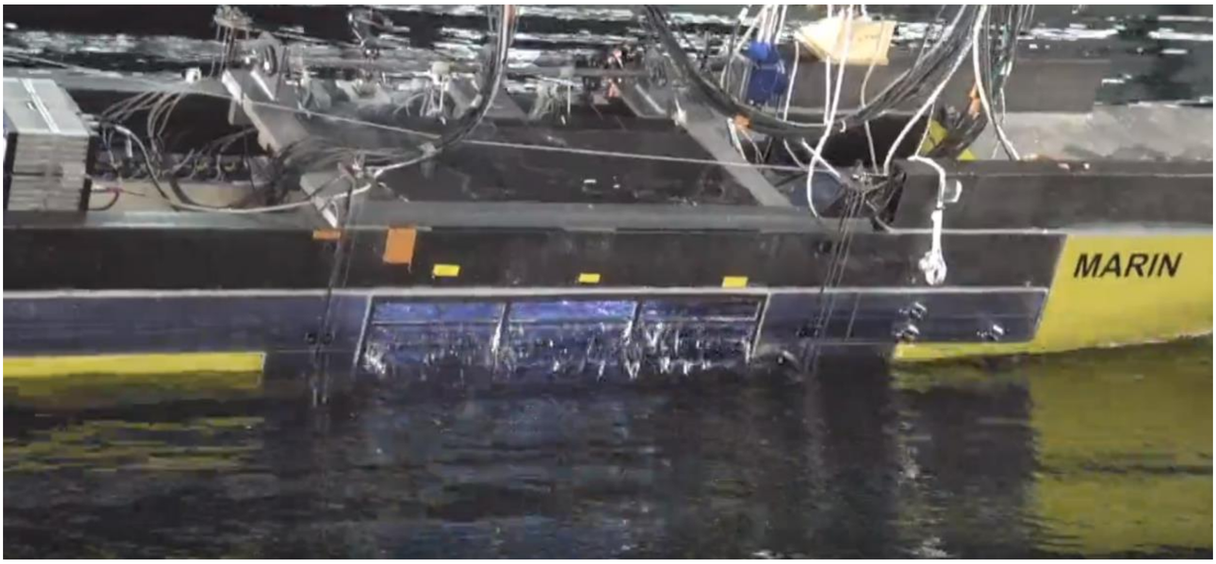

Figure 1-1 Model in irregular waves

1.1 Problem definition

- In the development and verification of codes that assess dynamic flooding of ships it is required to benchmark the result of numerical simulations and to gain insight into the most important drivers in the flooding of cruise vessels.

1.2 Technical approach and work plan

- A ship model with a floodable internal geometry was built to simulate a given flooding scenario
- Basin tests were executed in calm water and a selection of irregular waves for a range of metacentric heights
- The measurements were analysed and discussed

1.3 Results

- The measurements contribute to the understanding of the most important drivers in the flooding of cruise vessels.

1.4 Conclusions

- The flooding openings deviated at some points from the provided scenario and the most forward compartment on deck 3 had some leakage. This should be taken into account if used for benchmarking purposes. The tests in Volume 5 are in line with the given flooding scenario.
- As expected the metacentric height was the main driver in the capsizing behaviour. Higher metacentric heights resulted in fewer wave conditions where capsizes were observed.
- With a GM of 2.61 m (Intermediate), the vessel capsizes under progressive flooding.
- With a GM of 2.88 m (High), the vessel capsizes under progressive flooding, with a time to capsize about twice as long compared to GM of 2.61 m.
- With a GM of 3.15 m (Extra high), the vessel did not capsize. (The names of the conditions such as “Extra high” and “Intermediate GM” refer to their relative magnitude in the present test programme and do not correlate to loading conditions in reality)
- Wave realisations of irregular waves with a different seed resulted in the same outcome with respect to capsizes.
- A drift speed of 1m/s did not have a notable impact on the results.
- No capsizes were observed in head seas and in tests with the breach at the leeward side.
- In the high GM case the vessel capsizes when the damage is facing the waves, but remains afloat when the damage location is on leeward side. This points to progressive flooding onto the main deck due to relative wave action, that does not occur when the damage is to leeward.
- Given the previous conclusion, the survivability of the cruise vessel is thus noticeable different depending on the ship heading, and this should be respected in the capsize probability calculations in the framework.

2 INTRODUCTION

2.1 General

The goal of this work package is to provide measurements that can be used to benchmark simulation software that is able to predict the flooding of cruise or Ropax vessels.

Volumes 1 to 5 describe the model tests that were executed for Cruise vessels by MARIN. Volumes 5 to 8 describe the model tests that were executed to investigate the flooding of Ropax vessels. The latter tests were executed by HSVA.

Volumes 1 to 5 describe

1. Fundamental compartment flooding
2. Deck flooding
3. Fundamental hydrodynamics
4. **Cruise ship flooding (Part 1)**
5. Cruise ship flooding (Part 2)

Volumes 6 and higher describe the tests that were executed for the Ropax vessel at HSVA.

The model information, measured data and videos of the present model tests are provided on a USB memory stick. An HTML menu provides the metadata of each test and easy access of the results.

2.2 Volume 4

The present report describes a series of model tests that focus on the flooding of a cruise ship model that are executed within the EU FLARE project. The goal of the tests is to provide data for benchmarking and verification of the results of numerical codes that simulate the flooding process.

The model is based on the flooding scenario as provided by University of Strathclyde. The model is a ship model in which all the compartments and openings flooded in this scenario are modelled.

The measurements described in the present report showed that some of the connections between the bulkheads and the decks were not water-tight. This resulted in the vessel not flooding according to the prescribed scenario. Thereafter the model was corrected and a second set of tests was executed. The second set of tests is reported in Volume 5.

The test setup and adopted approaches are described in chapters 3 to7; a summary of the results including a concise discussion of the results is given in chapter 8. The analysed data and videos are included on a USB stick that is delivered with this report.

2.3 FLOODING ACCIDENT RESPONSE

Despite the fact that the maritime sector is continuously investing in increasing and maintaining safety on board ships, additional effort is needed in the pathway towards zero-loss of life and zero-pollution. The highest risk for persons on board ships comes with flooding accidents, but

consequences may be reduced when appropriate actions are taken following such an accident, thus greatly reducing the probability of loss of life or damage to the environment.

The FLARE project will target a risk-based methodology for "live" flooding risk assessment and control, by developing a generic (all incidents in one model) and holistic (active and passive measures) risk model with potential application to new buildings and, which is totally new, to existing ships. Innovative technical solutions in ship concepts and equipment for risk containment and control will be accompanied by proposals for the revision of relevant IMO regulations towards a risk-based approach to contain and control risk in passenger ships from flooding incidents, thereby significantly contributing to the safety of both passenger and ship.

2.4 Project partners

BALance Technology Consulting GmbH, with its headquarters in Bremen, Germany, will coordinate the project in close cooperation with the University of Strathclyde, Department of Naval Architecture, Ocean and Marine Engineering. Nineteen other leading maritime stakeholders will contribute to the results of FLARE: Aalto University, Brookes Bell, Bureau Veritas Marine & Offshore, Carnival, Color Line Marine, DNV GL, Fincantieri, Hamburgische Schiffbau-Versuchsanstalt, ICAM Nantes, Lloyd's Register, MARIN, Meyer Werft, Meyer Turku, NAPA, SEA Europe, Chantiers de l'Atlantique, Rina Services, RCCL and Stena Line. This project has received funding from the European Union's Horizon 2020 research and innovation programme under Grant Agreement No 814753.

3 MODEL

3.1 General

A ship model was made to a geometric scale of 1:60 (Model number 10155). A part of the interior was modelled according to the flooding scenario as described in email dated 2 March 2020 of University of Strathclyde. The model is assembled from the following parts:

- The bow and stern are Styrofoam filled and shown in yellow in Figure 2–1.
- The floodable compartments are made from transparent PVC and are shown in green. The damage opening is forward of amidships. The opening is covered with a magnetic sheet at the start of the tests.
- Two lower sections (fore and aft) are Styrofoam filled and displayed with sand-colour in the figure.
- The sections are stiffened by two carbon fibre box beams.

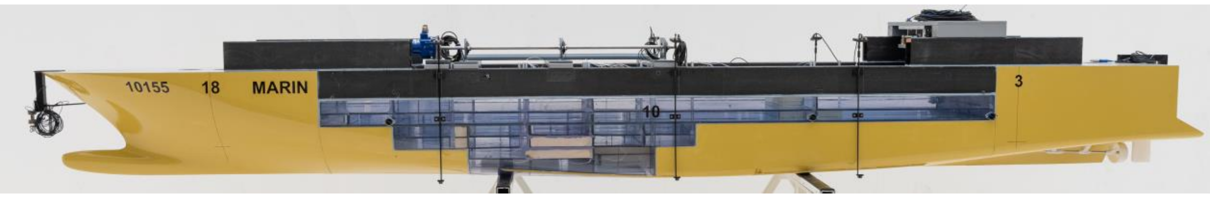

Figure 3-1: Side view of the model (intact side)

3.2 Breach

Figure 3-2 shows the breach in the model and the magnetic cover sheet that closes the breach at the start of the test. The size of the breach is given in the provided flooding scenario. The size was selected to provide suitable data that can be used to benchmark codes that simulate the flooding process. This does not reflect a realistic flooding scenario; it is unlikely that the side shell will be opened for such a large length and height.

At the start of the flooding of the model, the magnetic cover sheet was pulled upwards with a winch. The speed was about 2.5 m/s (model scale).

Figure 3-2: Breach

3.3 Compartments

Figure 3-2 shows the assembly of the compartments that are modelled in the flooding model. Each deck is denoted with a different colour. Figure 3-4 to Figure 3-9 show the individual decks.

The floodable compartments are made from transparent PVC. The thickness of these plates is 4mm. The (sub)compartments that are impermeable are filled with Styrofoam.

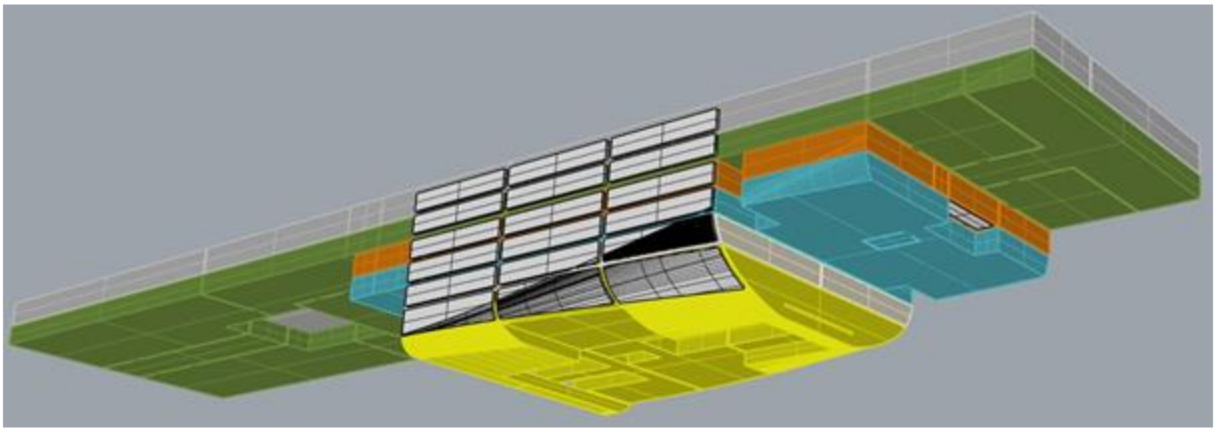

Figure 3-3: Assembly of compartments

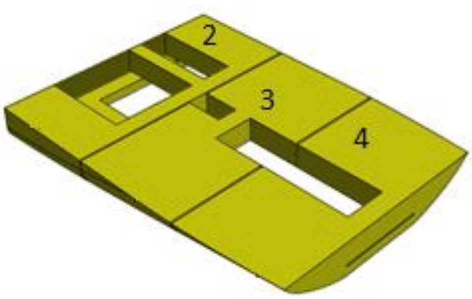

Figure 3-4: Compartments on decks 0 and 1

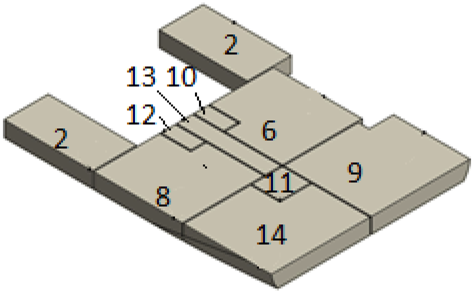

Figure 3-5: Compartments on deck 2

Note: At deck 2 the door opening at the centreline between Compartment 9 and 14 was not present in the model.

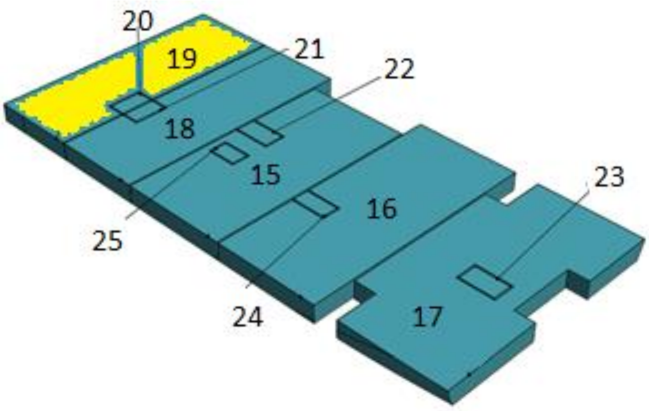

Figure 3-6: Compartments on deck 3

Compartment 18 was opened by the breach; this not in accordance with the given flooding scenario. The same is valid for compartment 33 on deck 4. The two compartments are marked yellow.

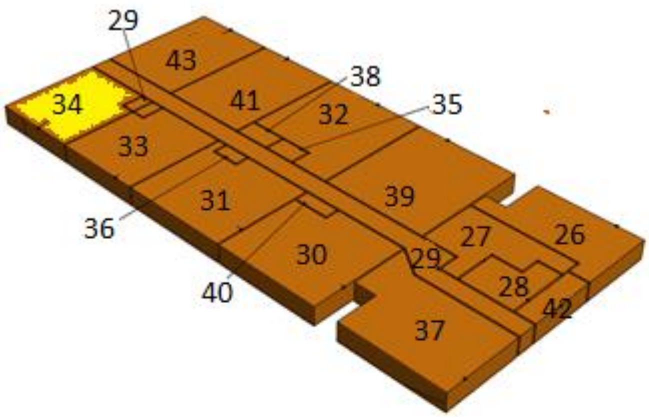

Figure 3-7: Compartments on deck 4

The geometry of deck 4 was used in the Fundamental Deck Flooding tests and is reported in Volume 2 of this report.

.

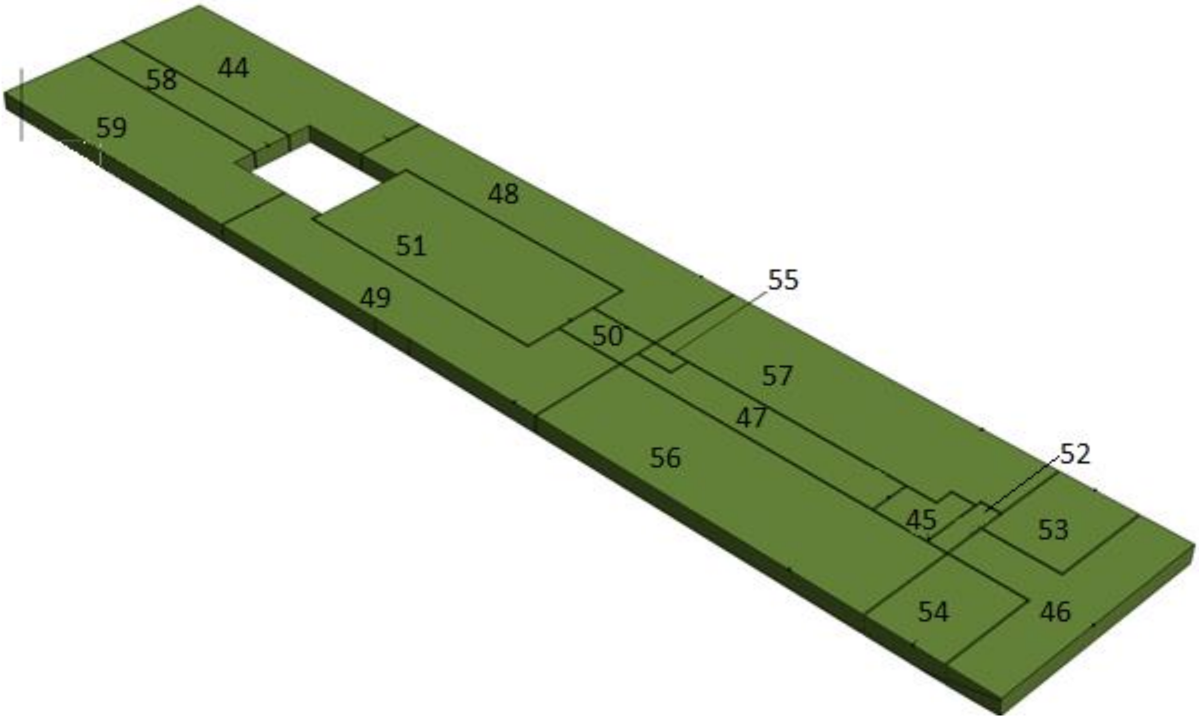

Figure 3-8: Compartments on deck 5

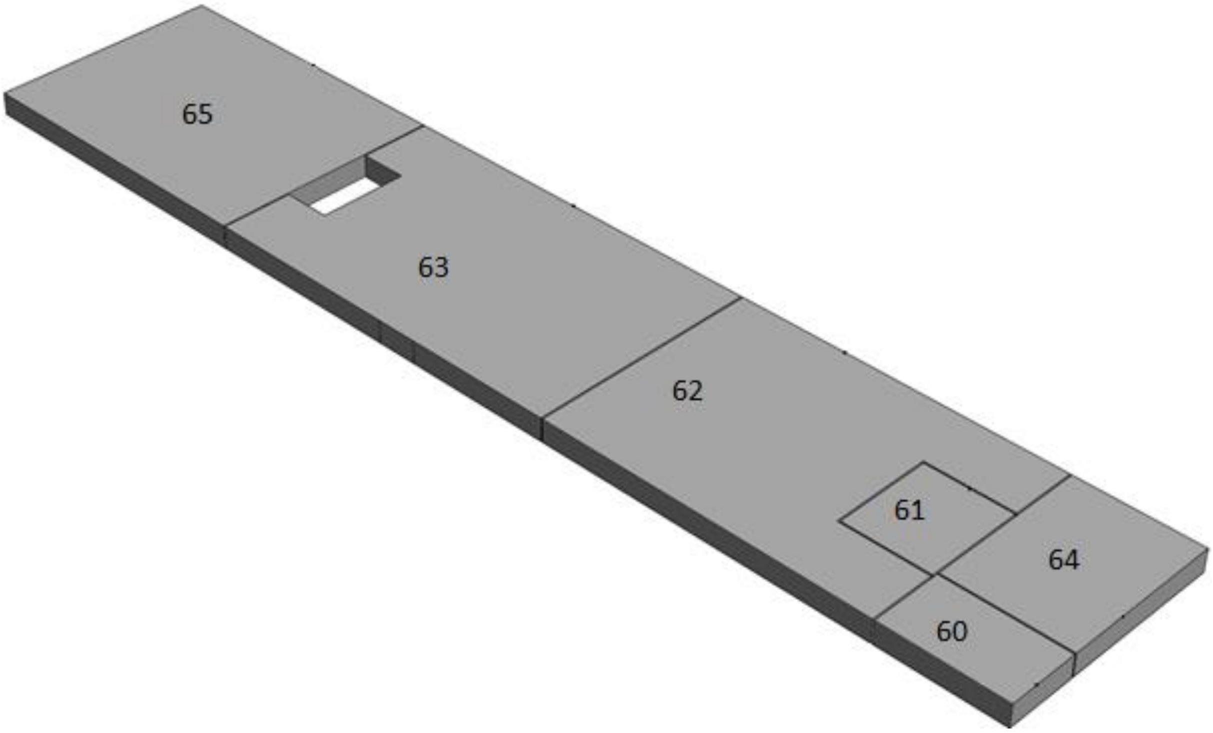

Figure 3-9: Compartments on deck 6

3.4 Ventilation pipes

The small diameter of the preinstalled ventilation pipes appeared to have a notable impact on the flooding speed. The air required some time to escape from the compartments. Hence, the compartments are vented, but not fully vented. Because the test results are to be used for benchmarking, the impact due to ventilation should be as small as possible.

This was solved by mounting external ventilation pipes to the model with a larger inner diameter of 17 mm. This is 1020 mm at full scale, which is expected to be a larger ventilation area than in reality for most of the compartments.

Figure 3-10: ventilation pipes

3.5 Appendages

The model is equipped with the following appendages:

- Passive rudders (rapid prototyping).
- Passive propeller arrangement (rapid prototyping).
- Wooden bilge keels with a total length of 90 m and a height of 430mm. The bilge keel is divided into a forward and aft part. The bilge keel is removed at the location of the damage opening.
- Drain plugs are fitted to enable drainage of all compartments after the tests.

3.6 Loading condition

The given loading conditions in the scenario are given Table 3-1. The table defines the type of capsize according to numerical assessments made by MSRC. The table indicates that a full scale change in vertical centre of gravity of 30mm will lead to a different capsize scenario. At model scale this is a difference of 0.5mm, and this is a smaller value than can be determined within the accuracy of the model tests. However, it indicates the sensitivity to changes in loading conditions in a flooding sequence.

It is believed that the KG location on full scale will not be known to the precision of 3cm, which makes, according to the dynamic flooding calculations of MSRC, the difference between a survival case or a capsize loss case.

Table 3-1: Provided loading conditions, intact KG values.

Case	KG [m]	T [m]	Trim [m]
Transient Capsize Case	17.1	8.2m	0
Transient Survival Case	17.0	8.2m	0
Progressive Flooding Loss	17.03	8.2m	0

Because of calculated sensitivity, the starting point was a centre of gravity of 17.0 m; based on the results of the tests, the CoG was adjusted and a new measurement in calm water was executed. In this way the CoG iterated to the values that were near the threshold of capsizing.

The properties of the loading condition are given in Table T 1 and Table T 2.

Note that in model tests the GM is measured via the inclination test. The intact KM is known from the hydrostatics, hence the intact KG is known when the GM is determined. The KG is not measured in dry condition. Table 3-2 summarises the results of the inclination tests.

Table 3-2: Summary of inclination tests.

Condition	Mass [t]	Transverse distance [m]	Heel [deg]	GM [m]
High GM	442800	24.8400	4.00	2.88
Intermediate GM	442800	24.8400	4.40	2.61
Low GM	442800	24.8400	4.78	2.41
Extra high GM	442800	24.8400	3.65	3.15

4 TEST SETUP AND FACILITY

4.1 Facility

This part of the test programme was executed in the Seakeeping and Manoeuvring Basin. This basin is equipped with a wave generator and a moving carriage. Current is mimicked by moving the model slowly through the basin in a soft spring mooring.

Figure 4-1: Seakeeping and Manoeuvring basin

4.2 Test setup

The vessel was kept at location by a soft spring mooring system. The mooring lines were connected at the bow and stern of the vessel. The angle of the mooring lines was 45 degrees with the centreline. Figure 4-2 and Figure 4-3 show a sketch of the mooring system and a photo of the model connected in the mooring.

Line stiffness: 241 kN/m

Pretension: 6516 kN

The stiffness of the lines was designed in such a way that resonance with the ship motions was avoided. The yaw motion is the shortest period in this type of mooring system; in the present setup the yaw period was about twice the natural period of roll with a yaw period of 37 s. The results of the mooring decay tests are included in Appendix II.

The mooring line attachment height on the vessel was located between the CoG and the waterline. The mooring lines run parallel to the calm water level.

A lightweight slack bundle of flexible measurement cables provided the transfer of data between the model and the carriage; care was taken that these wires did not restrict the motions of the model.

Four flexible synthetic safety wires were installed to retrieve the model at the end of the test and to make sure that the model did not sink or capsize in flooded condition.

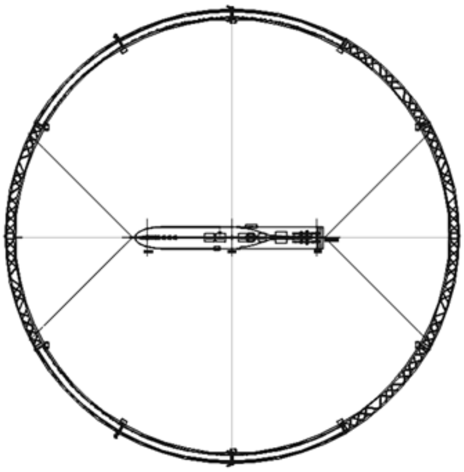

Figure 4-2: Soft spring mooring arrangement

Figure 4-3: Photo of the model in the test setup

5 MEASUREMENTS

The test setup was equipped with:

- An optical tracking system to measure the 6-DOF motions of the model in order to use the actual obtained position of the model in the test. Measured at a frequency of 100 Hz. The motions measured are translated to the CoG of the model.
- Incident wave height in the basin at 3 locations to measure the incoming wave. Measured at a frequency of 50 Hz.
- The relative wave elevation was measured at 35 locations inside the model; the locations of the wave probes are given in Table T 6 in Appendix I.
- Relative wave elevation at 6 positions at the side shell of the vessel. Measured at a frequency of 200 Hz.
- 3 DoF accelerations were measured at 4 positions.
- 3 DoF mooring forces (Surge, Sway and Yaw).

Drawings of the wave probe instrumentation can be found on the memory stick that is delivered with this report.

6 AXIS SYSTEMS AND SIGN CONVENTION

The ITTC axis and heading system was used in this report, as Figure 6-1.

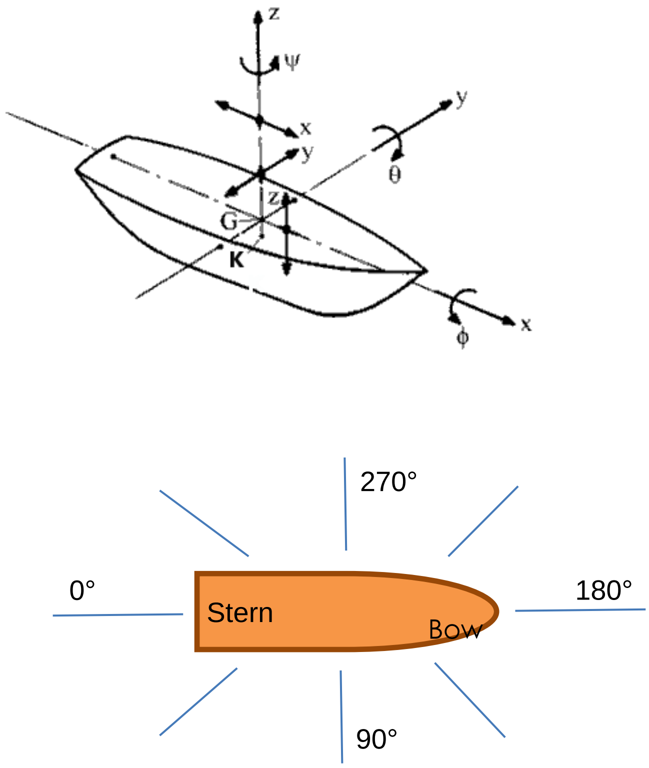

Figure 6-1: Axis system and heading convention.

The origin of the vessel is at the aft perpendicular, centreline and keel for longitudinal, transverse and vertical directions respectively.

Draught is defined as the vertical distance between the keel and calm water level.

7 TEST PROGRAMME AND PROCEDURES

7.1 Summary of the test programme

A total of 48 flooding tests were executed. Of which:

- 4 decay tests (roll and mooring)
- 10 tests in calm water
- 12 tests with high GM in irregular waves
- 12 tests with intermediate GM in irregular waves
- 4 tests with high GM in irregular waves in current
- 2 tests with extra high GM in waves
- 4 tests with High Gm in head seas

7.2 Test procedures

The following test procedures were followed:

Loading condition check

After each change in the loading condition the metacentric height was measured in an inclining test.

- At the start of the test a ballast weight which was already part of the loading condition was positioned at the side of the model. The static heel angle was measured.
- The weight was moved to the other side of the vessel over a known distance; again the static heel angle was measured.
- The ballast weight was mounted at its original position to establish zero heel.
- A roll decay was executed to measure the natural period of roll.

Flooding tests

Unless stated otherwise, the following steps were conducted in each test:

A. The model was prepared for the tests and was suspended above the water
B. The measurement starts
C. The wave generator starts and sufficient waiting time is taken into account for the waves to develop at the location of the model
D. The model is lowered into the water
E. The carriage starts moving at the given current speed
F. After a short waiting time the breach opens

G. The test ends after about 60 minutes full scale time, or if a roll angle of 40 deg is reached, whichever came first

H. The model is lifted out the water and prepared for the next test

8 SUMMARY AND DISCUSSION

This section gives a summary of the main observations, including a brief discussion.

8.1 Roll damping

Roll damping is discussed in Volume 3 of this report.

8.2 Tests in calm water

Tests in calm water were executed to find the lowest GM where the model does not capsize in calm water. The steps in the value of the GM were about 0.2m full scale; compared to the sensitivity, as described in the given flooding scenario, these are relatively large. The Low GM condition (GM=2.41 m) capsizes in calm water shortly after opening the breach. The Intermediate GM was selected to be the lowest GM value to be tested in waves.

Figure 8-1 shows the time trace of the heel angle in the calm water conditions tested. The left part of the graph is zoomed in at the moment after the breach opens; the right shows the whole time trace measured. The initial heel after opening the breach decreases with the GM value and is about 22 deg in the Extra High GM and 32 deg in the Low GM condition.

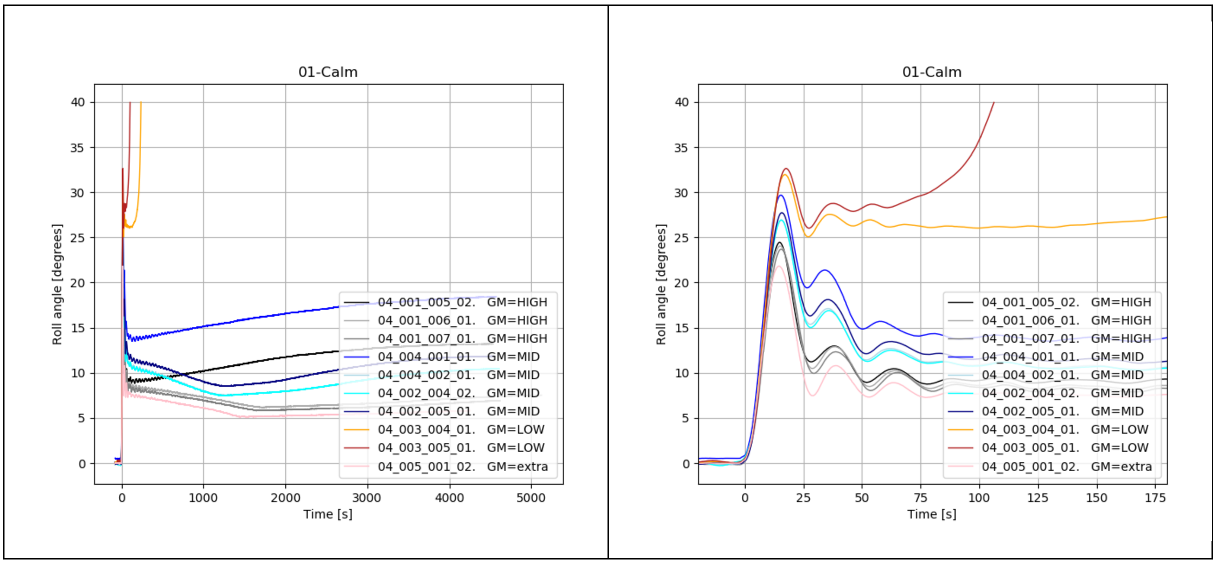

Figure 8-1: Heel angle in calm water

The heel angles show also a gradual change in the heel angle after the peak. This is because of leakage between some of the compartments. For instance, Figure 8-2 shows the water level at Rel 19, which is in the most forward compartment on deck 3. This compartment could not be filled through an internal opening. In a later investigation of the model some leakage points were found.

Because of these unintended compartment fillings the results in the present test programme are less suitable for benchmarking. However the impact of the differences in test conditions can still be investigated; the deviation is the same in all tests.

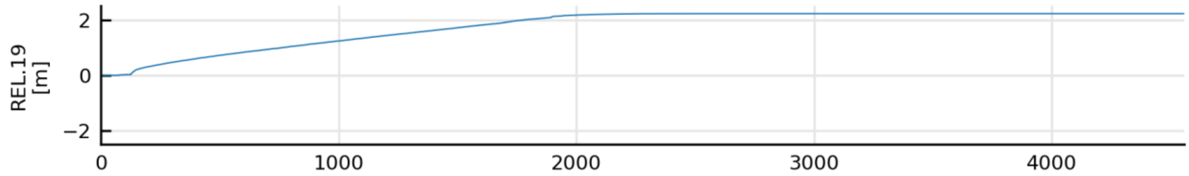

Figure 8-2: Water level at Rel 19 test 30703_07SMB_04_001_005_02 (High GM)

8.3 Intermediate GM

Figure 8-3 shows the heel angle in waves in the Intermediate GM loading condition (GM=2.61 m). Each wave (Hs and Tp combination) is denoted with a dedicated colour. It can be seen that colours are grouped, which means that the different wave seeds give similar results. Looking at the Hs=4m waves, the wave steepness seems to have a large impact: the steep waves result in an early capsize. At Hs=7m, this difference is less clear. The initial heel angle after the opening of the breach ranges between 25 and 31 deg.

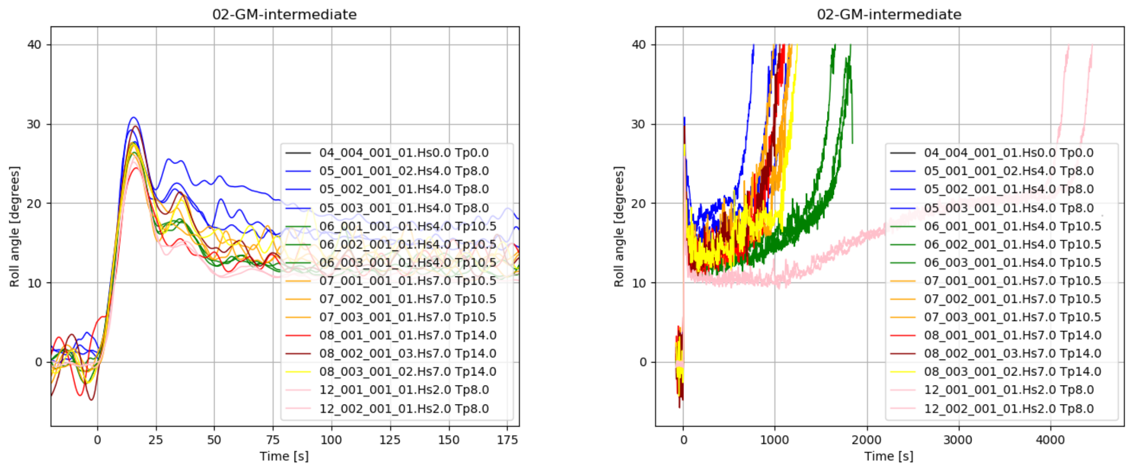

Figure 8-3: Heel angle – Intermediate GM in waves

8.4 High GM

Figure 8-4 shows the heel angle of the vessel in the High GM loading condition (GM=2.88 m). The 0.27 m increase of the GM relative to the Intermediate GM reduces the initial maximum heel angle to 27 deg and the vessel does not capsize in a significant wave height of 4 m. In a wave height of 7 m, the time to capsize is roughly doubled.

The impact of the wave steepness is however reversed: the longer waves with a peak period of 14 seconds result in a greater increase of the heel angle. Probably this is caused by the vessel having higher roll motions as this wave period is closer to the vessel's natural period of roll.

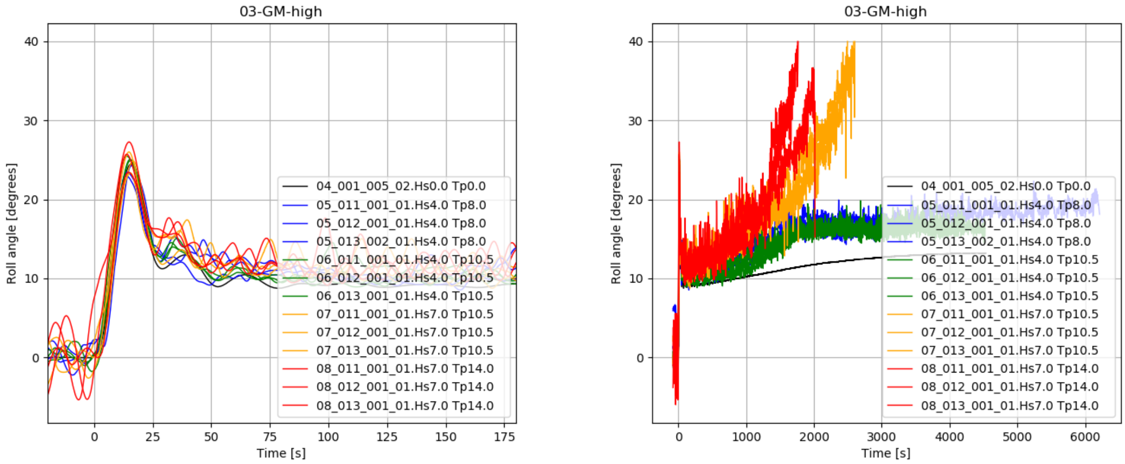

Figure 8-4: Heel angle – High GM in waves

8.5 High GM - Drift

Figure 8-5 shows the heel angle of the High GM loading condition in waves, while towed in transverse direction with the waves. It is expected that the simulation of drift in waves will reduce the ingress. However, the results are very similar to those of the test at zero transverse speed and therefore do not confirm the expectations.

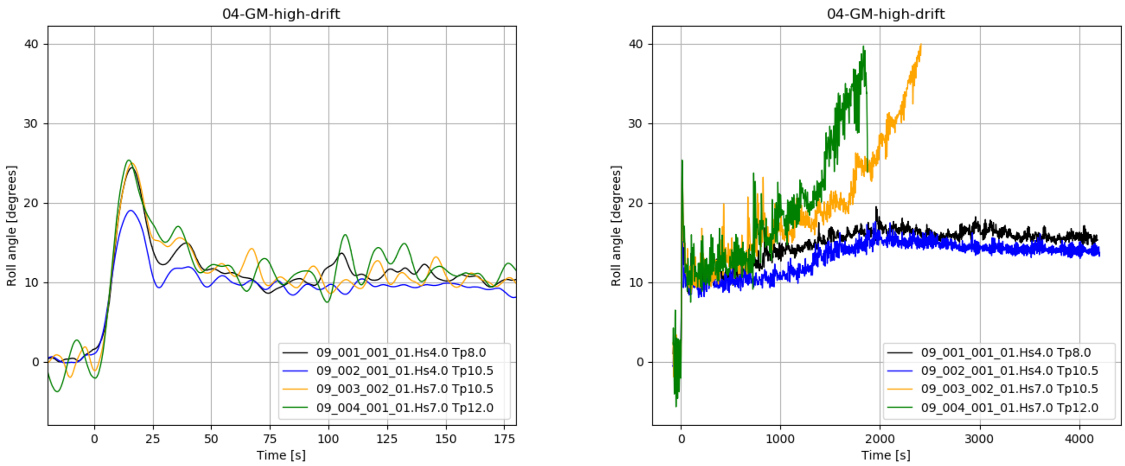

Figure 8-5: Heel angle – High GM in waves at 1m/s drift speed

8.6 High GM - Leeward

Figure 8-6 shows the heel angle in the High GM loading condition with the breach at the leeward side of the model. The present setup was tested with only 7 m waves. These tests did not result in a capsize.

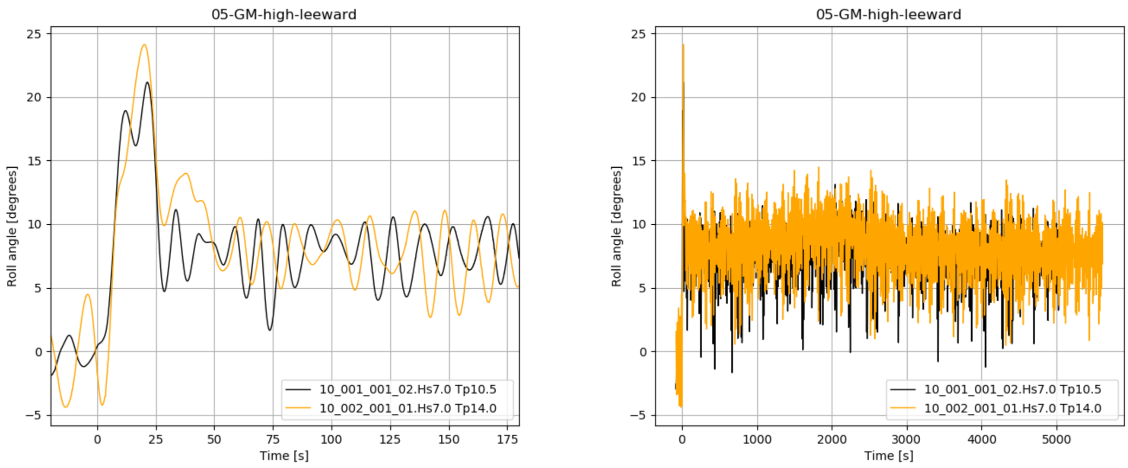

Figure 8-6: Heel angle – High GM breach at the leeward side

8.7 High GM – Head seas

Figure 8-7 shows the heel angle in the High GM in head seas; the conditions tested did not result in a capsize. Remarkable are the roll motions which are present in the head seas condition with a wave peak period of 14 s. The roll motions are apparently caused by the large opening at the starboard side of the model which make the vessel asymmetric. It must be noted that the breach in the model is very large and does not represent a condition that may occur in reality.

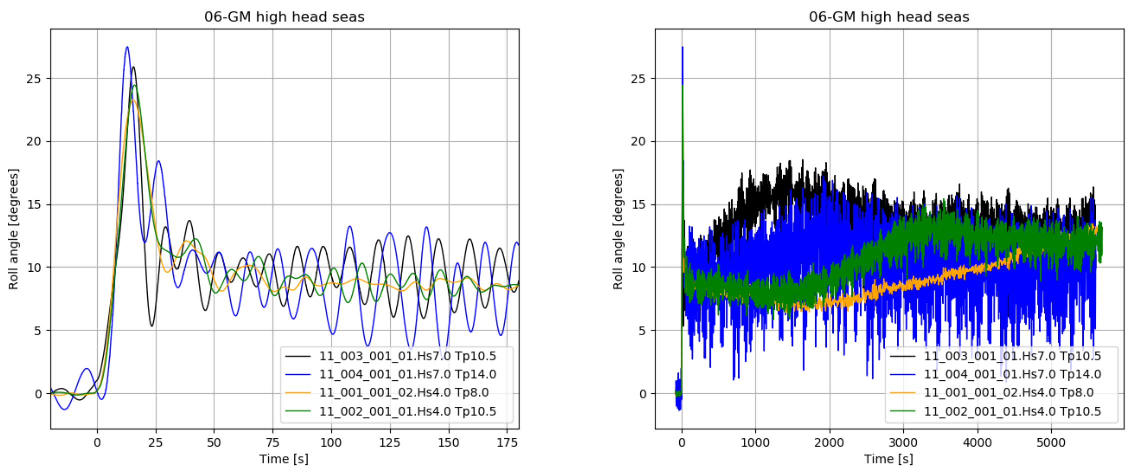

Figure 8-7: Heel angle – High GM in head seas

8.8 Extra high GM in waves

Figure 8-8 shows the heel of the Extra high GM loading condition (GM=3.15 m) in calm water and a wave height of 7 m. The initial heel angle at this GM was between 21 and 23 deg. In waves, the heel gradually increases to 15 deg and stays constant.

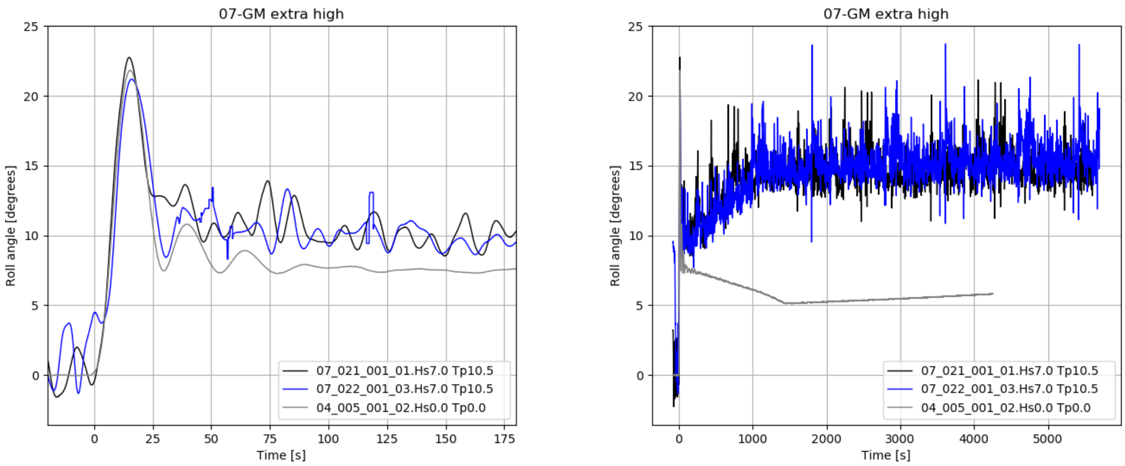

Figure 8-8: Heel angle – Extra high GM in waves

9 CONCLUSION

Model tests were conducted with a model of a cruise vessel with floodable internal compartments to investigate flooding in waves. The goal of the tests was to generate a data set which can be used to benchmark flooding software. Based on the results of the tests the following conclusions can be drawn:

- The flooding openings deviated at some points from the provided scenario and the most forward compartment on deck 3 had some leakage. This should be taken into account if used for benchmarking purposes. The tests in Volume 5 are in line with the given flooding scenario.
- As expected the metacentric height was the main driver in the capsizing behaviour. Higher metacentric heights resulted in fewer wave conditions where capsizes were observed.
- With a GM of 2.61 m (Intermediate), the vessel capsizes under progressive flooding.
- With a GM of 2.88 m (High), the vessel capsizes under progressive flooding, with a time to capsize about twice as long compared to GM of 2.61 m.
- With a GM of 3.15 m (Extra high), the vessel did not capsize. (The names of the conditions such as "Extra high" and "Intermediate GM" refer to their relative magnitude in the present test programme and do not correlate to loading conditions in reality)
- Wave realisations of irregular waves with a different seed resulted in the same outcome with respect to capsizes.
- A drift speed of 1m/s did not have a notable impact on the results.
- No capsizes were observed in head seas and in tests with the breach at the leeward side.
- In the high GM case the vessel capsizes when the damage is facing the waves, but remains afloat when the damage location is on leeward side. This points to progressive flooding onto the main deck due to relative wave action, that does not occur when the damage is to leeward.
- Given the previous conclusion, the survivability of the cruise vessel is thus noticeable different depending on the ship heading, and this should be respected in the capsize probability calculations in the framework.

Appendix I – Tables

Table T 1: Loading condition

Main particulars			
Designation	**Symbol**	**Magnitude**	**Unit**
Length	Lpp	270	m
Breadth	B	35	m
Height	H	12.6	m
Draught fore	T fore	8.2	m
Draught aft	T aft	8.2	m
Displacement mass	displ	52850	ton
VCG position from Keel (approx.)	KG	17	m
LCG position from AP	LCG	127.92	m
Radius of inertia for roll	Kxx	13.904	m
Radius of inertia for pitch	Kyy	70.708	m
Radius of inertia for yaw	Kzz	71.223	m

Table T 2: GM variations

Metacentric height	
Name	**GM[m]**
Extra High	3.15
High	2.88
Intermediate	2.61
Low	2.41

Note: The name of the conditions such as "Extra high" and "Intermediate GM" refer to their relative magnitude in the present test programme and do not correlate to loading conditions in reality

Table T 3: location of measurement devices

Wave probes	X [m]	Y [m]	Z [m] (zero level)	Compartment number	Deck
Number					
REL.1	142.92	-15	0.18	2	1
REL.2	157.2	-15	1.56	3	1
REL.4	157.2	-7.5	1.56	3	1
REL.5	172.74	-7.5	0.18	4	1
REL.6	142.92	15	1.56	2	1
REL.7	157.2	15	1.56	3	1
REL.8	172.74	15	0.18	4	1
REL.9	157.2	-15	5.3	8	2
REL.10	172.74	-15	5.3	9	2
REL.11	157.2	-15	8.22	15	3
REL.12	157.2	-7.5	5.3	8	2
REL.13	172.74	-7.5	5.3	9	2
REL.14	157.2	7.5	5.3	6	2
REL.15	172.74	7.5	5.3	9	2
REL.16	130.08	-15	8.22	19	3
REL.17	142.92	-15	8.22	18	3
REL.18	172.74	-15	8.22	16	3
REL.19	189.18	-15	8.22	-	3
REL.20	130.08	0	8.22	19	3
REL.21	142.9	0	8.22	18	3
REL.22	157.2	0	8.22	15	3
REL.23	172.74	0	8.22	16	3
REL.24	186.18	0	8.22	-	3
REL.25	130.2	-14.52	11	34	4
REL.26	142.92	-14.52	11	33	4
REL.27	157.2	-14.52	11	31	4
REL.28	172.74	-14.52	11	30	4
REL.29	189.6	-11.64	11	37	4
REL.30	130.2	-1.5	11	29	4
REL.31	172.74	-1.5	11	29	4
REL.32	86.22	-14.52	13.4	59	5
REL.33	142.92	-14.52	13.4	49	5
REL.34	189.6	-14.52	13.4	56	5
REL.35	142.92	-14.52	16.8	63	6
REL.36	189.54	-14.52	16.8	62	6
REL.PSA	82.2	18	8.2	outside	-
REL.SBA	82.2	-18	8.2	outside	-
REL.PSM	129	18	8.2	outside	-
REL.SBM	129	-18	8.2	outside	-
REL.PSF	190	18	8.2	outside	-
REL.SBF	190	-18	8.2	outside	-

Table T 4: Decay tests

Decay tests	Type
Test No	
30703_07SMB_03_001_001_02_1	Roll
30703_07SMB_03_002_001_01_1	Surge
30703_07SMB_03_003_001_01_1	Sway
30703_07SMB_03_004_001_01_1	Yaw

Table T 5: Model in calm water

Calm water	
Test No	**GM**
30703_07SMB_04_001_005_02	HIGH
30703_07SMB_04_001_006_01	HIGH
30703_07SMB_04_001_007_01	HIGH
30703_07SMB_04_004_001_01	MID
30703_07SMB_04_004_002_01	MID
30703_07SMB_04_002_004_02	MID
30703_07SMB_04_002_005_01	MID
30703_07SMB_04_003_004_01	LOW
30703_07SMB_04_003_005_01	LOW
30703_07SMB_04_005_001_02	Extra HIGH

Table T 6: High GM in waves

High GM - tests in waves		
Test No	**Hs[m]**	**Tp[s]**
30703_07SMB_05_011_001_01	4	8
30703_07SMB_05_012_001_01	4	8
30703_07SMB_05_013_002_01	4	8
30703_07SMB_06_011_001_01	4	10.5
30703_07SMB_06_012_001_01	4	10.5
30703_07SMB_06_013_001_01	4	10.5
30703_07SMB_07_011_001_01	7	10.5
30703_07SMB_07_012_001_01	7	10.5
30703_07SMB_07_013_001_01	7	10.5
30703_07SMB_08_011_001_01	7	14
30703_07SMB_08_012_001_01	7	14
30703_07SMB_08_013_001_01	7	14

Table T 7:Intermediate GM in waves

Intermediate GM - tests in waves		
Test No	**Hs[m]**	**Tp[s]**
30703_07SMB_05_001_001_01	4	8
30703_07SMB_05_002_001_01	4	8
30703_07SMB_05_003_001_01	4	8
30703_07SMB_06_001_001_01	4	10.5
30703_07SMB_06_002_001_01	4	10.5
30703_07SMB_06_003_001_01	4	10.5
30703_07SMB_07_001_001_01	7	10.5
30703_07SMB_07_002_001_01	7	10.5
30703_07SMB_07_003_001_01	7	10.5
30703_07SMB_08_001_001_01	7	14
30703_07SMB_08_002_001_03	7	14
30703_07SMB_08_003_001_02	7	14

Table T 8:High GM in waves – 1m/s current

High GM - tests in waves - 1m/s drift		
Test No	**Hs[m]**	**Tp[s]**
30703_07SMB_09_001_001_01	4	8
30703_07SMB_09_002_001_01	4	10.5
30703_07SMB_09_003_001_01	7	10.5
30703_07SMB_09_004_001_01	7	14

Table T 9: Extra High GM in waves

High GM - extra high		
Test No	**Hs[m]**	**Tp[s]**
30703_07SMB_07_021_001_01	7	10.5
30703_07SMB_07_022_001_02	7	10.5

Table T 10: High GM in head seas

High GM - head seas		
Test No	**Hs[m]**	**Tp[s]**
30703-07SMB-11-001-001-02	4	8
30703-07SMB-11-002-001-01	4	10.5
30703-07SMB-11-003-001-01	7	10.5
30703-07SMB-11-004-001-01	7	14

Appendix II – Decay tests

Flare 30703		
Roll decay - Vs = 0 kn		
Test ID: 30703_07SMB_03_001_001_02_1 - Intact, config 1 - Soft mooring		

Parameter	Magnitude	Unit
P	0.205	-
Q	0.018	1/deg
BCrit	7.70E+06	kNm/(rad/s)
BLin	3.3	%*
BQua	1.0	%/(deg·rad/s)*
Natural Period	18.3	s
Damped Period	18.4	s

* percentage critical damping

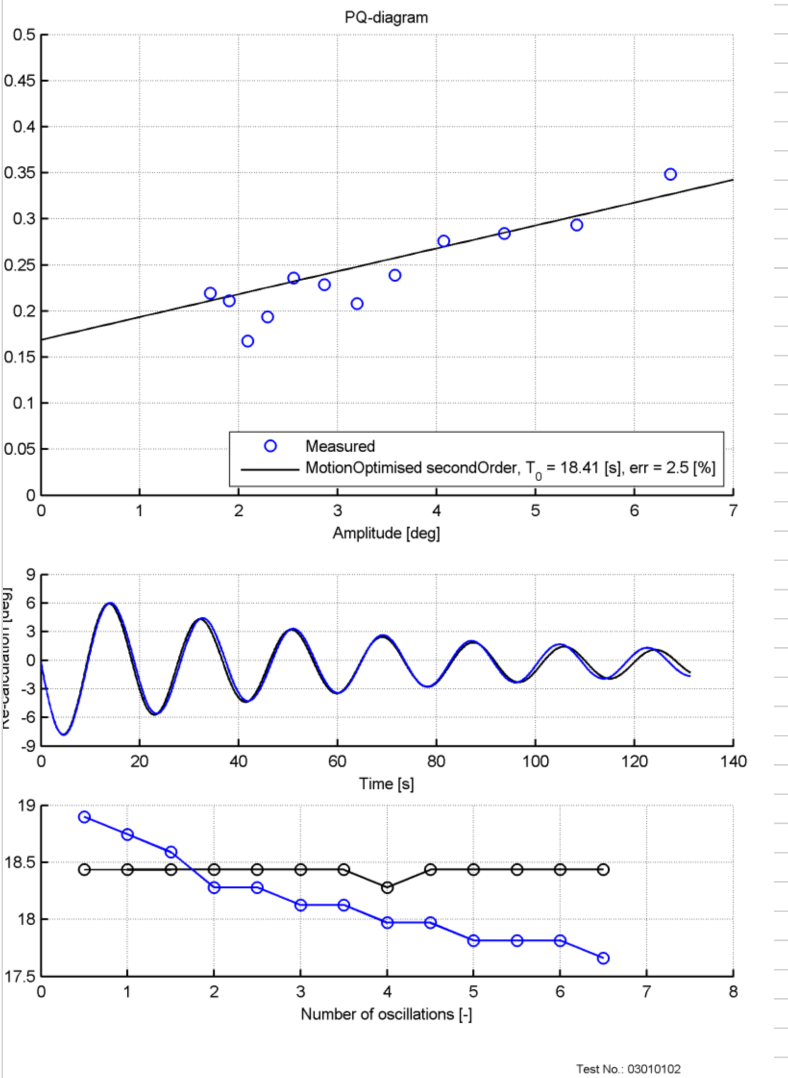

Flare 30703
Surge decay - Vs = 0 kn
Test ID: 30703_07SMB_03_002_001_01_1 - Intact, config 1 - Soft mooring

Parameter	Magnitude	Unit
P	0.117	-
Q	0.000	1/m
BCrit	2.75E+07	kN/(m/s)
BLin	1.9	%*
BQua	0.0	%/(m·rad/s)*
Natural Period	65.5	s
Damped Period	65.5	s

* percentage critical damping

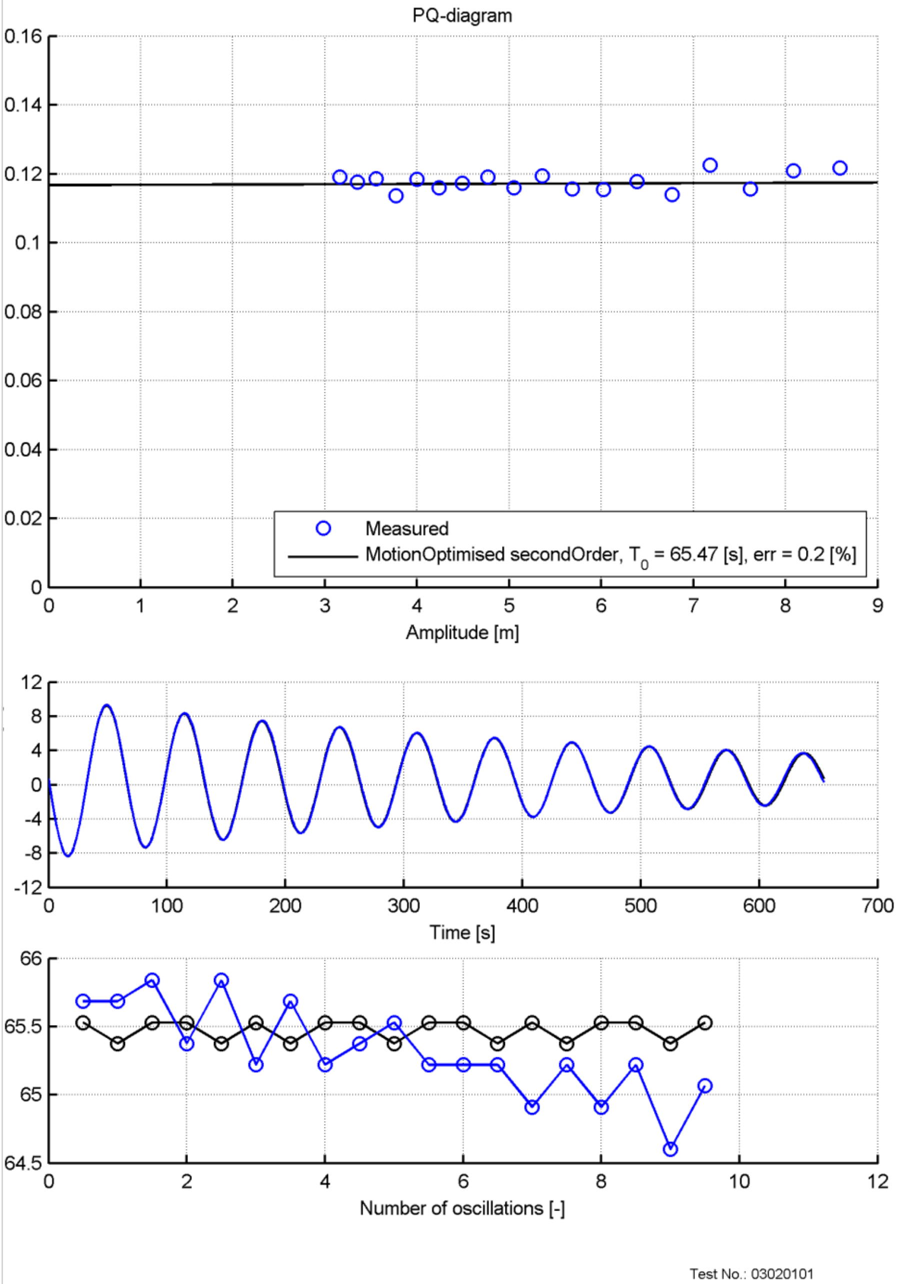

Flare 30703

Sway decay - Vs = 0 kn

Test ID: 30703_07SMB_03_003_001_01_1 - Intact, config 1 - Soft mooring

Parameter	Magnitude	Unit
P	0.099	-
Q	0.048	1/m
BCrit	3.52E+07	kN/(m/s)
BLin	1.6	%*
BQua	11.9	%/(m·rad/s)*
Natural Period	83.9	s
Damped Period	83.9	s

* percentage critical damping

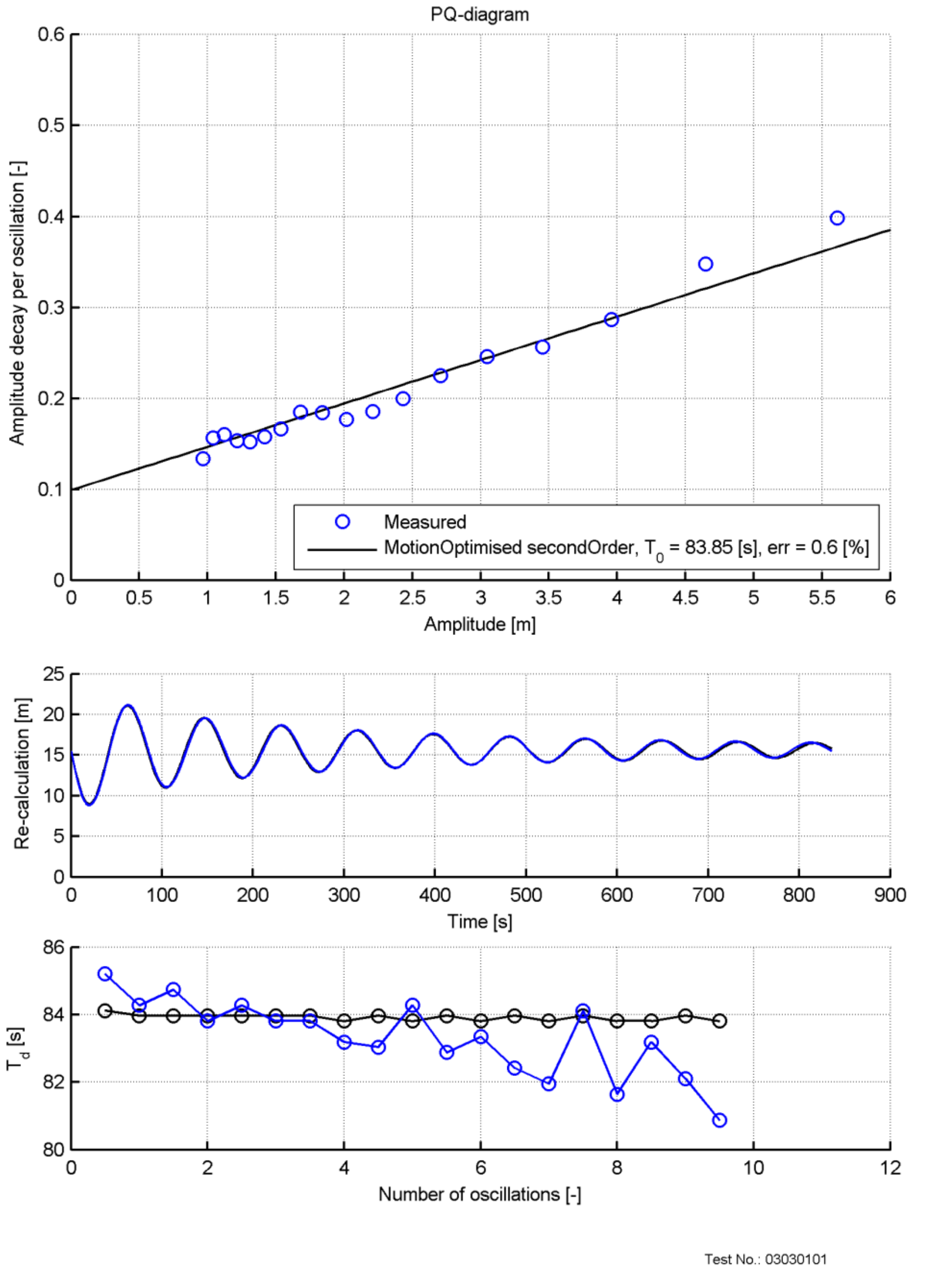

Flare 30703		
Yaw decay - Vs = 0 kn		
Test ID: 30703_07SMB_03_004_001_01_1 - Intact, config 1 - Soft mooring		

Parameter	Magnitude	Unit
P	0.018	-
Q	0.265	1/deg
BCrit	1.52E+07	kNm/(rad/s)
BLin	0.3	%*
BQua	28.7	%/(deg·rad/s)*
Natural Period	36.3	s
Damped Period	36.3	s

* percentage critical damping

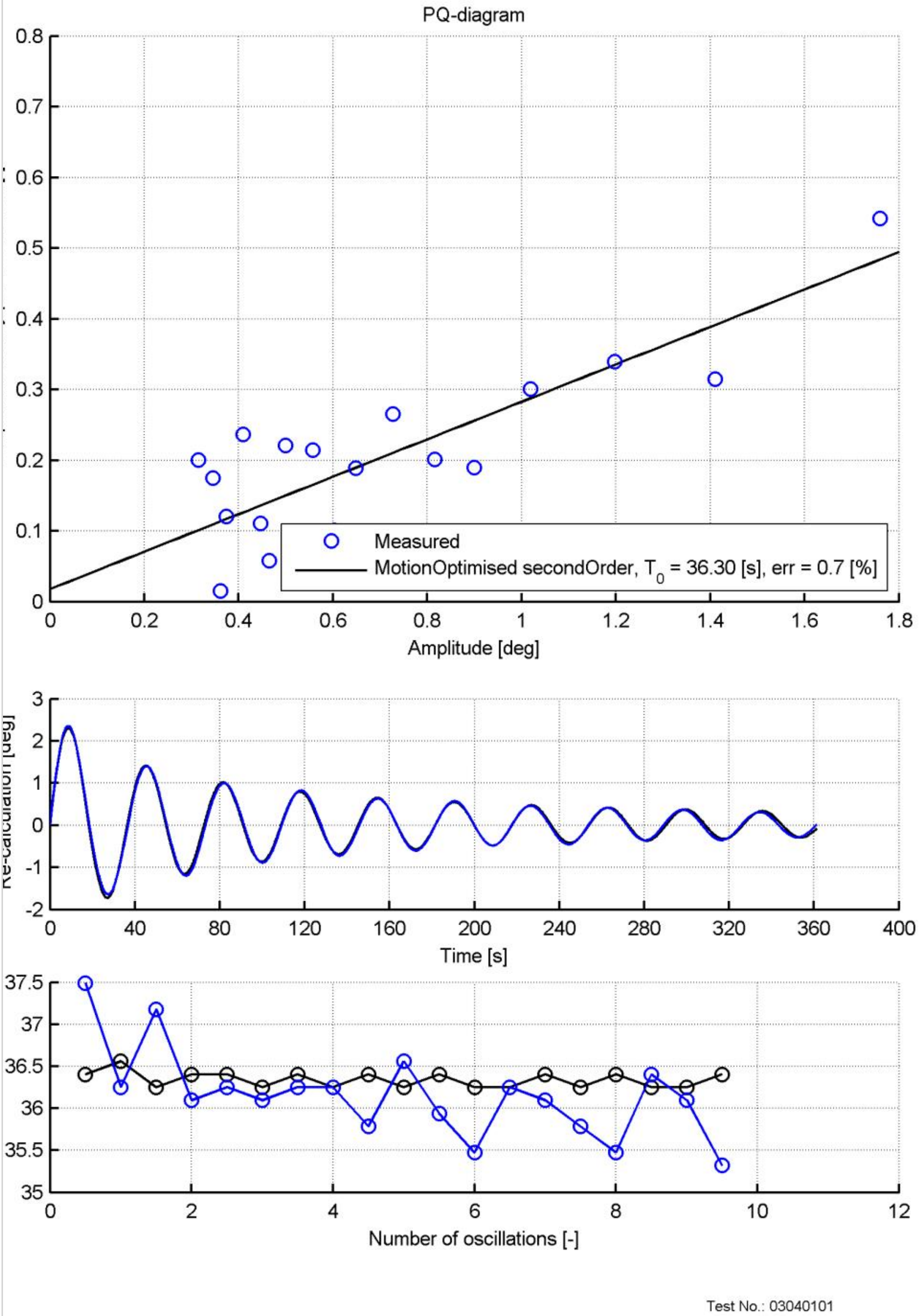

Acronym: FLARE
Project full title: Flooding Accident REsponse
Grant agreement No. 814753
Coordinator: BALance Technology Consulting GmbH

Deliverable 4.2 – Model tests

Volume 5 – Cruise ship flooding II

The project has received funding from the European's Horizon 2020 research and innovation programme (Contract No.: 814753)

Duration: 36 months - Project Start: 01/06/2019 - Project End: 31/05/2022

Deliverable data

Deliverable No	4.2 Volume 5		
Deliverable Title	Model tests: Cruise ship flooding II		
Work Package no: title	WP4.2 Model tests		

Dissemination level	Public	**Deliverable type**	Report
Lead beneficiary	HSVA		
Responsible author	R. van Basten Batenburg		
Co-authors	-		
Date of delivery	25-11-2020		
Approved	**Name (partner)**		**Date [DD-MM-YYYY]**
Peer reviewer 1	O. Rognebakke (DNVGL)		13-01-2021
Peer reviewer 2	O. K. Olufsen (DNVGL)		13-01-2021

Document history

Version	**Date**	**Description**
1	**24 Nov. 20**	Draft
2	**25 Nov. 20**	For peer review
2	**29 Nov. 20**	Final

The research leading to these results has received funding from the European Union Horizon 2020 Programme under grant agreement n° 814753.
This report reflects only the author's view. INEA is not responsible for any use that may be made of the information it contains.

CONTENTS

List of symbols and abbreviations

Cd	Discharge coefficient
CoG	Centre of Gravity
DoF	Degree of Freedom
ITTC	International Towing Tank Conference
CFD	Computational Fluid Dynamics
GM	Metacentric height
RAO	Response Amplitude Operator
TD	Time domain

1 EXECUTIVE SUMMARY

The present report describes a series of model tests that focus on the flooding of cruise ships that are executed within the EU FLARE project. The goal of the tests is to provide data for benchmarking and verification of the results of numerical codes that simulate the flooding process.

The present volume describes a second test programme with an improved ship model. This was executed based on the results of the tests reported in Volume 4.

Figure 1-1 Model in irregular waves

1.1 Problem definition

- In the development and verification of codes that assess flooding of ships it is required to benchmark the results of numerical simulations and to gain insight into the most important drivers in the flooding of cruise vessels.

1.2 Technical approach and work plan

- A ship model with a floodable internal geometry was built to simulate a given flooding scenario.
- Basin tests were executed in calm water and a selection of irregular waves for a range of metacentric heights.
- The measurements were analysed and discussed.

1.3 Results

- The measurements contribute to the understanding of the most important drivers in the flooding of cruise vessels.

1.4 Conclusions

- As expected the metacentric height was the main driver in the capsizing behaviour and time to capsize. Higher metacentric heights resulted in fewer wave conditions where capsizes were observed, and longer survival times
- The tests were quite consistent: different realisations of an irregular wave condition, with a different seed, always resulted in the same outcome with respect to capsizes and time to capsize..

- The wave period did not seem to have a clear impact on the capsizes and the time to capsize.
- The present results are obtained with a slightly different internal floodable space than the results presented in Volume 4. It led to similar capsize behaviour and time to capsize for the intermediate GM values (GM=2.50 m now versus 2.88 m (High GM in previous test programme) and GM=2.36 m versus GM 2.61 m (Intermediate GM in previous test programme)). Hence, the internal flooding had a noticeable effect
- With a GM of 2.27 m immediate capsize in waves occurred after the first water ingress and first heel towards the damage. The vessel recuperated to a safe upright flooding in calm water condition, but not in waves. The vessel capsizes under transient flooding.
- With a GM of 2.36 m, the vessel capsizes under progressive flooding.
- With a GM of 2.50 m, the vessel capsizes under progressive flooding, with a time to capsize about twice as long compared to GM of 2.36 m
- With a GM between 2.36 m and 2.93 m, the vessel reaches a large heel towards the damage in calm water, but always restores to an stable floating condition afterwards.
- The metacentric height was lower than in the previous tests. With a difference of about 0.3 m the behaviour of the two models was similar with respect to observed capsizes in specific wave conditions and the time to capsize.

2 INTRODUCTION

2.1 General

The goal of this work package is to provide measurements that can be used to benchmark simulation software that is able to predict the flooding of cruise or Ropax vessels.

Volumes 1 to 5 describe the model tests that were executed for cruise vessels by MARIN. Volumes 6 to 8 describe the model tests that were executed to investigate the flooding of Ropax vessels. The latter tests were executed by HSVA.

Volumes 1 to 5 describe

1. Fundamental compartment flooding
2. Deck flooding
3. Fundamental hydrodynamics
4. Cruise ship flooding (Part 1)
5. **Cruise ship flooding (Part 2)**

The model information, measured data and videos of the present model tests are provided on a USB memory stick. An HTML menu provides the metadata of each test and easy access of the results.

2.2 Volume 5

The present report describes the second series of model tests that focus on the flooding of a cruise ship model that was selected within the EU FLARE project. The goal of the tests is to provide data for benchmarking and verification of the results of numerical codes that simulate the flooding process.

The model is based on the flooding scenario as provided by University of Strathclyde. The model is a ship model in which all the compartments and openings flooded in this scenario are modelled.

Based on the measurements as reported in Volume 4, it was decided to execute a second set of flooding tests because the flooding scenario deviated from the desired flooding scenario. Some of the openings were not modelled according to specifications and leakage between some compartments was found to have occurred unnoticed during the tests.

The test setup and adopted approaches are described in chapters 3 to7; a summary of the results including a concise discussion of the results is given in chapter 8. The analysed data and videos are included on a USB stick that is delivered with this report.

2.3 FLOODING ACCIDENT RESPONSE

Despite the fact that the maritime sector is continuously investing in increasing and maintaining safety on board ships, additional effort is needed in the pathway towards zero-loss of life and zero-pollution. The highest risk for persons on board ships comes with flooding accidents, but

consequences may be reduced when appropriate actions are taken following such an accident, thus greatly reducing the probability of loss of life or damage to the environment.

The FLARE project will target a risk-based methodology for “live” flooding risk assessment and control, by developing a generic (all incidents in one model) and holistic (active and passive measures) risk model with potential application to new buildings and, which is totally new, to existing ships. Innovative technical solutions in ship concepts and equipment for risk containment and control will be accompanied by proposals for the revision of relevant IMO regulations towards a risk-based approach to contain and control risk in passenger ships from flooding incidents, thereby significantly contributing to the safety of both passenger and ship.

2.4 Project partners

BALance Technology Consulting GmbH, with its headquarters in Bremen, Germany, coordinates the project in close cooperation with the University of Strathclyde, Department of Naval Architecture, Ocean and Marine Engineering. Nineteen other leading maritime stakeholders will contribute to the results of FLARE: Aalto University, Brookes Bell, Bureau Veritas Marine & Offshore, Carnival, Color Line Marine, DNV GL, Fincantieri, Hamburgische Schiffbau-Versuchsanstalt, ICAM Nantes, Lloyd’s Register, MARIN, Meyer Werft, Meyer Turku, NAPA, SEA Europe, Chantiers de l’Atlantique, Rina Services, RCCL and Stena Line. This project has received funding from the European Union’s Horizon 2020 research and innovation programme under Grant Agreement No 814753.

3 MODEL

3.1 General

A ship model was made to a geometric scale of 1:60 (Model number 10155). A part of the interior was modelled according to the flooding scenario as described in email dated 2 March 2020 of University of Strathclyde. The model is assembled from the following parts:

- The bow and stern are Styrofoam filled and shown in yellow in Figure 3–1.
- The floodable compartments are made from transparent PVC The opening is covered with a magnetic sheet at the start of the tests.
- Two lower sections (fore and aft) are Styrofoam filled
- The sections are stiffened by two carbon fibre box beams on top of the model.

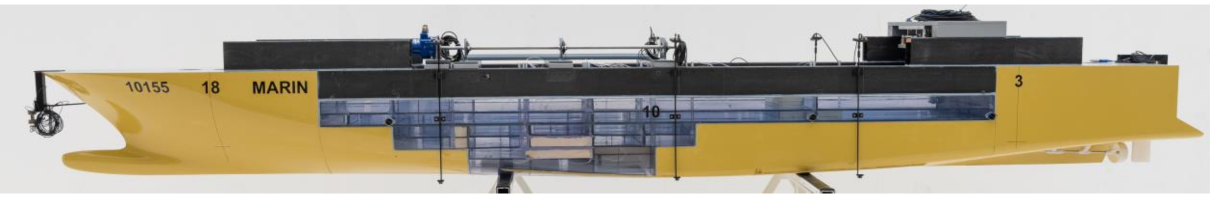

Figure 3-1: Side view of the model (intact side) without ventilation pipes

The changes to the model compared to the previous set of model tests (Volume 4) are described in Section 3.3

3.2 Breach

Figure 3-2 shows the breach in the model and the magnetic cover sheet that closes the breach at the start of the test. The size of the breach is given in the provided flooding scenario. The size was selected to provide suitable data that can be used to benchmark codes that simulate the flooding process. This does not reflect a realistic flooding scenario; it is unlikely that the side shell will be opened for such a large length and height.

At the start of the flooding of the model, the coversheet was pulled upwards with a winch. The speed was about 2.5 m/s (model scale value)

Figure 3-2: Breach

3.3 Compartments

Figure 3-2 shows the assembly of the compartments that are modelled in the flooding model. Each deck is denoted with a different colour. Figure 3-4 to Figure 3-9 show the individual decks.

The floodable compartments are made from transparent PVC. The thickness of these plates is 4mm (model scale). The (sub)compartments that are impermeable are filled with Styrofoam.

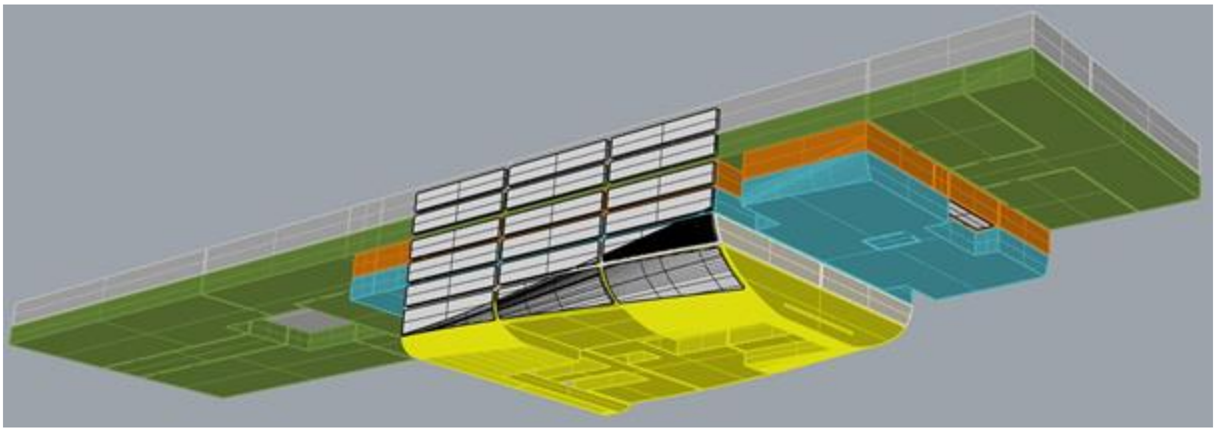

Figure 3-3: Assembly of compartments

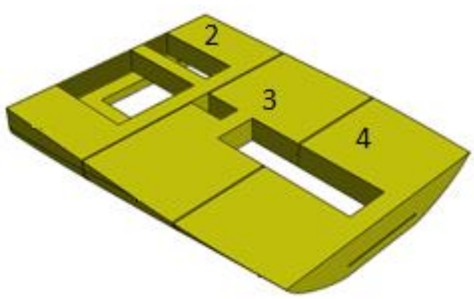

Figure 3-4: Compartments on decks 0 and 1

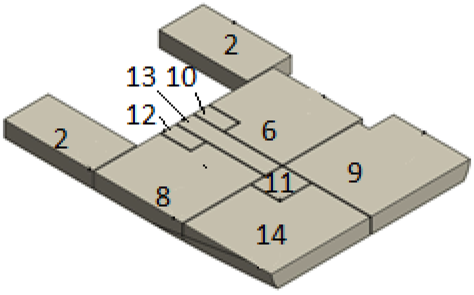

Figure 3-5: Compartments on deck 2

Note: At deck 2 the bulkhead between Compartments 9 and 14 (marked red)was removed in order to allow ingress into compartment 9.

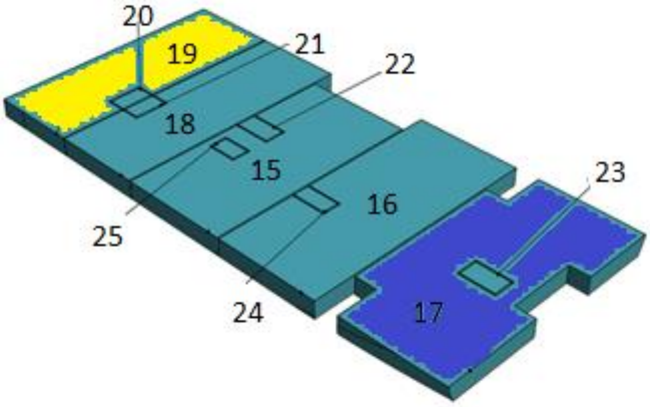

Figure 3-6: Compartments on deck 3

Compartment 17 (marked blue) was foam filled to prevent the unintentional ingress of water. This compartment should not be filled in the flooding scenario.

In the previous tests, Compartment 18 (marked yellow) was opened by the breach; this not in accordance with the given flooding scenario. For the present tests the opening was closed. Similarly for compartment 34 on deck 4 (marked yellow)

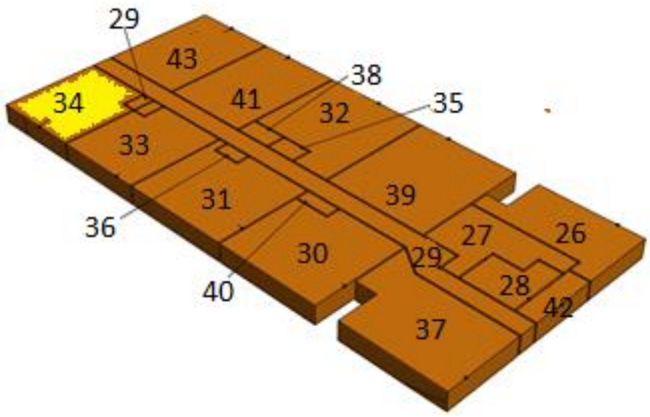

Figure 3-7: Compartments on deck 4

The geometry of deck 4 was used in the Fundamental Deck Flooding tests and is reported in Volume 2 of the WP4.2 deliverables.

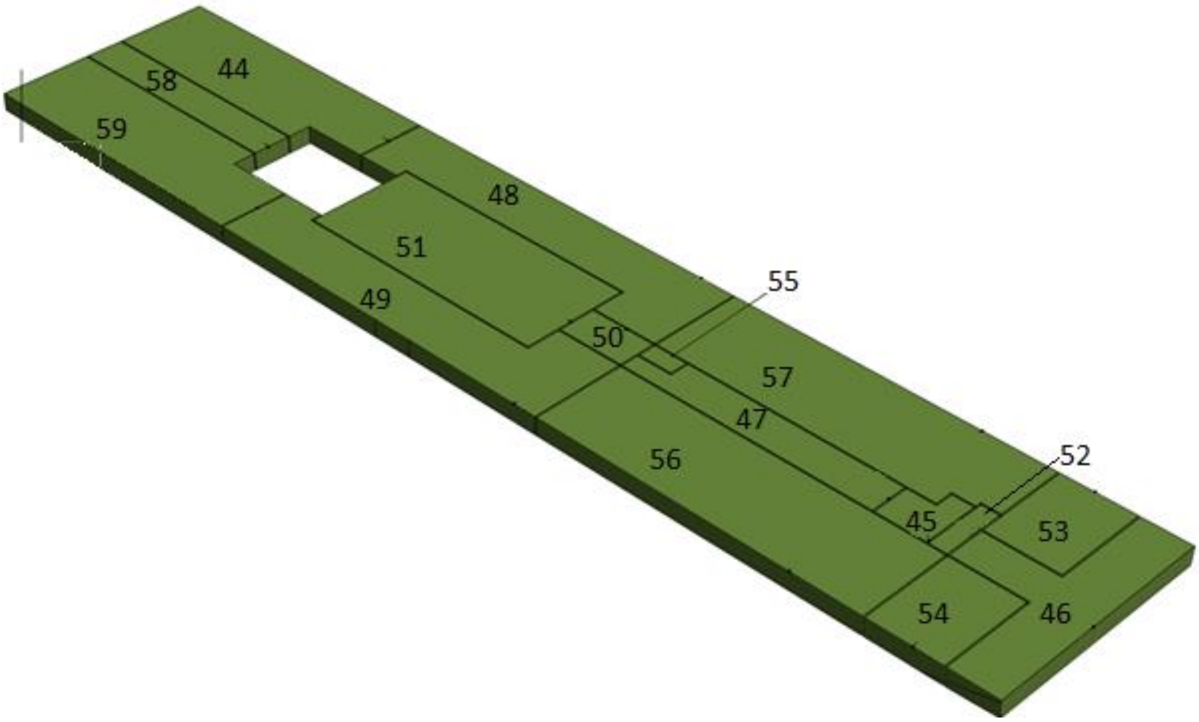

Figure 3-8: Compartments on deck 5

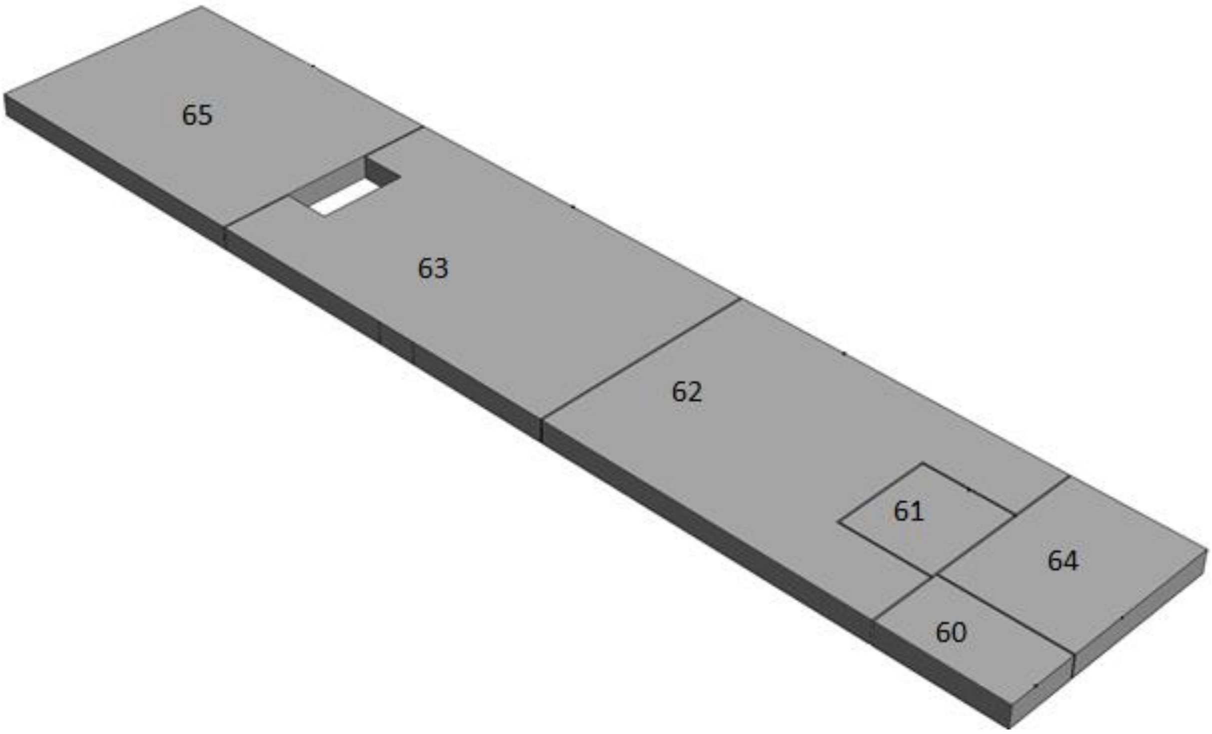

Figure 3-9: Compartments on deck 6

3.4 Ventilation pipes

The hoses that were mounted to improve the ventilation pipes in the tests reported in Volume 4 were replaced by 17 mm diameter PVC pipes on intact side of the model.

Figure 3-10: Ventilation pipes

3.5 Appendages

The model is equipped with the following appendages:

- Passive rudders, (rapid prototyping)
- Passive propeller arrangement (rapid prototyping)
- Wooden bilge keels with a total length of 90 m and a height of 430mm. The bilge keel is divided into a forward and aft part. The bilge keel is removed at the location of the damage opening
- Drain plugs are fitted to enable drainage of all compartments after the tests.

Figure 3-11: Appendages

3.6 Loading condition

The given loading conditions in the scenario are given Table 3-1. The table defines the type of capsize according to numerical assessments made by MSRC. The table indicates that a full scale change in vertical centre of gravity of 30mm will lead to a completely different capsize scenario. At model scale this is a difference of 0.5mm, and this is a smaller value than can be determined within the accuracy of the model tests. However, it indicates the sensitivity to changes in loading conditions.

It is believed that the KG location on full scale will not be known to the precision of 3cm, which makes, according to the dynamic flooding calculations of MSRC, the differ between a survival case or a capsize loss case.

Table 3-1: Provided loading conditions, intact KG values.

Case	KG	T	Trim
Transient Capsize Case	17.1m	8.2m	0m
Transient Survival Case	17.0m	8.2m	0m
Progressive Flooding Loss	17.03m	8.2m	0m

Because of calculated sensitivity, the starting point was a centre of gravity of 17.0 m; based on the results of the tests, the CoG was adjusted and a new measurement in calm water was executed. In this way the CoG iterated to the values that were near the threshold of capsizing.

The properties of the loading conditions as used in the tests are given in Table T 1. The metacentric heights are shown in Table T 2.

Note that in model tests the GM is measured via the inclination test. The intact KM is known from the hydrostatics, hence the intact KG is known when the GM is determined. The KG is not measured in dry condition. Table 3-2 shows a summary of the

Table 3-2: Provided loading conditions, intact KG values.

Condition	Mass [t]	Transverse distance [m]	Heel [deg]	GM [m]	Tϕ [s]
Config 1	221.4	24.84	1.96	2.93	17.82
Config 2	221.4	24.84	2.53	2.27	21.19
Config 3	221.4	24.84	2.31	2.50	19.13
Config 4	221.4	24.84	2.44	2.36	19.91

4 TEST SETUP AND FACILITY

4.1 Facility

This part of the test programme is executed in the Seakeeping and Manoeuvring Basin. This basin is equipped with a wave generator and a moving carriage. Current is mimicked by moving the model slowly through the basin.

Figure 4-1: Seakeeping and Manoeuvring basin

4.2 Test setup

The vessel was kept at location by a soft spring mooring system. The mooring lines were connected at the bow and stern of the vessel. The angle of the mooring lines was 45 degrees with the centreline. Figure 4-2 shows a sketch of the mooring system. The following line properties were used:

Line stiffness: 241 kN/m

Pretension: 6516 kN

The stiffness of the lines was designed in such a way that resonance with the ship motions was avoided. The yaw motion is the shortest period in this type of mooring system; in the present setup the yaw period was about twice the natural period of roll with a yaw period of 37 s. The results of the mooring decay tests are included in Appendix II.

The mooring line attachment height on the vessel was located between the CoG and the waterline. The mooring lines run parallel to the calm water level.

A lightweight slack bundle of flexible measurement cables provided the transfer of data between the model and the carriage, care was taken that these wires did not restrict the motions of the model.

Four flexible synthetic safety wires were installed to retrieve the model at the end of the test and to make sure that the model did not sink or capsize in flooded condition.

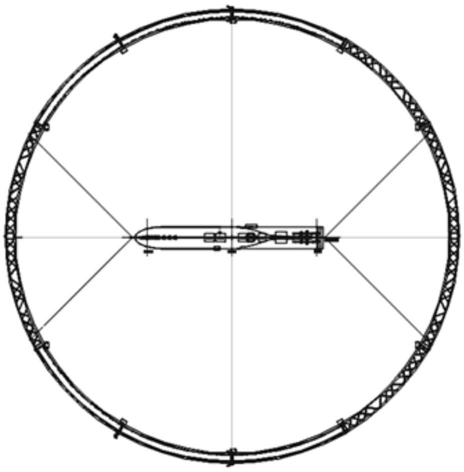

Figure 4-2: Soft spring mooring arrangement

5 MEASUREMENTS

The test setup was equipped with:

- An optical tracking system to measure the 6-DOF motions of the model in order to use the actual obtained position of the model in the test. Measured at a frequency of 100 Hz. The motions measured are translated to the CoG of the model.
- Incident wave height in the basin at 3 locations to measure the incoming wave. Measured at a frequency of 50 Hz.
- The relative wave elevation was measured at 35 locations inside the model; the locations of the wave probes are given in Table T 5 in Appendix I.
- Relative wave elevation at 6 positions at the side shell of the vessel. Measured at a frequency of 200 Hz.
- 3 DoF accelerations were measured at 4 positions.
- 3 DoF mooring forces (Surge, Sway and Yaw).

Drawings of the wave probe instrumentation can be found on the memory stick that is delivered with this report.

6 AXIS SYSTEMS AND SIGN CONVENTION

The ITTC axis and heading system was used in this report, as Figure 6-1.

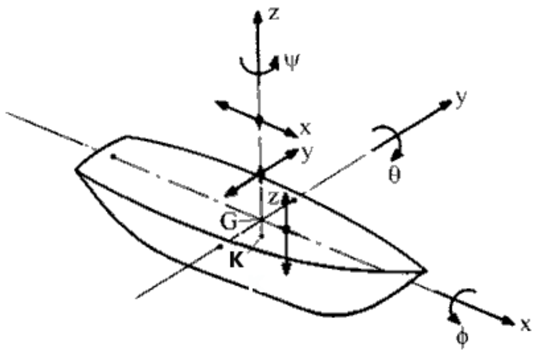

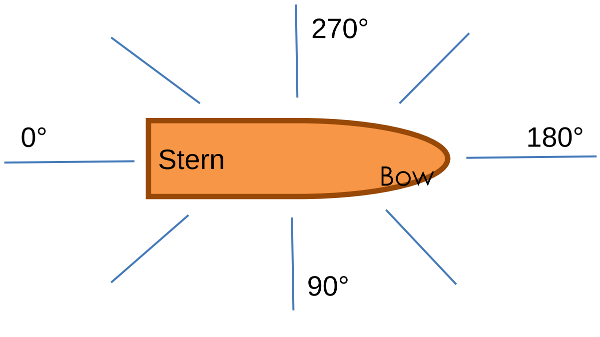

Figure 6-1: Axis system and heading convention.

The origin of the vessel is at the aft perpendicular, centreline and keel for longitudinal, transverse and vertical directions respectively.

Draught is defined as the vertical distance between the keel and calm water level.

7 TEST PROGRAMME AND PROCEDURES

7.1 Summary of the test programme

A total of 49 flooding tests were executed. Of which:

- 11 decay tests (roll and mooring)
- 10 tests in calm water
- 12 tests with high GM in irregular waves
- 12 tests with intermediate GM in irregular waves
- 4 tests with high GM in irregular waves

7.2 Test procedures

The following test procedures were followed:

Loading condition check

After each change in the loading condition the metacentric height was measured in an inclining test.

- At the start of the test a ballast weight which was already part of the loading condition was positioned at the side of the model. The static heel angle was measured.
- The weight was moved to the other side of the vessel over a known distance; again the static heel angle was measured.
- The ballast weight was mounted at its original position to establish zero heel.
- A roll decay was executed to measure the natural period of roll.

Flooding tests

Unless stated otherwise, the following steps were conducted in each test:

A. The model was prepared for the tests and was suspended above the water.

B. The measurement starts.

C. The wave generator starts and sufficient waiting time was taken into account for the waves to develop at the location of the model.

D. The model is lowered into the water.

E. The carriage starts moving at the given current speed.

F. After a short waiting time the breach opens.

G. The test ends after about 60 minutes full scale time, or if a roll angle of 40 deg is reached, whichever came first

H. The model is lifted out the water and prepared for the next test.

8 SUMMARY AND DISCUSSION

This section gives a summary of the main observations including a brief discussion.

8.1 Test in calm water

Figure 8-2 shows the angle of heel of configurations 2, 3 and 4. The metacentric height in these configurations was 2.27, 2.50 and 2.36 m respectively. The initial peak in the heel is shown on the left, the complete time trace on the right.

In the lowest two GMs (cfg2 and cfg4), the initial peak in the heel is about 30 deg, which is followed by a clear second peak due to the sloshing of the water inside the compartments. In the highest GM the first peak is about 26 degrees and no clear second peak is measured. Thereafter, the heel stays constant.

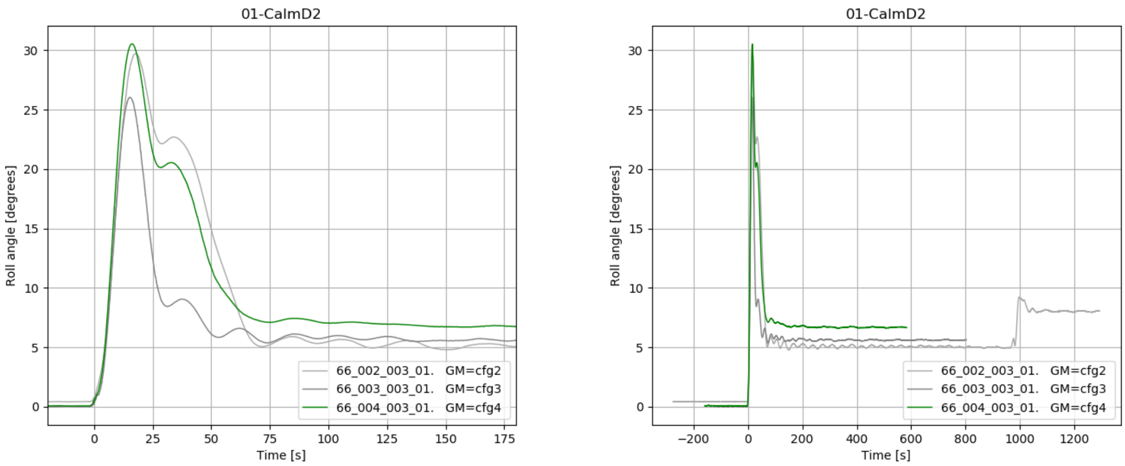

Figure 8-1: Heel angle in calm water

8.2 Configuration 2 (GM=2.27m)

Figure 8-2 shows the heel of the lowest GM in calm water and in waves. In waves, the vessel capsizes at the second peak. Please note that this is only one realisation in an extreme weather condition with a significant wave height of 7 m.

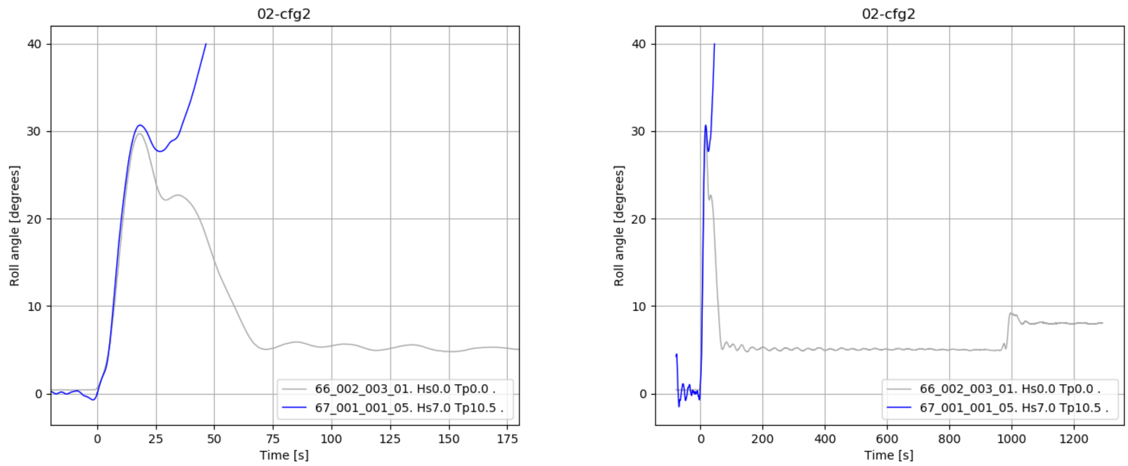

Figure 8-2: Heel angle – Configuration 2

8.3 Configuration 3 (GM=2.50 m)

Figure 8-3 shows the heel of the highest GM in calm water and in waves. The initial heel angle was between 25 and 31 deg. In a wave height of 4 m no capsizes were observed. In waves with a significant height of 5.5 m and higher, all measurements resulted in a capsize. The spread in the time to capsize per wave condition was relatively small. In contrast with the previous tests, at a significant wave height of 7 m the steeper waves resulted in a shorter time to capsize than the longer wave which are closer to roll resonance. In the present test the natural period of roll is longer due to the lower initial GM and less flood water at low positions in the hull. The behaviour was similar to that of the High GM in the previous test programme. However GM in the previous test programme was 0.38 m higher, which is in line with expectations: fewer compartments are being filled with water.

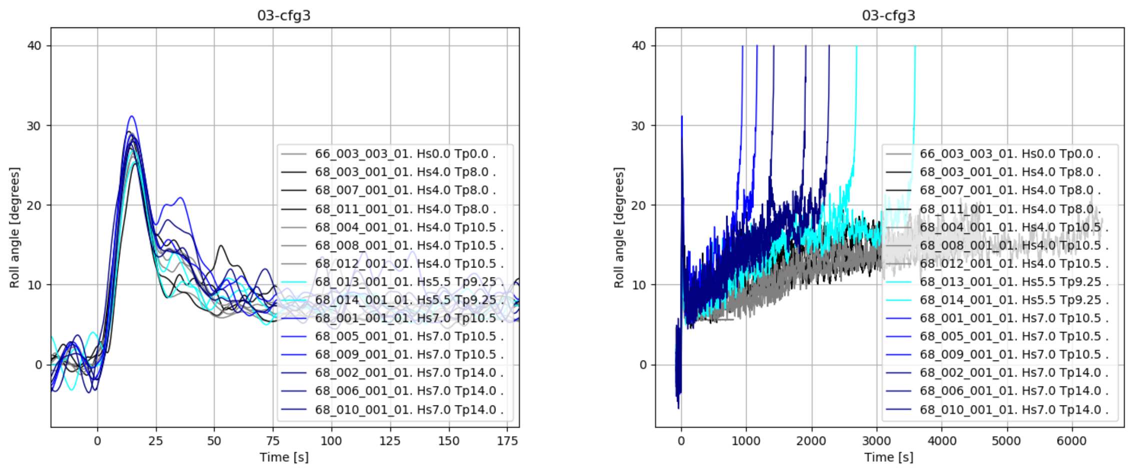

Figure 8-3: Heel angle – Configuration 3

8.4 Configuration 4 (GM=2.36 m)

Figure 8-4 shows the heel of Configuration 4, which was the loading condition with the intermediate GM. The times to capsize are significantly reduced compared to Configuration 3. Additionally all tests in Hs=4 m resulted in a capsize.

The times to capsize were roughly similar to the Intermediate GM in the previous tests (as reported in Volume 4). The GM in the previous test programme was 0.24 m higher.

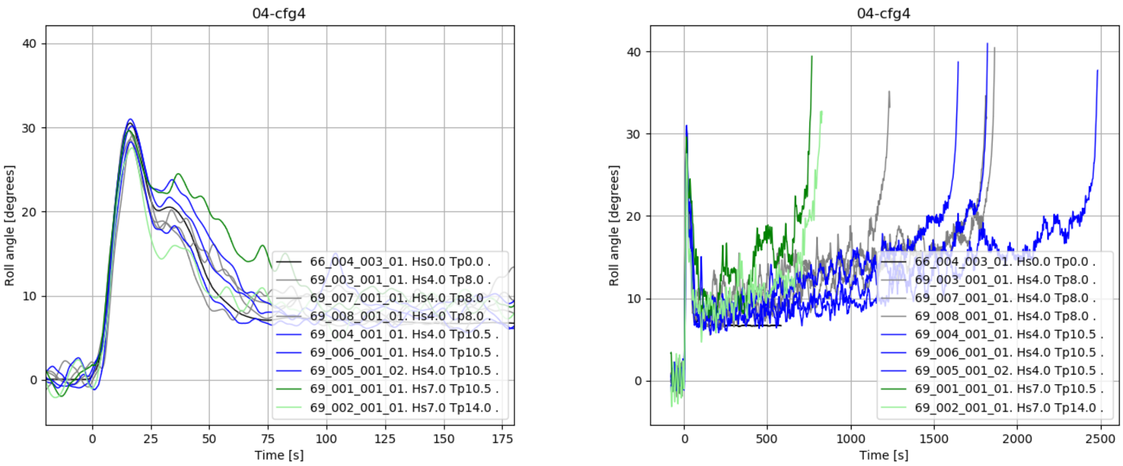

Figure 8-4: Heel angle – Configuration 4

9 CONCLUSION

Model tests were conducted for a cruise vessel (denoted Cruise Vessel #3 in FLARE) to investigate flooding in waves. The goal of the tests was to generate a data set which can be used to benchmark flooding software.

Based on the results of the tests the following conclusions can be drawn:

- As expected the metacentric height was the main driver in the capsizing behaviour and time to capsize. Higher metacentric heights resulted in fewer wave conditions where capsizes were observed, and longer survival times
- The tests were quite consistent: different realisations of an irregular wave condition, with a different seed, always resulted in the same outcome with respect to capsizes and time to capsize..
- The wave period did not seem to have a clear impact on the capsizes and the time to capsize.
- The present results are obtained with a slightly different internal floodable space than the results presented in Volume 4. It led to similar capsize behaviour and time to capsize for the intermediate GM values (GM=2.50 m now versus 2.88 m (High GM in previous test programme) and GM=2.36 m versus GM 2.61 m (Intermediate GM in previous test programme)). Hence, the internal flooding had a noticeable effect
- With a GM of 2.27 m immediate capsize in waves occurred after the first water ingress and first heel towards the damage. The vessel recuperated to a safe upright flooding in calm water condition, but not in waves. The vessel capsizes under transient flooding.
- With a GM of 2.36 m, the vessel capsizes under progressive flooding.
- With a GM of 2.50 m, the vessel capsizes under progressive flooding, with a time to capsize about twice as long compared to GM of 2.36 m
- With a GM between 2.36 m and 2.93 m, the vessel reaches a large heel towards the damage in calm water, but always restores to an stable floating condition afterwards.
- The metacentric height was lower than in the previous tests. With a difference of about 0.3 m the behaviour of the two models was similar with respect to observed capsizes in specific wave conditions and the time to capsize.

Appendix I – Tables

Table T 1: Loading condition

Main particulars			
Designation	**Symbol**	**Magnitude**	**Unit**
Length	Lpp	270	m
Breadth	B	35	m
Height	H	12.6	m
Draught fore	T fore	8.2	m
Draught aft	T aft	8.2	m
Displacement mass	displ	52850	ton
VCG position from Keel (approx.)	KG	17	m
LCG position from AP	LCG	127.92	m
Radius of inertia for roll	Kxx	13.904	m
Radius of inertia for pitch	Kyy	70.708	m
Radius of inertia for yaw	Kzz	71.223	m

Table T 2: GM variations

Metacentric height	
Name	**GM[m]**
Config 1	2.93
Config 2	2.27
Config 3	2.50
Config 4	2.36

Table T 3: location of measurement devices

Wave probes	X [m]	Y [m]	Z [m] (zero level)	Compartment number	Deck
Number					
REL.1	142.92	-15	0.18	2	1
REL.2	157.2	-15	1.56	3	1
REL.4	157.2	-7.5	1.56	3	1
REL.5	172.74	-7.5	0.18	4	1
REL.6	142.92	15	1.56	2	1
REL.7	157.2	15	1.56	3	1
REL.8	172.74	15	0.18	4	1
REL.9	157.2	-15	5.3	8	2
REL.10	172.74	-15	5.3	9	2
REL.11	157.2	-15	8.22	15	3
REL.12	157.2	-7.5	5.3	8	2
REL.13	172.74	-7.5	5.3	9	2
REL.14	157.2	7.5	5.3	6	2
REL.15	172.74	7.5	5.3	9	2
REL.16	130.08	-15	8.22	19	3
REL.17	142.92	-15	8.22	18	3
REL.18	172.74	-15	8.22	16	3
REL.19	Not mounted				
REL.20	130.08	0	8.22	19	3
REL.21	142.9	0	8.22	18	3
REL.22	157.2	0	8.22	15	3
REL.23	172.74	0	8.22	16	3
REL.24	Not mounted				
REL.25	130.2	-14.52	11	34	4
REL.26	142.92	-14.52	11	33	4
REL.27	157.2	-14.52	11	31	4
REL.28	172.74	-14.52	11	30	4
REL.29	189.6	-11.64	11	37	4
REL.30	130.2	-1.5	11	29	4
REL.31	172.74	-1.5	11	29	4
REL.32	86.22	-14.52	13.4	59	5
REL.33	142.92	-14.52	13.4	49	5
REL.34	189.6	-14.52	13.4	56	5
REL.35	142.92	-14.52	16.8	63	6
REL.36	189.54	-14.52	16.8	62	6
REL.PSA	82.2	18	8.2	outside	-
REL.SBA	82.2	-18	8.2	outside	-
REL.PSM	129	18	8.2	outside	-
REL.SBM	129	-18	8.2	outside	-
REL.PSF	190	18	8.2	outside	-
REL.SBF	190	-18	8.2	outside	-

Table T 4: Model in calm water

Calm water	
Test No	**GM**
30703_09SMB_66_002_003_01	cfg2
30703_09SMB_66_003_003_01	cfg3
30703_09SMB_66_004_003_01	cfg4

Table T 5: Config 2 in waves

High GM - tests in waves		
Test No	**Hs[m]**	**Tp[s]**
30703_09SMB_66_002_003_01	7	10.5

Table T 6: Config 3 in waves

Intermediate GM - tests in waves		
Test No	**Hs[m]**	**Tp[s]**
30703_09SMB_68_003_001_01	4	8
30703_09SMB_68_007_001_01	4	8
30703_09SMB_68_011_001_01	4	8
30703_09SMB_68_004_001_01	4	10.5
30703_09SMB_68_008_001_01	4	10.5
30703_09SMB_68_012_001_01	4	10.5
30703_09SMB_68_013_001_01	5.5	9.25
30703_09SMB_68_014_001_01	5.5	9.25
30703_09SMB_68_001_001_01	7	10.5
30703_09SMB_68_005_001_01	7	10.5
30703_09SMB_68_009_001_01	7	10.5
30703_09SMB_68_002_001_01	7	14
30703_09SMB_68_006_001_01	7	14
30703_09SMB_68_010_001_01	7	14

Table T 7: Config 4 in waves

High GM - tests in waves - 1m/s drift		
Test No	**Hs[m]**	**Tp[s]**
30703_09SMB_69_003_001_01	4	8
30703_09SMB_69_007_001_01	4	8
30703_09SMB_69_008_001_01	4	8
30703_09SMB_69_004_001_01	4	10.5
30703_09SMB_69_006_001_01	4	10.5
30703_09SMB_69_005_001_02	4	10.5
30703_09SMB_69_001_001_01	7	10.5
30703_09SMB_69_002_001_01	7	14